

**TISSUE RESIDENT AND MIGRATORY GROUP 2 INNATE LYMPHOID CELLS IN  
MICE**

by

Laura Mathae

B.Sc., The University of British Columbia, 2014

A THESIS SUBMITTED IN PARTIAL FULFILLMENT OF  
THE REQUIREMENTS FOR THE DEGREE OF

DOCTOR OF PHILOSOPHY

in

THE FACULTY OF GRADUATE AND POSTDOCTORAL STUDIES  
(Interdisciplinary Oncology)

THE UNIVERSITY OF BRITISH COLUMBIA  
(Vancouver)

August 2020

© Laura Mathae, 2020

The following individuals certify that they have read, and recommend to the Faculty of Graduate and Postdoctoral Studies for acceptance, the dissertation entitled:

Tissue resident and migratory group 2 innate lymphoid cells in mice

submitted by Laura Mathae in partial fulfillment of the requirements for

the degree of Doctor of Philosophy

in Interdisciplinary Oncology

**Examining Committee:**

Dr. Fumio Takei, Professor, Pathology and Laboratory Medicine, UBC  
Supervisor

Dr. Pauline Johnson, Professor, Microbiology and Immunology, UBC  
Supervisory Committee Member

Dr. Laura Sly, Associate Professor, Pediatrics, UBC  
University Examiner

Dr. Stuart Turvey, Professor, Pediatrics, UBC  
University Examiner

**Additional Supervisory Committee Members:**

Dr. Kelly McNagny, Professor, Medical Genetics, UBC  
Supervisory Committee Member

Dr. Kevin Bennewith, Associate Professor, Pathology and Laboratory Medicine, UBC  
Supervisory Committee Member

## Abstract

Group 2 innate lymphoid cells (ILC2s) primarily reside on mucosal surfaces and produce copious amounts of IL-5 and IL-13 upon activation by epithelium-derived cytokines, such as IL-33, leading to inflammation characterized by eosinophilia. Elevated numbers of ILC2s are found in the peripheral blood of patients with allergic diseases including asthma, suggesting their involvement in the disease.

Epidemiological studies have shown higher prevalence of asthma in women than men during reproductive age, but the mechanism is largely unknown. By using flow cytometric analyses, I found that post-pubertal female lung ILC2s are more responsive to IL-33 stimulation than male ILC2s. Gene expression analyses of purified ILC2s and measurement of epithelium-derived cytokines in the lung demonstrated ILC2 intrinsic and lung environmental differences between naïve female and male lungs, suggesting a more activated state of female ILC2s compared to male ILC2s at steady state conditions.

ILC2s have previously been shown to be tissue resident at steady state as well as during inflammation. However, recent reports have demonstrated migratory potential of ILC2s upon activation. Intranasal IL-33 administration into mice caused expansion of ILC2s not only in the lung but also in the blood and liver. Parabiosis experiments showed that ILC2s migrate out of the lung to the liver through circulation. Lung-derived ILC2s potently produced IL-5, IL-13 and IL-6, inducing eosinophilia and mild fibrosis. In contrast, intranasal IL-33 pre-treatment attenuated concanavalin A-induced acute hepatitis and cirrhosis.

Overall, these results highlight the complexity of ILC2 regulation and ILC2-mediated local and systemic immunity. These considerations need to be taken into account when investigating ILC2s in human diseases.

## **Lay Summary**

Group 2 innate lymphoid cells (ILC2s) are immune cells that reside in the lung. ILC2s are elevated in asthmatic patients' blood, implicating their involvement in asthma. Previous studies have shown increased prevalence of asthma in women than men after puberty. To understand the differences between female and male ILC2s and the fate of lung ILC2s during inflammation, I investigated ILC2s in various organs after stimulation in the lung. In adult mice, female lung ILC2s responded more vigorously than male ILC2s, resulting in enhanced inflammation in female lungs. Upon stimulation, a small number of ILC2s left the lung, circulated through blood and moved to the liver, where they modulated other immune cells and promoted or protected from fibrosis in different settings. These findings demonstrate complex regulation of ILC2s as well as multiple layers of protection provided by lung-resident and migratory ILC2s, which should be taken into consideration when studying human diseases.



## Preface

This work was conducted at the Terry Fox Laboratory by Laura Mathae, Hanjoo Shim, Yi Han Yin, Dr. Catherine Steer, Dr. Mónica Romera-Hernández, Dr. Itziar Martinez-Gonzalez, Mona Orangi, ChihKai Chang, Dr. Fabio Rossi and Dr. Fumio Takei as part of the requirements for Doctor of Philosophy in Interdisciplinary Oncology Program. The data presented in Figure 4.2 were generated in collaboration with Dr. Catherine Steer and Dr. Mónica Romera-Hernández, Figures 3.5F and 3.6C were generated by Hanjoo Shim, while data presented in Figure 4.6 were generated by Yi Han Yin. Dr. Catherine Steer and Dr. Itziar Martinez-Gonzalez helped with immunohistochemistry, and Dr. Mónica Romera-Hernández helped with optimization of small intestine processing protocol. Hanjoo Shim, Yi Han Yin, Dr. Catherine Steer, Dr. Mónica Romera-Hernández, Dr. Itziar Martinez-Gonzalez, and Mona Orangi helped with tissue harvesting and processing. ChihKai Chang and Dr. Fabio Rossi generated parabiosis mice at the Biomedical Research Centre. I was responsible for designing, performing and analyzing the majority of the experiments unless otherwise stated above.

A version of Chapter 3 has been published: Mathä L, Shim H, Steer CA, Yin YH, Martinez-Gonzalez I, Takei F (2019) Female and male mouse lung group 2 innate lymphoid cells differ in gene expression profiles and cytokine production. *PLoS ONE* **14** (3): e0214286. I designed, performed and analyzed most experiments and wrote the manuscript (contribution=60%). Hanjoo Shim performed gene ontology analyses of microarray data and performed experiments (12.5%). Dr. Catherine Steer and Dr. Itziar Martinez-Gonzalez helped with immunohistochemistry and tissue processing (5%). Yi Han Yin contributed to tissue processing (2.5%). Dr. Fumio Takei conceptualized the project, provided guidance and wrote the

paper (20%). A version of Chapter 2 has also been published in the same manuscript under Materials and Methods section.

A version of Chapter 4 and 5 has been submitted as a manuscript entitled “Migration of lung resident group 2 innate lymphoid cells link allergic lung inflammation and liver fibrosis” for publication in a peer-reviewed journal.

All animal use was approved by the animal care committee of the University of British Columbia in accordance with the guidelines of the Canadian Council on Animal Care under protocols: A14-0182 (2014/07/04-2018/08/31), A15-0119 (2015/09/01-2019/09/28), A16-0131 (2016/06/17-2020/08/17), A18-0231 (2018/07/24-2020/09/10), and A19-0215 (2019/09/28-2020/12/06). All laboratory work has been approved under biosafety certificate # B18-0088 (2018/04/20-2020/07/25).

# Table of Contents

<b>Abstract.....</b>	<b>iii</b>
<b>Lay Summary .....</b>	<b>iv</b>
<b>Preface.....</b>	<b>v</b>
<b>Table of Contents .....</b>	<b>vii</b>
<b>List of Tables .....</b>	<b>xii</b>
<b>List of Figures.....</b>	<b>xiii</b>
<b>List of Symbols .....</b>	<b>xv</b>
<b>List of Abbreviations .....</b>	<b>xvi</b>
<b>Acknowledgements .....</b>	<b>xxi</b>
<b>Dedication .....</b>	<b>xxiii</b>
<b>Chapter 1: Introduction .....</b>	<b>1</b>
1.1 Immune responses.....	1
1.1.1 Overview.....	1
1.1.1.1 Innate immunity .....	1
1.1.1.2 Adaptive immunity .....	2
1.1.2 Types of immunity.....	3
1.1.2.1 Type 1 immunity.....	4
1.1.2.2 Type 2 immunity.....	6
1.1.2.3 Type 3 immunity.....	7
1.2 ILC2 .....	9
1.2.1 Discovery and characterization.....	9

1.2.2	Development .....	11
1.2.3	Activation.....	13
1.2.3.1	IL-33 .....	15
1.2.3.2	IL-25 .....	16
1.2.3.3	TSLP .....	17
1.2.3.4	Co-stimulatory cytokines .....	18
1.2.3.5	Lipid mediators .....	21
1.2.3.6	Neurotransmitters.....	23
1.2.3.7	Other molecules .....	25
1.2.3.8	Cell-cell interactions .....	25
1.2.4	Inhibition.....	26
1.2.4.1	Cytokines .....	26
1.2.4.2	Lipid mediators .....	28
1.2.4.3	Neurotransmitters.....	29
1.2.4.4	Androgen.....	29
1.2.4.5	Cell-cell interactions .....	30
1.2.5	Function .....	30
1.2.6	Memory.....	34
1.3	Diseases.....	34
1.3.1	Asthma .....	34
1.3.1.1	Overview.....	34
1.3.1.2	Pathogenesis.....	35
1.3.2	Hepatic fibrosis .....	37

1.3.2.1	Overview .....	37
1.3.2.2	Pathogenesis.....	38
1.3.3	Cancer .....	39
1.4	Thesis objective .....	40
<b>Chapter 2: Materials and Methods .....</b>		<b>42</b>
2.1	Materials .....	42
2.1.1	Mice .....	42
2.1.2	Parabiosis .....	43
2.1.3	Antibodies and flow cytometry.....	44
2.1.4	Reagents .....	48
2.2	Methods.....	49
2.2.1	In vivo stimulation .....	49
2.2.2	Primary leukocyte preparation.....	49
2.2.3	BM transplantation.....	50
2.2.4	Intracellular staining .....	51
2.2.5	Immune cell identification .....	51
2.2.6	ILC/ILC2 enrichment.....	55
2.2.7	In vitro stimulation.....	55
2.2.8	Tissue homogenate preparation .....	55
2.2.9	Quantification of cytokines.....	56
2.2.10	IL-33 immunohistochemistry.....	56
2.2.11	Liver histology .....	56
2.2.12	RNA extraction .....	57

2.2.13	Microarray.....	57
2.2.14	Genes set enrichment analysis .....	58
2.2.15	Visualization of Cytoscape network analyses.....	58
2.2.16	Reactome pathway analyses .....	58
2.2.17	cDNA synthesis .....	59
2.2.18	RT-qPCR.....	59
2.2.19	Statistics .....	60
<b>Chapter 3: Female and male mouse lung ILC2s differ in gene expression profiles and cytokine production .....</b>		<b>61</b>
3.1	Introduction.....	61
3.2	Results.....	62
3.3	Discussion .....	74
<b>Chapter 4: Activation-induced migration of lung ILC2s to the liver .....</b>		<b>78</b>
4.1	Introduction.....	78
4.2	Results.....	79
4.3	Discussion .....	94
<b>Chapter 5: Lung-derived liver ILC2s induce changes in the liver immune environment ....</b>		<b>99</b>
5.1	Introduction.....	99
5.2	Results.....	102
5.3	Discussion .....	114
<b>Chapter 6: Conclusion .....</b>		<b>117</b>
6.1	Summary .....	117
6.2	Significance.....	122

6.3	Strengths and limitations.....	123
6.4	Future directions .....	125
<b>References .....</b>		<b>128</b>
<b>Appendices.....</b>		<b>150</b>
Appendix A.....		150
A.1	Sex has no effects on ILC2 development .....	150
A.2	Female and male ILC2s respond similarly in female host.....	150
Appendix B.....		151
B.1	Perfusion has little effect on the frequencies of liver ILC2s and eosinophils .....	151
B.2	Analyses of parabiosis mice after i.n. IL-33 administration into Pep3b mice.....	152
B.3	Lin <sup>-</sup> Thy1 <sup>+</sup> cells contain non-ILC2s .....	153
Appendix C .....		154
C.1	Characterization of CD127 cKO mouse SI, spleen and BM .....	154

## List of Tables

Table 1.1: Summary of ILC2 phenotype in different tissues.....	11
Table 1.2: Summary table of ILC2 functions in various organs.....	34
Table 2.1: Table of antibodies used in this study.....	44
Table 2.2: Table of probes/primers used for RT-qPCR analyses .....	59
Table 4.1: Phenotype of naïve and IL-33 treated lung and liver ILC2s .....	91
Table 4.2: Table of $R^2$ values for each microarray dataset comparison .....	93



## List of Figures

Figure 1.1: Types of immunity .....	4
Figure 1.2: ILC2 regulatory network and effector functions.....	14
Figure 2.1: Gating strategies used to identify various lymphoid populations .....	52
Figure 2.2: Gating strategies used to identify various myeloid populations.....	54
Figure 3.1: Post-pubertal female lung ILC2s are more responsive to IL-33 than male ILC2s.....	64
Figure 3.2: Pre-pubertal female and male lung ILC2s respond similarly to IL-33 stimulation....	65
Figure 3.3: Kinetics of ILC2 activation in female and male lungs.....	67
Figure 3.4: IL-33, IL-7 and TSLP are differentially expressed in naïve female and male lungs .	69
Figure 3.5: Gene expression analyses of naïve female and male lung ILC2s .....	71
Figure 3.6: Gene expression analyses of activated female and male lung ILC2s.....	73
Figure 4.1: ILC2s expand in peripheral tissues after stimulation in the lung .....	81
Figure 4.2: Activated lung ILC2s migrate to the liver: analysis of parabiosis mice .....	83
Figure 4.3: LNs are not required for ILC2 migration from the lung to the liver .....	85
Figure 4.4: Lung-derived liver ILC2s produce more IL-5, IL-13 and IL-6 than lung ILC2s.....	87
Figure 4.5: Surface marker expression on ILC2s in the lung, liver and PB .....	90
Figure 4.6: Gene expression analyses of CD103 <sup>+</sup> and CD103 <sup>-</sup> lung, liver and PB ILC2s .....	93
Figure 5.1: Lung-derived liver ILC2s induce changes in the liver immune environment.....	103
Figure 5.2: Characterization of CD127 cKO mice .....	105
Figure 5.3: Liver inflammation is diminished in ILC2 deficient mice .....	106
Figure 5.4: Repeated i.n. IL-33 injections cause eosinophilic hepatitis and mild fibrosis .....	109
Figure 5.5: Hepatic inflammation upon IL-33 challenge is attenuated in CD127 cKO mice ....	111
Figure 5.6: I.n. IL-33 pre-treatment attenuates ConA-induced hepatitis.....	113

Figure 6.1: Post-pubertal female lung ILC2s are more responsive than male lung ILC2s.....	118
Figure 6.2: Lung ILC2s migrate to the liver upon activation and alter the immune environment .....	120
Figure 6.3: Lung-derived ILC2s exert pro- and anti- fibrotic effects in the liver.....	121

## List of Symbols

$\alpha$	alpha
$\beta$	beta
$\delta$	delta
$\gamma$	gamma
$\varepsilon$	epsilon
$\kappa$	kappa
$\mu$	micro
$\%$	percent
$+$	plus
$\pm$	plus or minus
$\geq$	greater than or equal to
$>$	greater than
$<$	smaller than
$\#$	number

## List of Abbreviations

2-ME	2-mercaptoethanol
<i>A. alternata</i>	<i>Alternaria alternata</i>
AD	atopic dermatitis
AHR	airway hyperresponsiveness
$\alpha$ -LP	$\alpha$ lymphoid progenitor
ALD	alcoholic liver disease
ALX/FOR2	a lipoxin and formyl peptide receptor 2
AMacs	alveolar macrophages
ANOVA	analysis of variance
APC	allophycocyanin
APCs	antigen presenting cells
APL	acute promyelocytic leukemia
AR	androgen receptor
ARC	Animal Resource Centre
Areg	amphiregulin
$\beta$ 2AR	$\beta$ 2 adrenergic receptor
BALF	bronchoalveolar lavage fluid
BAT	beige adipocytes
BCCRC	British Columbia Cancer Research Centre
BCL11b	B-cell leukemia 11b
BCR	B cell receptor
BiNGO	biological network gene ontology tool
BM	bone marrow
BMT	bone marrow transplantation
BRC	Biomedical Research Centre
BV	brilliant violet
CD	cluster of differentiation
cDC1	type 1 conventional dendritic cell
cDC2	type 2 conventional dendritic cell
cDNA	complementary deoxyribonucleic acid
CHILP	common helper ILC progenitor
cKO	conditional knock out
CLP	common lymphoid progenitor
CLR	calcitonin receptor-like receptor
CGRP	calcitonin gene-related peptide
ConA	concanavalin A
CRS	chronic rhinosinusitis
CRTH2	chemoattractant receptor-homologous molecule expressed on Th2 cells
Cys	cysteinyl
DAMP	damage-associated molecular pattern
DMEM	Dulbecco's Modified Eagle's Medium
DC	dendritic cell
DNA	deoxyribonucleic acid

DP	D prostanoid receptor
DR3	death receptor 3
ECM	extracellular matrix
EDTA	ethylenediaminetetraacetic acid
EILP	early innate lymphoid progenitor
ELISA	enzyme-linked immunosorbent assay
EOMES	omesodermin
FACS	fluorescence-activated cell sorting
FALC	fat-associated lymphoid clusters
FBS	fetal bovine serum
FITC	fluorescein isothiocyanate
GABA	$\gamma$ -aminobutyric acid
GATA3	GATA binding protein 3
$\gamma$ c	common gamma chain
GI	gastrointestinal
GITR	glucocorticoid-induced tumor necrosis factor receptor
GITRL	glucocorticoid-induced tumor necrosis factor receptor ligand
GM-CSF	granulocyte-macrophage colony-stimulating factor
GO	gene ontology
GPCR	G protein-coupled receptor
GSEA	Gene Set Enrichment Analysis
HBSS	Hank's Balanced Salt Solution
HDM	house dust mite
H&E	hematoxylin and eosin
HSC	hepatic stellate cell
ICAM1	intercellular adhesion molecule 1
ICOS	inducible costimulator
ICOSL	ICOS ligand
ID2	inhibitor of DNA binding 2
iILC2	inflammatory ILC2
IL	interleukin
IL-1RAcP	IL-1 receptor accessory protein
ILC	innate lymphoid cell
ILC1	group 1 innate lymphoid cell
ILC2	group 2 innate lymphoid cell
ILC2P	ILC2 precursor
ILC3	group 3 innate lymphoid cell
ILCP	ILC precursor
IFN	interferon
Ig	immunoglobulin
IMacs	interstitial macrophages
i.n.	intranasal
IP	prostacyclin receptor
i.p.	intraperitoneal
IRAK	interleukin-1 receptor-associated kinase

ITG	integrin
i.v.	intravenous
JAK	Janus kinase
KC	Kupffer cell
kg	kilogram
KLRG1	killer cell lectin like receptor G1
KO	knock out
LN	lymph node
LMPP	lymphoid-primed multipotent progenitor
LSEC	liver sinusoidal endothelial cell
LT	leukotriene
LTi	lymphoid tissue inducer
LX	lipoxin
mAChR	muscarinic acetylcholine receptor
Macs	macrophages
MAPK	mitogen-activated protein kinases
MDSC	myeloid-derived suppressor cell
medLN	mediastinal lymph node
mg	milligram
μg	microgram
MHC	major histocompatibility complex
mins	minutes
μL	microliter
mL	milliliter
mLN	mesenteric lymph node
μm	micrometer
μM	micromolar
MMP	matrix metalloproteinase
Mo	monocytes
MoMacs	monocyte-derived macrophages
MS	multiple sclerosis
MyD88	myeloid differentiation primary response 88
nAChR	nicotinic acetylcholine receptor
NAFLD	non-alcoholic fatty liver disease
<i>N. brasiliensis</i>	<i>Nippostrongylus brasiliensis</i>
NF	nuclear factor
NFIL3	nuclear factor, interleukin 3 regulated
ng	nanogram
NK	natural killer
NKT	natural killer T
NMU	neuromedin U
OVA	ovalbumin
PAMP	pathogen-associated molecular pattern
PB	peripheral blood
PBS	Phosphate-buffered saline

PD-1	programmed cell death protein 1
PDAC	pancreatic ductal adenocarcinoma
PE	phycoerythrin
PG	prostaglandin
PLZF	promyelocytic leukemia zinc finger protein
PMA	phorbol 12-myristate 13-acetate
PNEC	pulmonary neuroendocrine cell
PRRs	pattern recognition receptors
P/S	penicillin/streptomycin
R	receptor
RA	rheumatoid arthritis
Rag	recombination activating gene
RAMP	receptor activity modifying protein
RBC	red blood cell
RELM	resistin-like molecule
RIN	RNA integrity number
RMA	robust multi-array average
RNA	ribonucleic acid
ROR	retinoic acid receptor-related orphan receptor
rpm	revolutions per minute
RPMI	Roswell Park Memorial Institute
RT-qPCR	real-time quantitative polymerase chain reaction
S1P	sphingosine-1-phosphate
<i>S. mansoni</i>	<i>Schistosoma mansoni</i>
SEM	standard of the mean
SI	small intestine
SNP	single nucleotide polymorphism
STAT	signal transducer and activator of transcription
TCF	T cell factor
TCR	T cell receptor
TGF	transforming growth factor
Th1	T helper type 1
Th2	T helper type 2
Th17	T helper type 17
TIMP	tissue inhibitors of metalloproteinase
TL1A	tumor necrosis factor-like ligand 1A
TNF	tumor necrosis factor
TNFSF	TNF superfamily
TRAF6	tumor necrosis factor receptor-associated factor 6
TOX	thymocyte-selection-associated high mobility group box protein
Tregs	regulatory T cells
TSLP	thymic stromal lymphopoietin
U	units
VIP	vasoactive intestinal peptide
vs.	versus

WAT	white adipose tissue
WT	wild type
Yeti	YFP-enhanced transcript for IFN $\gamma$



## Acknowledgements

First and foremost, I would like to express my enormous gratitude to my thesis supervisor, Dr. Fumio Takei. Without his support, guidance, and patience, this thesis work could not have been accomplished. His scientific curiosity provided me with inspiration, and I could not have asked for a better mentorship through the process of becoming a scientist. I would also like to thank Dr. Yuh-Ching Twu and Dr. Timotheus Halim for training me during the first year in the Takei laboratory and Dr. Timotheus Halim for providing me with the opportunity to contribute to the article published in *Immunity* **40**: 425-35. I would also like to acknowledge my supervisory committee members Dr. Kelly McNaghy, Dr. Kevin Bennewith and Dr. Pauline Johnson for their encouragement and constructive feedback throughout my PhD and reviewing this thesis.

I would also like to thank British Columbia Cancer Research Centre animal facility and flow core staff for their support with mice work and help with cell sorting and analyses, Dr. Maryam Ghaedi for generating ILC2 deficient mouse line (CD127 cKO) and Dr. Fabio Rossi and ChihKai Chang for providing us with parabiosis mice. I would also like to acknowledge the co-operative education students Hanjoo Shim and Yi Han Yin and a visiting student Hüma Tuğçe Sezgin for their invaluable help in the laboratory.

I have received tremendous support from past and present members of the Takei laboratory including Dr. Itziar Martinez-Gonzalez, Dr. Grace Poon, Dr. Catherine Steer, Dr. Maryam Ghaedi, Dr. Mónica Romera-Hernández, and Mona Orangi. I am deeply grateful for all the help in the laboratory, lab meeting discussions, constructive feedback and friendship. I would also like to thank all the fellow scientists in the Terry Fox Laboratory and in the Interdisciplinary Oncology Program.

Additionally, I would like to acknowledge Canadian Institutes for Health Research for funding my work and Vanier Canada Graduate Scholarship and University of British Columbia 4 Year Fellowship for studentship, which supported me throughout my PhD.

Finally, I am especially thankful to my amazing parents, sisters, grandparents and wonderful friends who have continued to have faith in me and supported me throughout this process. I could not have accomplished this without you.

*I dedicate this thesis to my grandfather, who was endlessly proud of my achievement and always  
believed in my success as a scientist.*

# **Chapter 1: Introduction**

## **1.1 Immune responses**

### **1.1.1 Overview**

We are constantly exposed to infectious agents and irritants, such as bacteria, viruses or allergens, in our daily life. To prevent their entry, host defense mechanisms are in place, which consist of two levels of protection: (i) anatomical and physiological barriers and (ii) immune system (1). Anatomical and physiological barriers including the skin and mucosal surfaces, pH regulation and antimicrobial enzymes present in body fluids block their entry or prevent their survival, but occasionally, the barriers are breached (1). To protect ourselves from damage caused by invading pathogens or irritants, our body is equipped with the immune system, which is composed of various types of specialized immune cells and effector molecules that work together to provide layers of protection. The overall goal of the immune system is to eliminate invading microorganisms and irritants to prevent adverse effects and potential harm, but also to repair tissue damage caused by the pathogens. However, excessive or insufficient activation of the immune system can be harmful and therefore, immune responses need to be properly regulated. To achieve proper and efficient immunity against pathogens, our immune system is divided into two levels that work closely together: innate and adaptive immunity.

#### **1.1.1.1 Innate immunity**

Innate immunity provides the first line of defense by initiating a fast and non-specific response towards invading pathogens. It developed early during evolution and it is found in all multicellular organisms (1). This type of immune response includes soluble molecules, enzymes and peptides that aim to destroy pathogens or facilitate their clearance and the complement

system that aids removal of pathogens by effector cells (1). Effector cells of the innate immunity consist of myeloid and lymphoid cells, which develop from different hematopoietic cell lineages. Myeloid cells include monocytic phagocytes (monocytes, macrophages), dendritic cells (DCs), which are professional antigen presenting cells (APCs) and granulocytes (eosinophils, neutrophils, basophils and mast cells), which contain cytoplasmic granules. The lymphoid compartment consists of natural killer T (NKT) cells, and innate lymphoid cells (ILCs), which are deficient in lineage (T, B and myeloid cell) markers and are categorized into cytotoxic natural killer (NK) cells, group 1, 2 and 3 “helper” ILCs (ILC1s, ILC2s, ILC3s) and lymphoid tissue inducer (LTi) cells (2). Innate immune cells lack antigen-specific receptors and their activation relies on recognition of soluble signals, such as alarmins that are released upon necrotic cell death, or molecular patterns, such as pathogen-associated molecular patterns (PAMPs), derived from invading pathogens, and damage-associated molecular patterns (DAMPs), derived from host cells (3). PAMPs and DAMPs are recognized by a variety of pattern recognition receptors (PRRs) expressed on immune cell surface (4). While innate immune cells keep the invading pathogens in check, they also propagate signals to activate adaptive immunity, which provides more robust and specialized protection in an antigen-specific manner.

#### **1.1.1.2 Adaptive immunity**

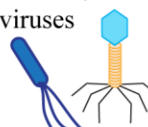


Adaptive immunity is evolutionarily recent, and it is seen in jawless fish (agnathans) and higher organisms (5). Adaptive immunity consists of T and B lymphocytes that have a large repertoire of antigen specific receptors generated by rearrangement of their receptor genes. T cells recognize a wide variety of antigens by T cell receptors (TCRs), while B cells use B cell

receptors (BCRs), membrane-bound immunoglobulins (Igs). Upon cross-linking of their receptors by cognate antigens, they undergo clonal expansion, providing a robust response to eliminate pathogens. Their antigen specificity relies on somatic diversification of the TCRs and BCRs by deoxyribonucleic acid (DNA) rearrangement of the genes encoding these receptors during their development (5). One of the most significant outcomes of the activation of adaptive immune system is the generation of immunological memory. Once activated by their cognate antigens, T and B cells are able to recall their previous encounter with these molecules and respond more quickly and efficiently upon secondary encounter.

In addition to TCRs, T cells express co-receptors cluster of differentiation (CD) 4 and CD8, which classify them into CD4<sup>+</sup> helper and CD8<sup>+</sup> cytotoxic T cells, respectively (6). CD8<sup>+</sup> T cells are activated upon antigen recognition in the context of the major histocompatibility complex (MHC) I molecule, while CD4<sup>+</sup> T cells recognize antigens associated with the MHCII (6). Depending on the cytokine milieu present in the microenvironment during their activation, CD4<sup>+</sup> T cells can be further differentiated into T helper type 1 (Th1), 2 (Th2), 17 (Th17) and regulatory T cells (Tregs).

### **1.1.2 Types of immunity**

Our immune system is constantly challenged by a variety of microorganisms and irritants and therefore, it is armed with different types of immune responses tailored to efficiently remove pathogens and provide maximum protection for the hosts. Based on the activation stimuli, types of immune cells involved and their effector functions, the cell-mediated immune response is classified into three major types: type 1, type 2 and type 3 immunity (Figure 1.1).

Immunity	Simuli	Innate	Effector molecules	Adaptive	Function	Pathology
Type 1	Intracellular bacteria, viruses 	NK T-bet EOMES ILC1 T-bet	IFN $\gamma$ TNF $\alpha$ Perforin Granzyme	CD8 <sup>+</sup> T T-bet EOMES Th1 T-bet	killing (perforin/granzyme)	auto-immunity, inflammation
Type 2	Helminth Allergens 	ILC2 GATA3 ROR $\alpha$	IL-4 IL-5 IL-13 IL-9 Areg	Th2 GATA3	-helminth/allergen expulsion -tissue repair	allergy, fibrosis
Type 3	Extracellular bacteria, fungi 	ILC3 ROR $\gamma$ t	IL-17 IL-22	Th17 ROR $\gamma$ t	-killing (antimicrobial molecules) -epithelial regeneration	auto-immunity, inflammation

**Figure 1.1: Types of immunity**

A summary figure of the types of immunity. Type 1 immunity is elicited by intracellular pathogens and involves NK cells, ILC1s, CD8<sup>+</sup> T cells and Th1 cells, which together produce IFN $\gamma$ , TNF $\alpha$ , perforin and granzyme. Overall, this results in elimination of pathogens by cytotoxicity. Type 2 immunity provides protection from helminth and allergens via ILC2s and Th2 cells, which secrete IL-4, IL-5, IL-13, IL-9 and Areg. Type 2 responses result in helminth/allergen expulsion but also in repair of damaged tissue. Type 3 immunity is mediated by ILC3s and Th17 cells, which secrete IL-17 and IL-22 to elicit killing of pathogens by antimicrobial peptides. IL-22 also promotes epithelial regeneration. Excessive amount of each type of immune response is associated with pathological conditions. Transcription factors expressed by each cell type is indicated at the centre of each cell. NK=natural killer, ILC=innate lymphoid cells, EOMES=Eomesodermin, GATA3=GATA binding protein 3, ROR=retinoic acid receptor-related orphan receptor, IFN=interferon, TNF=tumor necrosis factor, Areg=amphiregulin.

### 1.1.2.1 Type 1 immunity

Type 1 immunity provides protection against intracellular bacteria and viruses, and it is characterized by the presence of pro-inflammatory cytokines such as interferon (IFN)  $\gamma$  and tumor necrosis factor (TNF)  $\alpha$ . This type of immunity is mainly orchestrated by cytotoxic cells such as NK cells and CD8<sup>+</sup> T cells, and IFN $\gamma$ -producing ILC1s and Th1 cells.

Infection by intracellular microbes causes activation of NK cells and ILC1s. NK cells and ILC1s both highly express the transcription factor T-bet and require interleukin (IL) -15 for maintenance (7), while NK cells additionally express Eomesodermin (EOMES) (8). Although

they are phenotypically similar, expression of killer cell lectin like receptor G1 (KLRG1) and CD49b distinguishes NK cells from ILC1s, which express CD49a and CD200R (2,9).

Both NK cells and ILC1s have a series of activating and inhibitory receptors to regulate their activities upon recognition of the ligands expressed on target cells (10). Additionally, they can also be activated by cytokines IL-15, IL-12 and IL-18 (10). Upon activation, they produce IFN $\gamma$  (10), which together with IL-12 provided by activated APCs, create an environment that allow for activation of CD8<sup>+</sup> T cells and CD4<sup>+</sup> T cell differentiation towards Th1 (11), in the presence of antigens presented by APCs. Th1 cells and CD8<sup>+</sup> T cells mirror ILC1s and NK cells, respectively, in that the former is defined by T-bet, while the latter express both T-bet and EOMES (12–14). NK cells and CD8<sup>+</sup> T cells directly kill infected cells by their cytolytic activities mediated by granzyme and perforin, while ILC1s and Th1 cells release cytokines such as IFN $\gamma$  and TNF $\alpha$  (15). These pro-inflammatory cytokines induce macrophage differentiation into M1 cells (16), which produce anti-proliferative nitric oxide and citrulline, further promoting killing of invading pathogens (17).

Type 1 immune response is critical in providing protection from invasive pathogens such as viruses and bacteria. However, pro-inflammatory mediators secreted during type 1 immune responses can be destructive and detrimental to the host as exemplified by the development of pneumonia and respiratory failure during respiratory virus infections (18). Additionally, strong anti-viral immune responses mounted during hepatitis virus infections also result in inflammation and irreversible tissue damage (19). Dysregulated type 1 immunity can also result in disease conditions including some autoimmune diseases such as rheumatoid arthritis (RA) and multiple sclerosis (MS) (11). However, increasing numbers of reports indicate involvement of



IL-17 in these conditions, which suggest that they may also be mediated by type 3 immunity (20), which will be discussed in section 1.1.2.3.

#### **1.1.2.2 Type 2 immunity**

Type 2 immunity provides protection from parasitic infection and allergens. As parasites and allergens do not directly infect cells, type 2 immunity recognizes tissue damage caused by these seemingly unrelated antigens. Type 2 immune responses involve cytokines IL-4, IL-5, IL-13 and IL-9, and is mediated by ILC2s, Th2 cells and granulocytes.

Type 2 immunity is triggered upon release of alarmin cytokines such as IL-33, IL-25 and thymic stromal lymphopoietin (TSLP) from damaged epithelium (21). These cytokines potentially activate ILC2s, which produce IL-5, IL-13, IL-9 and amphiregulin (Areg) (22–28), providing cues for CD4<sup>+</sup> T cells to differentiate into Th2 cells upon antigen recognition.

IL-4 is thought to be a critical cytokine for Th2 differentiation as it induces GATA binding protein 3 (GATA3) expression, which is essential for type 2 polarization (29). In contrast, we have previously shown, in an allergen-induced lung inflammation model, that IL-4 is dispensable, while ILC2-derived IL-13 is required for Th2 differentiation (30). Upon differentiation, GATA3 induces production of IL-4, IL-5 and IL-13 from Th2 cells, further amplifying the signals to activate downstream effector cells (31–33).

IL-5 induces recruitment of eosinophils, which release their cytoplasmic granular contents including cytotoxic proteins (34). IL-13 stimulates goblet cells to produce mucus (35), which interferes with the ability of worm to establish contacts with the host (36) or facilitates clearance of aeroallergens (37). IL-4 and IL-13 are essential for B cell class switch to IgE type (38,39), which activates basophils and mast cells upon cross linking of the high affinity-receptor FcεRI

expressed on their cell surface (40). IL-9 provides additional survival and activation signals to mast cells (41,42). Basophils and mast cells, in turn, undergo degranulation to release cytokines, enzymes and lipid mediators that result in vascular permeability and smooth muscle constriction (21).

The cytokines produced during activation of type 2 cells also cause macrophage polarization towards an M2 phenotype (43,44). M2 macrophages specialize in wound healing/growth promotion, which is mediated by arginine metabolism skewed to ornithine and polyamines production, promoting cell proliferation and tissue repair (17,45). ILC2-derived Areg also promotes tissue remodeling and wound healing (28). These responses orchestrated by various cell types together result in expulsion of parasites or allergens and repair of tissue damage.

Type 2 immunity is critical for protection against parasites and its role in wound healing is essential to maintain barrier integrity. However, excessive type 2 immune response can also be pathogenic. For example, excessive tissue remodeling and extracellular matrix (ECM) deposition can lead to fibrosis (46), while repeated exposure to environmental allergens can result in allergic diseases including atopic dermatitis (AD) and asthma (11).

### **1.1.2.3 Type 3 immunity**

A type 3 immune response is mounted upon invasion by extracellular bacteria and fungi. This type of protection is characterized by the presence of cytokines IL-17 and IL-22 and provided by ILC3s, Th17 cells and neutrophils.

When phagocytes are stimulated by invading extracellular bacteria or fungi through their PRRs, they produce IL-1 $\beta$  and IL-23, which activate ILC3s (47). Although there are various

subsets among ILC3s, they are defined by their retinoic acid receptor-related orphan receptor (ROR)  $\gamma$ t expression and they exert their functions by production of IL-17 and/or IL-22 (47).

In parallel, naïve T cells undergo differentiation towards Th17 cells upon antigen recognition. T cell differentiation into IL-17<sup>+</sup> type is complex, orchestrated by multiple cytokines, each playing important roles at different stages. IL-6 and transforming growth factor (TGF)  $\beta$  together upregulate expression of ROR $\gamma$ t (48), which is the master regulator critical for Th17 differentiation (49). IL-6 induces IL-23R expression on Th17 cells through IL-21, sensitizing them towards IL-23 signaling (50). IL-23 signaling, in turn, sustains Th17 phenotype (51). Like ILC3s, Th17 cells also produce type 3 cytokines, IL-17 and IL-22 (50).

The protective effect of type 3 immunity is exerted by IL-17, which is a key cytokine for recruitment of neutrophils by inducing production of neutrophil chemoattractants from stromal cells (52,53). Neutrophils discharge the contents of their granules, which contain antimicrobial molecules and enzymes such as lysozyme, defensin and myeloperoxidase, killing pathogens (54). Additionally, IL-22 is also important for antimicrobial defense (53) and promotes proliferation of epithelial cells (55), contributing to tissue regeneration.

Dysregulated type 3 immunity is also detected in autoimmune diseases including RA, MS, and psoriasis (20). Traditionally, they were considered to be type 1 immune diseases due to the involvement of IFN $\gamma$ , but the pathologic roles of IL-17 have been recognized with the discovery of Th17 cells. The immune profile of these diseases is much more complicated than initially thought, and significant contribution of both types of immunity is becoming evident (20). In addition to autoimmune diseases, excessive type 3 immunity also results in chronic inflammatory conditions as seen in inflammatory bowel disease and neutrophilic asthma (56).

## 1.2 ILC2

### 1.2.1 Discovery and characterization

The research on parasitic immunity and allergic inflammation had heavily focused on Th2 cells and B cells, as they were believed to be the major sources of type 2 cytokines IL-4, IL-5 and IL-13, and IgE, which are key mediators of type 2 immunity. Therefore, the innate sources of type 2 cytokines went unrecognized for a long time. However, the existence of innate type 2 cells was brought to light together with the discovery of an epithelium-derived cytokine, IL-25. The presence of ILC2-like cells were first reported in recombination activating gene (Rag) knock out (KO) mice, which lack T and B cells, as non-T non-B cells that produce type 2 cytokines, IL-4, IL-5 and IL-13, upon stimulation with IL-25 were observed (57–59). A few years later in 2010, a series of articles were published, identifying populations of type 2 cytokine-producing cells devoid of lineage markers in mesenteric fat-associated lymphoid clusters (FALC) (22), mesenteric lymph node (mLN) and intestine (23), and multiple tissues including mLN, liver, lung and spleen (24), which were termed “natural helper cells”, “nuocytes” and “Ih2 cells”, respectively. They lacked markers commonly expressed by T, B, and myeloid cells, such as CD3 $\epsilon$ , CD4, CD8 $\alpha$ , TCR $\beta$ , TCR $\gamma\delta$ , CD5, CD19, B220, NK1.1, Ter119, Gr-1, CD11b, CD11c and Fc $\epsilon$ R1 $\alpha$  (Lin<sup>-</sup>) and potently produced IL-5 and IL-13 upon stimulation with IL-25 and/or IL-33 or helminth infection. The past 10 years of efforts in studying mouse and human tissues have identified similar cells in various mucosal and non-mucosal tissues including the lung (28,60,61), skin (62–64), liver (65), adipose tissues (66–68), pancreas (69) and heart (70,71). In 2013, a group of researchers proposed unification of their nomenclature and these cells are now called group 2 innate lymphoid cells or ILC2s (72).

ILC2s in mouse tissues express CD45, a pan-leukocyte marker, IL-7R $\alpha$  (CD127), CD90 (Thy1), IL-2R $\alpha$  (CD25) and inducible costimulator (ICOS) (22–24,26,28,61–63,65–69,71), while expression of IL-25R and T1/ST2 (IL-33R) varies depending on the tissues. T1/ST2 is expressed by lung (28,61), liver (65) and fat ILC2s (66–68), while its expression is low in small intestine (SI) ILC2s (73) and varies in the skin (62,73,74). IL-25R is highly expressed by SI ILC2s (75) and approximately 60% of liver ILC2s (unpublished data). Both IL-25R positive and low/negative ILC2s have been reported in the skin (64,74,75), while adipose tissue ILC2s do not express IL-25R (74). In the lung, while naïve ILC2s have low expression of IL-25R, its expression is induced by activation and remains high for a long time after activation (76). Skin ILC2s uniquely express CD103 (64), and more recently, Ricardo-Gonzalez et al. demonstrated tissue specific expression of IL-18R by skin ILC2s (74). The presence of a similar IL-18R<sup>+</sup> subset has also been described in the lung, although it is likely a progenitor rather than mature ILC2 population (77). KLRG1 was identified as a reliable marker for SI ILC2s (78) and its expression was also detected in the skin (79) and adipose tissue ILC2s (66,68). However, in our hands, less than 50% of naïve lung and liver ILC2s express KLRG1 (unpublished data).

ILC2s have also been identified in human tissues including the fetal and adult intestine (25,80), lung (25,28,80), blood (25,80), nasal tissue (25), liver (81,82), skin (62,63), cord blood (80), tonsil (80) and adipose tissue (67). Human ILC2s are phenotypically similar to mouse ILC2s, but chemoattractant receptor-homologous molecule expressed on Th2 cells (CRTH2) and CD161 are specifically used for identification of human ILC2s in various tissues (25).

The majority of ILC2s seed tissues early after birth (83–85) and remain largely tissue resident onward (86), thus adopting a tissue-specific phenotype depending on the environmental cues they receive in their resident organs (74,87). Therefore, identification of ILC2s has been

challenging due to a lack of universal markers for ILC2s and the use of a combination of surface markers is necessary. Moreover, some of the surface markers are downregulated or upregulated upon ILC2 activation, making it difficult to definitively identify these cells. However, the transcription factor GATA3 is highly and stably expressed by ILC2s in mouse and human (78,88), suggesting that it is a useful marker for ILC2 identification. The markers identified in ILC2s are summarized in Table 1.1.

	Lung	Intestine	Mouse Skin	Liver	Fat	Human
<b>CD127</b>	+	+	+	+	+	+
<b>Thy1</b>	+	+	+	+	+	N/D
<b>CD25</b>	+	+	+	+	+	+
<b>ST2</b>	+	low	+/low	+	+	+/-
<b>IL25R</b>	low	+	+/low	+	low	+
<b>ICOS</b>	+	+	+	+	+	+
<b>CD103</b>	-	N/D	+	-	N/D	-
<b>C-kit</b>	+	+/low	low	N/D	+	+/-
<b>Sca-1</b>	+	+	var	+	+	N/D
<b>IL-18R</b>	-	-	+	-	-	+
<b>KLRG1</b>	low	+	+	low	+	+
<b>CRTH2*</b>						+
<b>CD161*</b>						+
<b>GATA3</b>	+	+	+	+	+	+

**Table 1.1: Summary of ILC2 phenotype in different tissues**

A comprehensive table showing common markers used to identify ILC2s. N/D=not determined. \*human ILC2 markers. Human markers are indicated as + if they have been identified in at least 1 organ.

## 1.2.2 Development

ILC development is finely regulated by a series of transcription factors that are expressed at various developmental stages. ILC2s are believed to develop from common lymphoid progenitors (CLPs), which are a progenitor population committed to lymphoid lineage (7,89,90). In contrast, we have previously reported that an upstream progenitor population, termed CD127<sup>+</sup> lymphoid-primed multipotent progenitor (LMPP), is the major producer of ILC2s, particularly

during the neonatal period when CLPs are barely detected (91). Similarly, various progenitors of ILCs have been described in adult BM, but the exact developmental relationship between them is unclear. A progenitor population that expresses the transcription factors nuclear factor, interleukin 3 regulated (NFIL3), thymocyte selection-associated high mobility group box protein (TOX), and  $\alpha 4\beta 7$  integrin (ITG), termed  $\alpha$  lymphoid progenitor ( $\alpha$ -LP) have potential to give rise to T cells and all ILCs, including NK cells (92,93). A similar population termed early innate lymphoid progenitor (EILP), which highly expresses the transcription factor T cell factor (TCF) 1 has also been described (94). EILPs, similar to  $\alpha$ -LPs, do not efficiently generate adaptive T and B cells, but give rise to all ILCs including NK cells (94). A common helper ILC progenitor, or CHILP, which is dependent on inhibitor of DNA binding 2 (ID2), is likely a further downstream progenitor as CHILPs lack potential to efficiently generate NK cells but give rise to helper ILCs and LT<sub>i</sub> cells (7,94). CHILPs contain two populations with respect to the expression of the transcription factor promyelocytic leukemia zinc finger protein (PLZF). PLZF<sup>+</sup> population, termed ILC precursor (ILCP), is a more restricted ILC progenitor, which can generate all helper ILC subsets, but not NK or LT<sub>i</sub> cells (89). This population is also identified by the expression of programmed cell death protein 1 (PD-1), an immune checkpoint molecule, although PD-1 is not required for ILC development (95,96). It was recently shown, however, that both ID2<sup>+</sup> and PLZF<sup>+</sup> progenitors retain NK cell potential, suggesting that CHILPs and ILCPs may not be as committed to helper ILC lineage as they were considered to be (97).

The transcription factors GATA3 (78,98) and ROR $\alpha$  (60,99) are considered to be important for ILCP lineage commitment to type 2 ILCs as they are required for the development of ILC2s. However, GATA3 was later found to be required for development of all IL-7R $\alpha$ <sup>+</sup> ILCs (100,101), while ROR $\alpha$  also seems to be expressed in some other ILC populations (77,78). More

recently, B-cell leukemia 11b (BCL11b) was identified as a specific marker of ILC2 fate determination as it is required for the development of ILC2 precursor (ILC2P) ( $\text{Lin}^- \text{CD127}^+ \text{Sca1}^+ \text{CD25}^+ \alpha 4\beta 7^+$ ) in the bone marrow (BM) after ILCP stage and maintained in mature ILC2s in the periphery (95,101–104).

While transcription factors regulate fate decisions during lymphopoiesis, ILC2 development also depends on cytokine signaling. ILC2s are absent in *Il2rg*<sup>-/-</sup> (22) and *Il7*<sup>-/-</sup> mice (22), while their number is significantly reduced in *Il7ra*<sup>-/-</sup> mice (99,105), indicating the requirement of signaling provided by these cytokines and cytokine receptors. More recently, it was also reported that ILC2 development was impaired in mice deficient in an adhesion molecule, intercellular adhesion molecule (ICAM) -1 (106), suggesting that ILC2-poiesis may also require cell-cell contact.

### 1.2.3 Activation

ILC2s play central roles in initiation of type 2 immunity. While they are crucial for providing protection from helminth infections, excessive activation of ILC2s can be pathogenic as seen in allergic diseases and fibrosis. Therefore, proper regulation of ILC2s is critical in order to achieve benefits without having disease consequences. As ILC2s lack antigen-specific receptors, ILC2s integrate extrinsic and intrinsic signals provided by small molecules such as cytokines, lipid mediators and hormones and cell-cell interactions (Figure 1.2).



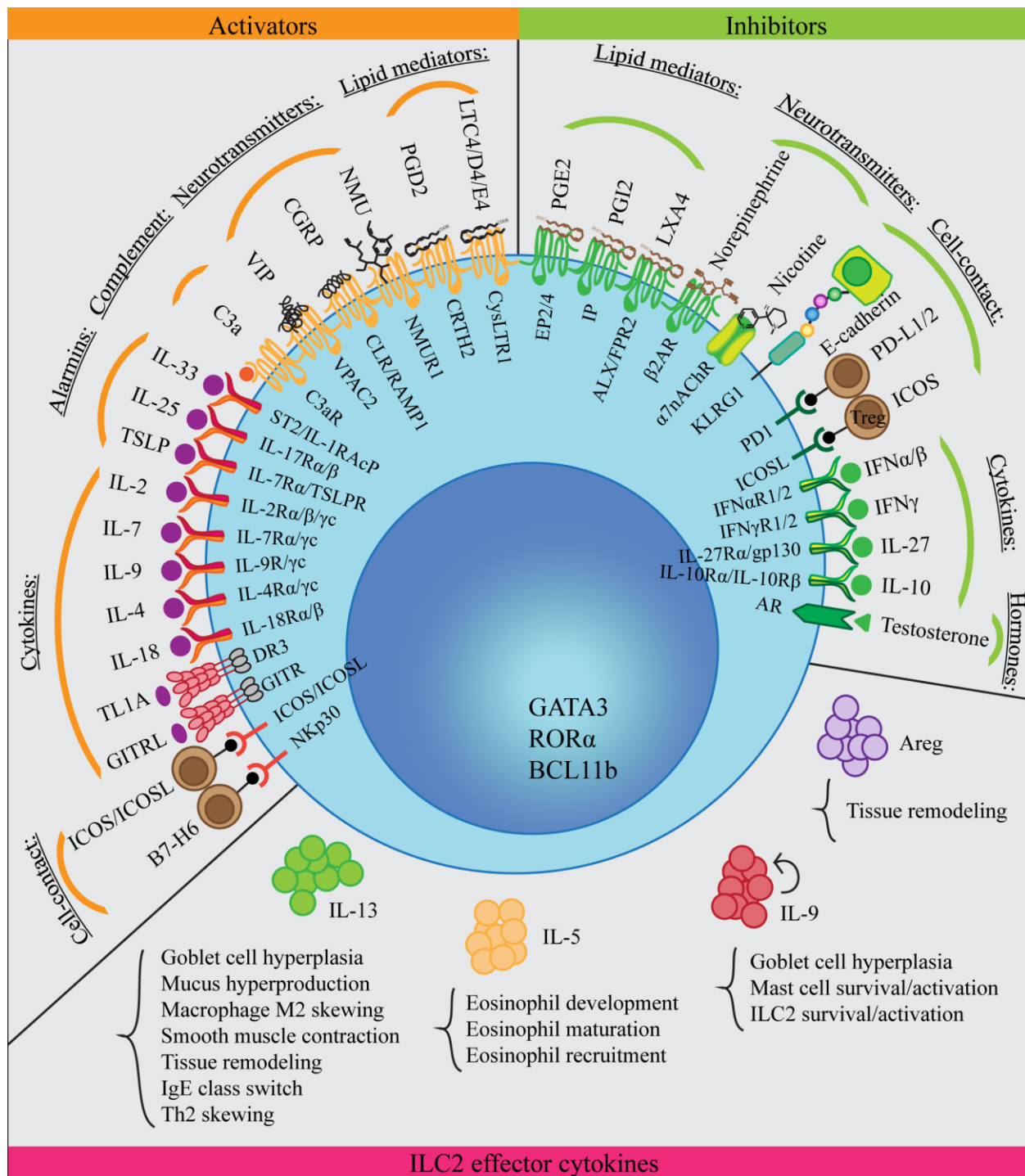


**Figure 1.2: ILC2 regulatory network and effector functions**

A figure showing positive and negative regulators and effector functions of ILC2s. Activators and inhibitors are labeled outside of the cell, while signaling receptors are indicated inside of the cell. LT=leukotriene, CysLTR=cysteinyl leukotriene receptor, PG=prostaglandin, CRTH2=chemoattractant receptor-homologous molecule expressed on Th2 cells, NMU=neuromedin U, CGRP=calcitonin gene-related peptide, CLR/RAMP=calcitonin receptor-like receptor/receptor activity-modifying protein 1, VIP=vasoactive intestinal

peptide, IL-1RAcP=interleukin 1 receptor accessory protein, TSLP=thymic stromal lymphopoietin,  $\gamma$ c=common  $\gamma$  chain, TL1A=tumor necrosis factor-like cytokine 1A, DR3=death receptor 3, GITR=glucocorticoid-induced tumor necrosis factor receptor, ICOS=inducible costimulator, IP=prostacyclin receptor, LXA4=lipoxin A4, ALX/FPR2=A lipoxin and formyl peptide receptor 2,  $\beta$ 2AR= $\beta$ 2 adrenergic receptor,  $\alpha$ 7nAChR= $\alpha$ 7 nicotinic acetylcholine receptor, KLRG1=killer cell lectin like receptor G1, PD=programmed cell death protein 1, IFN=interferon, AR=androgen receptor.

### 1.2.3.1 IL-33

IL-33 is an IL-1 family of cytokine together with IL-1 $\alpha$ , IL-1 $\beta$  and IL-18 (107). IL-33 is constitutively expressed in the nuclei of endothelial cells (108–110), epithelial cells, fibroblastic reticular cells (109,111) and adventitial stromal cells (112). IL-33 lacks a sequence necessary for secretion and trafficking through endoplasmic reticulum and Golgi (113), and therefore is released upon cellular injury or during necrosis (109,111,114,115). Similar to IL-1 $\alpha$ , IL-33 has a nuclear localization sequence, which allows it to interact with chromatin, preventing unnecessary release of this cytokine (107,116). IL-33 in its full length precursor form is already biologically active, and it is inactivated upon cleavage by caspase-1 (117). Interestingly, cleavage of full length IL-33 by inflammatory proteases, such as neutrophil cathepsin G and elastase, or mast cell chymase and tryptase, results in generation of a mature form of IL-33 protein, which has a 10-30 fold higher activity compared to the full length IL-33 (115,118).

IL-33 binds to a receptor consisting of T1/ST2 and IL-1 receptor accessory protein (IL-1RAcP) (119), which induces intracellular signaling through an adaptor protein myeloid differentiation primary response 88 (MyD88), interleukin-1 receptor-associated kinase (IRAK) 1/4, tumor necrosis factor receptor-associated factor 6 (TRAF6), nuclear factor (NF)  $\kappa$ B and mitogen-activated protein kinases (MAPK) (120). This results in phosphorylation of GATA3, promoting its binding to *Il5* and *Il13* promoter and regulating proliferation of ILC2s (121).

We have previously demonstrated that ILC2 activation induced by papain, a protease allergen known to cause airway inflammation, is significantly reduced in *Il33*<sup>-/-</sup> mice, indicating that IL-33 is necessary for ILC2 activation (30). While intranasal (i.n.) IL-33 administration into mice potently activates ILC2s in vivo (76), we and others have also found that IL-33 is not sufficient to stimulate ILC2s in vitro as activation of ILC2s by IL-33 requires a secondary signal provided by co-stimulatory cytokines (25,26).

### 1.2.3.2 IL-25

IL-25, also known as IL-17E, belongs to the IL-17 family of cytokines that consist of IL-17A-F (122). IL-25 is constitutively expressed in tuft cells, chemosensory cells in the lining of the intestinal epithelium (123), but it is also expressed in immune cells, including Th2 cells (57), alveolar macrophages (124), mast cells (125), basophils and eosinophils (126) upon stimulation. ILC2s in some organs including the mLN, spleen and liver greatly expand upon intraperitoneal (i.p.) IL-25 treatment (23,24). In the SI, IL-25 deficiency causes significant reduction in the frequency of ILC2s in steady state and after worm infection, suggesting an important role in ILC2 maintenance (123). Although IL-25 induces a mild increase in ILC2s in the lung upon in vivo administration via i.n. route, it is not as potent as IL-33 in activating naïve ILC2s because expression of IL-25R is low in lung ILC2s (76,127,128). However, we have previously shown that when ILC2s acquire memory-like properties after primary stimulation by allergens or IL-33, they become responsive to IL-25 in vivo (76). Interestingly, KO studies showed that in BALB/c mice, IL-25, together with IL-33, is the predominant cytokine in activating skin ILC2s (63). However, like IL-33, optimal stimulation of ILC2s with IL-25 in vitro requires a secondary cytokine (22,63).

More recently, Huang et al. described a population of ILC2-like cells that are induced in the lung, liver, mLN and spleen after i.p. injections of IL-25 (129). These cells, termed inflammatory ILC2s (iILC2s), are KLRG1<sup>+</sup> ST2<sup>lo</sup> and upon activation, migrate from the intestine to peripheral tissues through lymphatics in an sphingosine-1-phosphate (S1P) dependent manner (129,130). IL-25 is the major cytokine in activating this subset of ILC2s as they do not respond to IL-33 and they are largely absent in IL-25R deficient mice upon i.p. IL-25 treatment (129).

Although IL-25 signaling is not extensively studied in ILC2s, it has been shown that IL-25 binds to a receptor consisting of IL-17RA and IL-17RB, which, similar to IL-33, activates NFκB and MAPK signaling pathway through an adaptor protein Act 1 and TRAF6 (122). This signaling results in phosphorylation of GATA3 in ILC2s (121), inducing production of type 2 cytokines.

### **1.2.3.3 TSLP**

TSLP is an IL-2 family of cytokine and the signaling is initiated upon its binding to the receptor comprised of IL-7Rα and TSLPR (131). The signaling induces phosphorylation of signal transducer and activator of transcription (STAT) 5 through Janus kinase (JAK) 1/2, which are associated with IL-7Rα and TSLPR, respectively (132). STAT5 activates GATA3, which, in turn, activates ILC2s (133). In the lung, TSLP alone does not induce activation of ILC2s, while a small amount of TSLP synergistically stimulates ILC2s together with IL-33 (26,134). It has also been shown to be the only epithelial cytokine that promotes survival of human ILC2s in culture when given alone, and greatly enhances viability of ILC2s when given together with other cytokines (135). Interestingly, studies with IL-33 or IL-33R KO, IL-25R KO and TSLPR KO mice showed that it is the predominant cytokine in activating C57BL/6 mouse skin ILC2s

(62,63). However, a follow-up report showed that skin ILC2 proliferation required IL-4 produced by basophils, which are stimulated by TSLP, and thus, the effect of TSLP may be indirect (79).

TSLP is expressed by epithelial cells in the lung, such as alveolar type II cells, intestinal epithelial cells, and inflamed tonsils (134,136–138). TSLP is highly detectable in keratinocytes of AD patients, while it is undetectable in normal skin, indicating its involvement in the development of allergic inflammation in the skin (136).

#### **1.2.3.4 Co-stimulatory cytokines**

Many of the co-stimulatory cytokines including IL-2, IL-9, IL-7 and IL-4 belong to the common gamma chain ( $\gamma_c$ ) family of cytokines. These cytokines signal through receptors comprised of the shared  $\gamma_c$ , also known as IL-2R $\gamma$  (CD132) and a cytokine specific receptor component.

IL-2, a cytokine primarily produced by activated CD4<sup>+</sup> T cells (139), binds to IL-2 receptor complex, which consists of three subunits, IL-2R $\alpha$  (CD25), IL-2R $\beta$  (CD122) and  $\gamma_c$ . ILC2s consistently express CD25 (22,26,61–64,66,67) and low levels of CD122 (66,105) and therefore, IL-2 stimulation enhances survival and proliferation of ILC2s (140). IL-2 by itself only causes slow proliferation of ILC2s, but together with IL-33 and IL-25, it can greatly enhance ILC2 in vitro survival and cytokine production (140).

IL-9R is expressed on ILC2s at the transcript (24,78) and protein (27) levels. This receptor forms a receptor complex with  $\gamma_c$  (141). Wilhelm et al. demonstrated that in vitro and in vivo stimulation of ILC2s with IL-9 enhances ILC2 production of IL-5 and IL-13 (27). Interestingly, ILC2s themselves transiently produce IL-9 early during papain-induced airway inflammation,

suggesting an autocrine feedback mechanism (27). This is further supported by reduced IL-5 and/or IL-13 production in IL-9 deficient mice during chitin stimulation and *Nippostrongylus brasiliensis* (*N. brasiliensis*) infection (134), and decreased ILC2 numbers as well as type 2 cytokine production in IL-9R deficient mice during *N. brasiliensis* infection (142).

IL-7 is primarily produced by radioresistant non-hematopoietic cells (143) including BM and thymic stromal cells (144,145) and thymic epithelial cells (145) and play critical roles in the development of lymphocytes (146). However, it can also be induced in peripheral tissues including the lung (epithelial cells) (147), skin (keratinocytes) (148), intestine (epithelial cells) (149) and liver (hepatocytes) (150), where ILC2s reside. IL-7 receptor is formed by  $\gamma_c$  and IL-7R $\alpha$ , which is also shared with the TSLP receptor complex. Although IL-7 by itself does not support proliferation or activation of ILC2s (22,23,140), it induces slow proliferation of ILC2s together with IL-25 and potent expansion and activation of ILC2s with IL-33 in vitro (23,26,134,140).

IL-4 signals through the IL-4 receptor consisting of  $\gamma_c$  and IL-4R $\alpha$ , which is also shared by the IL-13 receptor complex (151). Kim et al. demonstrated that IL-4 derived from basophils is critical for skin ILC2 proliferation (79), while Motomura et al. used papain-induced airway inflammation model to demonstrate that basophil-derived IL-4 is required for expansion of ILC2s and induction of eosinophilia (152). ILC2s constitutively express IL-4R $\alpha$  and short-term culture of lung ILC2s with IL-4 alone induces production of small amount of IL-13, but very little IL-5. Interestingly, neither IL-33 nor IL-2 enhances IL-4-induced IL-13 production, while IL-33 and IL-4 synergistically stimulate IL-5 production (152), implying differential regulation of these two cytokines by IL-4. In humans, IL-4 is critical to induce maximum proliferation and activation of ILC2s isolated from peripheral blood (PB) upon stimulation by IL-33 (153).

More recently, human PB ILC2s (80), mouse skin (74) and some lung (74,77) ILC2s have been reported to express IL-18R $\alpha$ , which forms IL-18 receptor complex together with IL-18R $\beta$  (154). IL-18 is not as potent as IL-33, as only small amounts of type 2 cytokines are produced by mouse ILC2s in vitro (74) or in vivo (77) upon IL-18 stimulation. However, IL-18-mediated ILC2 activation play important roles in a mouse model of AD, as IL-18 deficient mice have reduced inflammation (74). Human ILC2s, on the other hand, respond to IL-18 + IL-7 stimulation by potently producing cytokines (80), suggesting more essential involvement of this cytokine in human ILC2 biology. Of note, activation of ILC2s by IL-18 is independent of epithelial cytokine signaling, as ILC2s from TLSPR, IL-33R and IL-25 triple KO mice still respond to IL-18 stimulation in a similar way as wild type (WT) mice (74).

TNF superfamily (TNFSF) of cytokines, which includes TNF-like ligand 1A (TL1A or TNFSF15) and glucocorticoid-induced tumor necrosis factor receptor ligand (GITRL or TNFSF18) also act as co-stimulators for ILC2s. This family of cytokines regulates cell proliferation, differentiation, survival, and apoptosis (155). TL1A is produced by activated myeloid cells, epithelial cells and endothelial cells (156). It signals through death receptor 3 (DR3), which is expressed by human PB and mouse mLN, lung, intestine and BM ILC2s (157,158). TL1A alone stimulates mouse and human ILC2s in vitro, but its effect is enhanced in the presence of IL-25, IL-33 or IL-7 (157,158). In contrast, its role on ILC2 activation in vivo is controversial. While Yu et al. reported positive regulatory effects of TL1A by i.p. injections of TL1A and its requirement for mounting proper immunity against *N. brasiliensis* infection using *Dr3*<sup>-/-</sup> mice, Meylan et al. did not observe any effects (157,158). Interestingly, both groups showed reduced ILC2-mediated type 2 inflammation in *Dr3*<sup>-/-</sup> compared to WT mice during papain-induced airway inflammation, suggesting tissue-specific requirement of TL1A. The effect

of TL1A on ILC2s was independent of IL-25 or IL-33 as similar activation of ILC2s occurred in *Il17rb<sup>-/-</sup>* and *ST2<sup>-/-</sup>* mice compared to WT mice upon i.p. TL1A treatment (157).

GITRL, also known as TNFSF18, is another TNFSF cytokine which is induced in some myeloid cells, T and B cells and endothelial cells during inflammation (159). The receptor of GITRL, GITR, is expressed on human and mouse ILC2s (160–162). Engagement of GITR by GITR agonist potently induces type 2 cytokine production from activated, but not naïve adipose tissue ILC2s in vitro (161). Studies with GITR deficient mice and blockade of GITR signaling demonstrated ILC2 activating role of this cytokine during lung inflammation (160). Furthermore, in the context of metabolic syndrome, GITR agonist treatment results in ILC2 expansion and activation in mice fed high fat diet, improving glucose homeostasis and preventing obesity (161).

#### **1.2.3.5 Lipid mediators**

Eicosanoids such as leukotrienes (LTs) and prostaglandins (PGs) are lipid signaling molecules derived from arachidonic acids. These immune-regulatory lipid mediators are potently produced by innate immune cells including mast cells and basophils, and signal through G protein-coupled receptors (GPCRs) (163,164). Various LTs and PGs activate or suppress mouse and human ILC2s. Here, ILC2 activating eicosanoids will be discussed, while inhibitory molecules will be introduced later in section 1.2.4.2.

I.n. administration of *Alternaria alternata* (*A. alternata*) into mouse induces expression of cysteine containing LTs, or cysteinyl (Cys) LTs (LTC<sub>4</sub>, LTD<sub>4</sub> and LTE<sub>4</sub>), in bronchoalveolar lavage fluid (BALF) (165), while helminth infection causes production of CysLTs from tuft cells in the SI (166). ILC2s highly express the LT receptors *Cystltr1* and *Ltb4r1*, and LTB<sub>4</sub>, LTC<sub>4</sub>, LTD<sub>4</sub>, and LTE<sub>4</sub> directly activate ILC2s in vitro (166–168), whereas i.n. administration of



LTC4 or LTD4 enhances *A. alternata* or IL-33 induced airway inflammation, respectively (165,168).

LTC4 is the most robust stimulator of ILC2 activation, followed by LTD4, while LTB4 and LTE4 are less potent (166,167). LTC4 and D4 signaling depends on the receptor CysLTR1, while LTB4R1 is necessary for optimal LTB4 signaling (165,167,168). Deficiency of individual LT signaling only causes mild reduction in ILC2 numbers and activation in vivo, suggesting that various LTs contribute together in ILC2 activation (167). Interestingly, deficiencies in IL-33 or LT signaling show similar impairment of type 2 inflammation in vivo, demonstrating their non-redundancy, most likely due to differences in their signaling pathways (167). While both IL-33 and LTD4 induce similar levels of IL-5 and IL-13 production from ILC2s purified from *A. alternata* treated lungs, only LTD4, but not IL-33, induces IL-4 production from ILC2s (165), further supporting distinct signaling pathways of ILC2 activation by these molecules. The kinetics of ILC2 activation by LTC4 and IL-33 also differs, where LTC4 potently stimulates ILC2 cytokine production at an early stage of activation, whereas IL-33 becomes more potent at later time points (167).

Human ILC2s also express LT receptor CysLTR1 and it is significantly upregulated in AD patients (169). LTC4, LTD4 and LTE4 do not only enhance ILC2 cytokine production, but also induce migration of ILC2s towards their gradient. LTE4 is the most potent LT in inducing migration of human ILC2s and this effect is highly enhanced by PGD2, but not by epithelium-derived cytokines such as IL-33, IL-25 or TSLP (169).

PGD2 is mainly produced by mast cells (170) and known to be abundantly present in asthmatic patients' airways (171). It signals through D prostanoid receptor (DP) 1 and DP2, also known as CRTH2 (171), which is expressed on human ILC2s (25). Mouse lung ILC2s have low

expression of *Gpr44*, which encodes CRTH2, and accordingly, PGD2 alone or in combination with epithelial cytokines do not cause activation or chemotaxis in vitro (172). However, ILC2s in the periphery express *Gpr44* and PGD2 induces their chemotaxis (172). Moreover, PGD2 receptor deficiency (*Gpr44*<sup>-/-</sup>) results in impaired ILC2 recruitment to the lung during helminth infection (172), suggesting its potential ILC2 regulatory activity.

In humans, PGD2 alone potently promotes ILC2 chemotaxis and stimulates type 2 cytokine production from PB and skin ILC2s in vitro (173,174). PB ILC2s of atopic patients have increased migratory ability towards PGD2 compared to ILC2s from healthy donors (175). PGD2 treatment induces upregulation of IL-33R and IL-25R, but downregulation of CRTH2 (173), suggesting a key role of PGD2 in human ILC2 regulation.

#### **1.2.3.6 Neurotransmitters**

Lymphoid organs and mucosal tissues are highly innervated and consequently, immune system is systemically and locally regulated by central and peripheral nervous systems (176). ILC2 research in recent years has revealed that ILC2s are not an exception. ILC2 activating neurotransmitters are introduced here and inhibitory neurotransmitters will be discussed in section 1.2.4.3.

In 2017, three papers were published in Nature around the same time, reporting regulation of ILC2s by neuromedin U (NMU) (177–179). NMU is a neuropeptide that regulates many different processes including muscle contraction, blood pressure and blood flow regulation, but it is also a known immune modulator (180). Mouse and human ILC2s express one of the NMU receptors, NMUR1, while NMUR2 expression is undetectable (177–179). NMU is expressed by cholinergic neurons, where ILC2s closely localize (177,179). While NMU induces only mild

upregulation of *Il5* and *Il13* in cultured lung ILC2s, co-treatment with IL-25 potentiates expression of these cytokines (178). Co-administration of NMU and IL-25 in vivo results in lung inflammation characterized by eosinophilia and airway hyperreactivity, while its effect is less potent in combination with IL-33 (178). In contrast, intestinal ILC2s respond potently to in vitro stimulation with NMU, which stimulates proliferation of ILC2s in an NMUR1 dependent manner (177,179). NMU also activates ILC2s and promotes efficient worm expulsion early during helminth infection (177,179). Treatment of neuron organoid cultures with IL-33 or *N. brasiliensis* secretory products induces *Nmu* expression, and i.n. administration of the culture supernatant causes ILC2 activation (179). This suggests an elegant neuron-immune crosstalk, where neuron cells efficiently sense and respond to alarmins or PAMPs by producing NMU, which in turn stimulates ILC2s to mount proper immune responses against allergens or helminths.

Calcitonin gene-related peptide (CGRP) is a neurotransmitter produced by pulmonary neuroendocrine cells (PNECs), which comprise airway epithelium (181). CGRP signals through a receptor complex consisting of a GPCR known as calcitonin receptor-like receptor (CLR) and receptor activity modifying protein (RAMP) 1 (182). ILC2s localize in the vicinity of PNECs and in vitro stimulation with CGRP synergistically activates ILC2s in the presence of IL-33 or IL-25 and IL-7 (183). In line with this, deficiency in CGRP signaling impairs eosinophilia and type 2 inflammation in the lung, which can be restored by administration of CGRP together with  $\gamma$ -aminobutyric acid (GABA), another product of PNECs (183).

Although only limited studies exist, vasoactive intestinal peptide (VIP), a neuropeptide widely expressed in the nervous system, also positively regulates ILC2s (184,185). VIP preferentially signals through VPAC1 and VPAC2, which are GPCRs, and regulates hormone

release, metabolism, immune responses and circadian rhythms (186). VIP is elevated in BALF of mice treated with ovalbumin (OVA), indicating that VIP may be released during inflammation (185). Both lung and intestinal ILC2s express VPAC1 and VPAC2, and VIP or VPAC2 agonist potently induces IL-5 production in the presence of IL-7 in vitro (184). VPAC2 blockade inhibits activation, but not expansion of ILC2s in vivo, while VPAC1 antagonist does not have any effect, suggesting that VPAC2 is likely the main receptor (185).

#### **1.2.3.7 Other molecules**

C3a, which is released upon activation of the complement pathway during inflammation, is elevated in BALF of house dust mite (HDM) treated mice. C3a does not only stimulate activation of ILC2s in vitro and enhance airway inflammation in vivo, but its signaling through the receptor C3aR is required for optimal airway inflammation. Interestingly, ILC2s produce C3a upon IL-33 stimulation, suggesting that C3a may regulate ILC2s in an autocrine manner (187).

#### **1.2.3.8 Cell-cell interactions**

ICOS is one of the markers used to identify ILC2s. ICOS deficiency or disruption of ICOS-ICOS ligand (ICOSL) interaction impairs ILC2-mediated airway inflammation by inhibiting ILC2 expansion and activation, in a cell-contact dependent manner (162,188). ICOS most likely provides survival signals through regulation of IL-2 signaling and apoptosis (188). ILC2s also express ICOSL and interact with each other to promote survival (188).

Human PB ILC2s express NKp30 and its engagement with its ligand B7-H6 induces IL-13 production in a cell-contact dependent manner (189). NKp30 is highly expressed by ILC2s in acute promyelocytic leukemia (APL) patients and B7-H6 is highly expressed by primary APL

blasts and APL cell lines (190). Stimulation of ILC2s with APL cell lines induces ILC2 production of IL-13, which in turn, activates myeloid-derived suppressor cells (MDSCs), generating immunosuppressive microenvironment (190). NKp30-mediated stimulation may also play roles in atopic diseases, as B7-H6 expression is higher and more widely expressed in AD patients' skin compared to healthy skin (189), but it requires further investigation.

#### **1.2.4 Inhibition**

ILC2s are very potent producers of type 2 cytokines and consequently dysregulated activation can result in pathogenic conditions. Thus, negative regulation of ILC2s is critical (Figure 1.2).

##### **1.2.4.1 Cytokines**

Type I IFNs include IFN $\alpha$  and  $\beta$ , which signal through the shared receptors IFN $\alpha$ R1 and IFN $\alpha$ R2 (191). ILC2s express IFN $\alpha$ Rs and in vitro stimulation of mouse ILC2s with IFN $\alpha$  or IFN $\beta$  inhibits their activation in an IFN $\alpha$ R1-dependent manner (140,192,193). Similarly, in vivo treatment of mice with IL-33 + IFN $\alpha$  or  $\beta$  inhibits ILC2 activation, type 2 inflammation and airway hyperresponsiveness (AHR) through increasing apoptosis and inhibiting proliferation (192,193). Human ILC2s are similarly inhibited by IFN $\alpha$  (193).

A type II IFN, IFN $\gamma$ , which signals through receptors consisting of IFN $\gamma$ R1 and IFN $\gamma$ R2, also inhibits ILC2s. ILC2s express IFN $\gamma$ R1 and IFN $\gamma$  stimulation prevents IL-33-induced activation of ILC2s in vitro in an IFN $\gamma$ R1-dependent manner (140,192,194–196). In vivo co-administration of IL-33 or *A. alternata* and IFN $\gamma$  also potently inhibits lung ILC2 proliferation and activation (140,192,195). The suppressive effects of IFN $\gamma$  on ILC2s are not model or tissue specific, as similar inhibitory effects have been shown in lung ILC2s during *N. brasiliensis*

infection and FALC ILC2s (140). Endogenous IFN $\gamma$  similarly inhibits ILC2s as demonstrated by reduction of adipose tissue ILC2s in YFP-enhanced transcript for IFN $\gamma$  (Yeti) heterozygous mice, which constitutively express IFN $\gamma$  (195). Moreover, lung ILC2s are also suppressed during co-infection with *N. brasiliensis* and intracellular bacteria *Listeria monocytogenes*, the latter of which induces production of IFN $\gamma$  from CD8<sup>+</sup> T cells (195). Interestingly, IFN $\gamma$  suppresses ILC2s when it is pre-existent prior to ILC2 activation (194), or administered after ILC2s have been activated (140).

IL-27 is an IL-12 family of cytokine, which signals through IL-27R $\alpha$  (also known as WSX1) and gp130 (197). IL-27R is expressed by BM and lung ILC2s, and in vitro culture of ILC2s in the presence of IL-27 inhibits IL-33-induced proliferation and activation of ILC2s (140,192,198). ILC2-mediated type 2 inflammation in mouse models of airway inflammation and parasite infection is also suppressed by IL-27 (140,198). IL-27-mediated inhibition of ILC2s is not likely tissue specific, as FALC ILC2s are also suppressed by this cytokine (140).

IL-10 belongs to the IL-10 family of cytokines and signals through the tetrameric receptor consisting of two IL-10R $\alpha$  and IL-10R $\beta$  chains (199,200). IL-10R is expressed on naïve and activated mouse ILC2s and human ILC2s (140,201,202), but the effect of IL-10 on ILC2s is controversial. While IL-10 mildly suppresses IL-33 stimulated ILC2 activation in vitro, it does not inhibit ILC2s stimulated with IL-2 or IL-2 + IL-25 (201,203). In contrast, Molofsky et al. and Moro et al. reported that IL-10 has no suppressive effects on lung or FALC ILC2s, respectively (140,195). In humans, however, IL-10-mediated inhibition of ILC2s seems more potent, as stimulation of human PB ILC2s with IL-33 + TSLP + IL-10 strongly inhibits ILC2 cytokine production and activation-induced morphological changes (202).

#### 1.2.4.2 Lipid mediators

Both mouse and human ILC2s are consistently inhibited by PGE<sub>2</sub> in vitro and IL-33 driven airway inflammation in mouse is suppressed in vivo (204,205). PGE<sub>2</sub> signals through GPCRs, EP1, EP2, EP3 or EP4 (206). While mouse ILC2s express *Ptger1* and *Ptger4* encoding EP1 and EP4 (204), respectively, human ILC2s express *PTGER2* and *PTGER4* encoding EP2 and EP4 (205). By using receptor antagonists and agonists, it was found that both EP2 and EP4 contribute to inhibition of human ILC2s (205), while EP4 is the primary receptor in mouse, which was also confirmed by exacerbated *A. alternata*-induced airway inflammation in EP4 deficient mice (204). The inhibitory effects of PGE<sub>2</sub> is likely exerted by downregulation of GATA3 (human and mouse), ST2 (mouse) and CD25 (human) and subsequent inhibition of proliferation (204,205).

ILC2s express prostacyclin receptor (IP), a PGI<sub>2</sub> receptor, and treatment with PGI<sub>2</sub> analog inhibits IL-33-mediated activation of mouse and human ILC2s in vitro (207). PGI<sub>2</sub> signaling also has similar inhibitory effects in vivo in an airway inflammation model (207). However, IP deficient mouse lungs have elevated numbers of NK cells, which more potently secrete IFN $\gamma$  compared to WT mice (208). Since ILC2s are inhibited by IFN $\gamma$  as described above (140,192,194–196), it is possible that the inhibitory effects of PGI<sub>2</sub> may partially be mediated by NK cell-derived IFN $\gamma$  (208).

Lastly, although the number of studies is limited, ILC2s also express ALX/FPR2, which are GPCRs for lipoxin (LX) A<sub>4</sub> (174). LXA<sub>4</sub>, which is elevated in asthmatic patients, has been shown to suppress IL-13 production from human ILC2s in the presence of other activating signals provided by IL-25, IL-33, IL-2 and PGD<sub>2</sub> (174).

#### **1.2.4.3 Neurotransmitters**

Catecholamines such as epinephrine, norepinephrine and dopamine are neurotransmitters released by the sympathetic nervous system (209). Norepinephrine signals through adrenergic receptors and they are known to mediate brain and immune cell cross-talk (209). ILC2s express  $\beta_2$  adrenergic receptor ( $\beta_2$ AR), which is one of the adrenergic receptors that mediate norepinephrine signaling, and colocalize with adrenergic neurons in the SI (210).  $\beta_2$ AR deficiency results in exacerbated type 2 inflammation in the SI and lung in various infection and disease models, while treatment with  $\beta_2$ AR agonist inhibits type 2 inflammation and ILC2 expansion (210).  $\beta_2$ AR signaling exerts its inhibitory effects by negatively regulating ILC2 proliferation, rather than enhancing apoptosis (210). Suppressive effects of norepinephrine on ILC2s have also been suggested in adipose tissue (211).

Acetylcholine, which also inhibits ILC2s, is a neurotransmitter released by the parasympathetic nervous system (212). Acetylcholine signals through muscarinic acetylcholine receptors (mAChRs), which are GPCRs, and nicotinic acetylcholine receptors (nAChRs), which are cationic channels (213). ILC2s express a subtype of nAChRs,  $\alpha_7$ nAChR, which is upregulated upon in vitro IL-33 treatment and in vivo i.n. IL-33 or IL-25 injections (212).  $\alpha_7$ nAChR agonist treatment attenuates proliferation and activation of ILC2s and GATA3 expression, leading to reduced eosinophilia and AHR during lung inflammation (212).

#### **1.2.4.4 Androgen**

Both ILC2 progenitors in the BM and mature ILC2s in the lung express androgen receptors. Testosterone has been shown to negatively regulate ILC2 maturation, proliferation and function (214–216). This topic will be explored further in Chapter 3.



#### 1.2.4.5 Cell-cell interactions

KLRG1, an inhibitory receptor expressed on NK cells and effector CD8<sup>+</sup> T cells, is known to interact with cadherins (217–219). Increased expression of KLRG1 is found on skin ILC2s isolated from AD patients (63). In vitro stimulation of human skin ILC2s with one of its ligands, E-cadherin, causes reduction in expression of *GATA3*, type 2 cytokines and *AREG* as well as ILC2 proliferation, suggesting negative regulation through this receptor (63).

An immune checkpoint protein PD-1 is expressed by T and B cells and APCs, and exerts inhibitory effects upon binding to its ligand PD-L1 or PD-L2 (220). PD-1 is expressed by a KLRG1<sup>+</sup> subset of ILC2s, and consequently PD-1 deficient mice have increased numbers of KLRG1<sup>+</sup> lung ILC2s (221). PD-1 expression is induced upon treatment with IL-33 + IL-2 + IL-7 and it negatively regulates proliferative capacity of KLRG1<sup>+</sup> ILC2s through STAT5. Moreover, PD-1 signaling inhibits ILC2s during parasite infections and airway inflammation. PD-1 also plays similar suppressive roles in human ILC2s (221).

While ICOS-ICOSL interaction provides pro-survival signals to ILC2s (188), Tregs, which also express ICOS, exert their suppressive effects on ILC2s through this interaction. The suppressive effect is dependent on ICOSL expression on ILC2s and cell-contact between Tregs and ILC2s (203).

#### 1.2.5 Function

Upon activation, ILC2s produce copious amounts of type 2 cytokines, IL-5 and IL-13, but they also release IL-9 and Areg (Figure 1.2). IL-5 induces eosinophil differentiation, maturation and recruitment into inflamed tissues (34), while IL-13 stimulates goblet cell hyperplasia and mucus hyperproduction (222,223). Together with IL-4, IL-13 also provides cues for

macrophages to polarize towards an M2 type (43,44,224). We have previously described that ILC2-derived IL-13 also facilitates polarization of helper T cells towards Th2 pathway through indirectly acting on DCs (30). ILC2s' high capacity to produce these cytokines is highlighted by their involvement in various immune-mediated processes, such as parasite expulsion (22), tissue repair (28) and adipose tissue homeostasis (67,68), but also in pathogenesis of diseases including asthma (225), AD (62), chronic rhinosinusitis (CRS) (25) and liver fibrosis (65).

ILC2s were initially described in the gastrointestinal (GI) tract and FALC, demonstrating their roles in intestinal immunity (22–24). In the GI tract, ILC2s are readily activated upon *N. brasiliensis* infection and represent the major source of IL-13 (22–24). ILC2-derived IL-13 stimulates goblet cells to produce resistin-like molecule (RELM)  $\beta$  and mucus, which prevent establishment of their interactions with the host (36,226,227), resulting in efficient expulsion of the worms (23). Moreover, ILC2s upregulate the expression of PD-L1 and directly facilitate Th2 polarization through PD-1 during *N. brasiliensis* infection, further enhancing anti-helminth type 2 immune response (228). ILC2s have also been shown to contribute to pathology of oxazolone-induced colitis in an IL-25-dependent manner (229). ILC2s are also present in fetal and healthy adult human intestines and similarly respond to IL-25 and IL-33 stimulation by producing IL-13 (25), suggesting that ILC2s likely exert protective effects against parasites in humans as well.

ILC2s are best described in pathology of allergic diseases including asthma, CRS and AD. We and others have shown pathogenic roles of ILC2s during airway inflammation using various mouse models of asthma (26,230–233). In these models, ILC2s produce large amounts of IL-5 and IL-13, which induce eosinophilia and mucus hyperproduction, respectively, resulting in AHR. Additionally, ILC2-derived IL-13 disrupts epithelial tight junction, leading to leakiness of the airways as seen in asthmatic patients (234). Lung ILC2s also transiently produce IL-9, which

induces goblet cell hyperplasia, mast cell accumulation and airway remodeling (41,42) early during inflammation (27,134,142). Regulation of IL-9 production from ILC2s is likely different from that of IL-5 or IL-13, however, as it is dependent on adaptive cell-derived IL-2 (27). Interestingly IL-9 amplifies IL-5 and IL-13 production from ILC2s by promoting their survival (142) and/or activation (134), suggesting autocrine regulation of ILC2s by IL-9 (27,134). Given that ILC2s are also present in human lungs (25,28) and are elevated in asthmatic patients' BALF (235) and PB (236), there is no doubt that they play critical roles in human lung diseases.

The pathogenic contribution of ILC2s in allergic diseases is not limited to the lung as the frequency of ILC2s is also increased in the skin of AD patients (62,63). Topical application of MC903, a vitamin D analog calcipotriol, or IL-2 treatment induces ILC2 accumulation and IL-5 and IL-13 production, followed by eosinophil infiltration and skin thickening (62,64). Similarly, subcutaneous HDM challenge results in ILC2 accumulation in human subjects (63), demonstrating their role in allergic responses. As dermal ILC2s constitutively express IL-13 in mouse and MC903 treatment did not induce significant increase in IL-13 production in one of the studies, the role of ILC2-derived IL-13 in the skin needs further investigation (64).

ILC2s also expand in the lung and produce large amounts of IL-5 and IL-13 during influenza infection (61). Although the role of ILC2-derived IL-5 is not clear as influenza infection does not cause eosinophilia, the importance of IL-13 is highlighted by the requirement of ILC2-derived IL-13 in the development of influenza-induced AHR (61). In contrast, ILC2s produce a growth factor, Areg, and mediate repair of the tissue damage and maintenance of the epithelial integrity during influenza infection (28). However, their capacity to repair tissues can be pathogenic, as exemplified in the case of hepatic fibrosis, where ILC2-derived IL-13 promotes activation of ECM producing hepatic stellate cells (HSCs), resulting in excessive

deposition of ECM and development of fibrosis (65). On the other hand, IL-33-mediated ILC2 activation exerts mild protective effects in viral hepatitis, while further studies are needed to determine the underlying mechanisms (237).

Most of ILC2 research has focused on their roles at mucosal barrier sites. However, ILC2s also play critical roles in adipose tissue homeostasis as suggested by reduction of white adipose tissue (WAT) ILC2s in obese human and mice fed high fat diet (67). Type 2 immunity mediated by eosinophils and M2 macrophages are crucial for maintaining leanness and insulin sensitivity (238). ILC2s in visceral adipose tissue play a central role in this process as they are the major source of IL-5 and IL-13, which are important for sustaining eosinophils and M2 macrophages (66). Furthermore, ILC2s mediate “beiging” of WAT, by producing methionine-enkephalin (67), which directly induce conversion of WAT to beige adipocytes (BAT). Additionally, ILC2-derived IL-13 together with eosinophil-derived IL-4 also stimulate adipocyte progenitors to commit to BAT lineage (68).

ILC2s also respond to environmental cues to coordinate local and systemic immunity. ILC2 activation is enhanced after caloric intake and suppressed after fasting (184). Such regulation of ILC2s by feeding cycle likely has an impact on basal eosinophil homeostasis as serum IL-5 and PB eosinophil levels oscillate in a similar manner as ILC2s upon feeding/fasting (184). This hypothesis is further supported by sensitivity of ILC2s towards VIP, which is a neurotransmitter tightly regulated by feeding cycles (239). Moreover, ILC2s sense nutrition status as shown by increase in intestinal ILC2s and their activation during vitamin A deficiency (240). This results in type 2 skewing of intestinal immunity, which consequently allows increased anti-parasite immunity (240). This suggests evolutionary adaptation of the host's

defense mechanism against helminth infections during nutrients deficiency, which can be induced by parasite infections. Functions of ILC2s are summarized in Table 1.2.

	<b>Protective</b>	<b>Pathogenic</b>
<b>Intestine</b>	Elimination of parasites	Colitis
<b>Lung</b>	Tissue repair after influenza infection	Allergic inflammation, AHR
<b>Skin</b>	N/D	Atopic dermatitis
<b>Liver</b>	Protection from viral hepatitis	Fibrosis
<b>Fat</b>	Maintenance of homeostasis	N/D

**Table 1.2: Summary table of ILC2 functions in various organs**

A table showing protective and pathogenic roles of ILC2s in different organs. N/D=not determined.

### 1.2.6 Memory

Immunological memory, defined as the ability of immune cells to respond more rapidly and robustly during the secondary encounter, is a hallmark of the adaptive immunity. However, we have recently found that ILC2s also have memory-like features (76). Lung ILC2s remain high in number for a long time after initial stimulation and respond more vigorously during secondary encounter (76). The antigen non-specific nature of ILC2s allow them to respond to unrelated allergens, potentially describing a mechanism behind reactivity towards multiple allergens seen in allergic patients (241).

## 1.3 Diseases

### 1.3.1 Asthma

#### 1.3.1.1 Overview

Asthma is a chronic inflammatory disease of the airways characterized by airway narrowing, wheezing and shortness of breath. Asthma affects approximately 300 million people worldwide and the numbers are expected to keep rising (242). It is one of the most common chronic diseases in the world and it affects a wide range of age groups from children to elderly

(242). The cause of the disease can be attributed to many factors including life style, exposure to viruses, allergens and pollutants (243). However, the individual variation in susceptibility to allergen sensitization suggests contribution of genetic factors. In fact, genome-wide association studies have identified single nucleotide polymorphisms (SNPs) in genes including *IL1RL1*, *SRP9*, *TSLP*, *IL33*, *AURKB* and *MHC* as risk factors (244–247). It is also known that asthma is more common among boys than girls before puberty, while the trend reverses during reproductive age (248), suggesting contribution of sex hormones as one of the risk factors.

Asthma is a heterogeneous disease and categorization has been challenging. One of the traditional classifications based on disease phenotype is “intrinsic” versus (vs.) “extrinsic” asthma, also known as “non-atopic (non-allergic)” vs. “atopic (allergic)” asthma. The majority of atopic/allergic asthma, where patients have reactivity to common allergens in a skin prick test, is early onset. In contrast, non-atopic/non-allergic asthma, in which patients lack IgE for common allergens, is more prevalent in late-onset asthma (242,249). With rising interest in personalized medicine, asthma is more recently classified based on the endotype, which focuses on the cellular and molecular mechanisms behind the development of the disease (250). The endotypes include two major groups, T2-high and non-T2-high groups based on the types of inflammation observed in patients: type 2 immunity-driven and non-type 2 immunity-driven, respectively (250).

### **1.3.1.2 Pathogenesis**

Immunopathology of asthma is largely characterized by the presence of type 2 immunity including eosinophils and type 2 cytokines, although some asthma is presented with IL-17 and neutrophil-mediated phenotype (251). Type 2 inflammation is initiated when airway epithelial

cells are exposed to airborne irritants or aeroallergens, which induce production of alarmin cytokines, including IL-33, IL-25 and TSLP (21). These cytokines activate ILC2s, which respond by proliferation and production of IL-5, IL-13 and IL-9, initiating an inflammatory cascade (22–27). IL-5 causes eosinophilia (34), while IL-13 induces goblet cell hyperplasia and mucus hyperproduction, as well as smooth muscle contraction and tissue remodeling, leading to AHR (35,222). IL-9 promotes ILC2 survival and activation in an autocrine manner (252), but it also provides survival and activation signals to mast cells (41,42).

ILC2-derived IL-13 also orchestrates adaptive immune responses by facilitating Th2 differentiation of T cells (30). Th2 cells, in turn, secrete large amounts of IL-4, IL-13 and IL-5, further enhancing type 2 inflammation. Th2 cell-derived IL-4 together with IL-13 plays a crucial role in regulating B cell responses, by inducing IgE class switch (38,39,253).

This series of events causes sensitization of individuals to specific allergens, mediated by antigen-specific T and B cell responses. Upon secondary encounter with the same allergens, antigen specific Th2 cells and IgE mediate a vigorous response, leading to enhanced inflammation. IgE crosslinking of high affinity FcεRI on mast cells and basophils induces degranulation, resulting in release of inflammatory mediators including leukotrienes and histamine, which cause vascular permeability and smooth muscle constriction (21).

Although each episode of allergen-induced inflammation may be reversible, repeated exposure to allergens and subsequent tissue remodeling predisposes airways to exaggerated responses and increases susceptibility to exacerbations (254). Consequently, individuals recurrently experience asthma symptoms including shortness of breath and wheezing.

### 1.3.2 Hepatic fibrosis

#### 1.3.2.1 Overview

Regeneration is the ability to renew parts of the body after injury or as a normal physiological process. Regenerative potential is seen across animal kingdom and organ systems, but the regenerative capacity varies among species (255). Some invertebrates, such as Hydra can regenerate entire organism, while some amphibians are able to regenerate some parts of the body (256). Mammalian tissues are highly regenerative during embryogenesis, but the ability to regenerate decreases as we mature and regenerative responses are largely replaced by tissue repair mechanisms in adults (255,257). However, the liver is one of the few organs that remains regenerative into adulthood. The ability of the liver to regenerate allows reconstruction of its architecture and function after injury or partial hepatectomy, but dysregulated repair/regeneration can lead to irreversible scarring of the liver, resulting in the development of chronic liver diseases including fibrosis.

Fibrosis is chronic scarring of the liver tissues due to excessive deposition of ECM, which causes liver dysfunction and failure. The most common etiologies include infection with hepatitis viruses or *Schistosoma*, alcoholic liver disease (ALD) caused by alcohol abuse, non-alcoholic fatty liver disease (NAFLD) induced by persistent oxidative stress, and cholestatic and autoimmune liver disease (258). Fibrosis is often merely the beginning of series of hepatic diseases and can further progress into liver cirrhosis and hepatocellular carcinoma (259). Cirrhosis and liver cancer are 11<sup>th</sup> and 16<sup>th</sup> leading cause of death worldwide, respectively, and the numbers have increased in the past 20 years (260), which highlights the necessity for preventative measures and treatment.



### 1.3.2.2 Pathogenesis

There are very few proliferating cells and very little ECM in a homeostatic liver (261). Upon injury induced by insults including viral infection, alcohol/drug intake or toxins, a series of events is initiated to repair damaged tissue. The repair response is finely orchestrated by various cell types such as epithelial, endothelial, mesenchymal and immune cells, and consists of three stages: regeneration, resolution and fibrosis (257).

Upon hepatic injury, damaged hepatocytes secrete DAMPs to induce activation of immune cells (262), such as liver-resident Kupffer cells, or recruitment of monocyte-derived macrophages. These cells phagocytose damaged epithelium and provide signals for hepatocytes regeneration, such as TNF $\alpha$  and IL-6 (263–265). In parallel, liver sinusoidal endothelial cells (LSECs) also provide hepatocytes with mitogenic signals to support their proliferation (257). HSCs, the major fibroblasts in the liver, transdifferentiate into myofibroblasts upon receiving TGF $\beta$  and other signals from macrophages (266). HSC differentiation is accompanied by the expression of smooth muscle  $\alpha$  actin, which increases their contractility and motility, allowing them to infiltrate injured area (267), where they deposit ECM such as collagen to repair damage. In this regenerative phase of the repair response, damaged cells are replaced by new cells and there is no long-term scarring of the tissue.

When the injury is acute and transient, the repair response is eventually terminated, and homeostasis is restored. This is mediated by macrophages that have a Ly6C<sup>lo</sup> phenotype, which produce matrix metalloproteinases (MMPs) that degrade ECMs (257). Immune cells, such as NK cells and  $\gamma\delta$ T cells clear myofibroblasts by inducing their apoptosis (268–271). Alternatively, myofibroblasts can also become inactivated (272,273). Overall, this series of events results in resolution of inflammation and removal of scar tissues.

When the injury becomes chronic or repetitive, however, persistent repair/regeneration responses can proceed to fibrosis. During this stage, increased numbers of monocyte-derived macrophages that have a Ly6C<sup>hi</sup> phenotype are recruited from circulation (274). They, together with LSECs produce large amounts of pro-fibrotic factors including TGFβ, promoting survival and activation of myofibroblasts, which, in turn, produce ECM and tissue inhibitors of metalloproteinases (TIMPs) (257). TIMPs inhibit degradation of ECM by MMPs, resulting in accumulation of ECM fibers. Complex meshwork resulting from extensive ECM deposition prevents access of MMPs and degradation of ECM fibers, resulting in a dysfunctional acellular structure (257).

### **1.3.3 Cancer**

Cancer is one of the leading causes of mortality as demonstrated by 18 million new cases and 9 million deaths reported in 2018 worldwide (275). While cancer is treatable when detected early, it often progresses into advanced disease and patients eventually succumb to death, highlighting the importance of developing improved therapeutics. Despite the presence of our body's inherent mechanism of eliminating cancerous or pre-cancerous cells, known as tumor immunosurveillance, cancer cells often escape detection by cytotoxic immune cells and alter immune landscape towards immunosuppressive microenvironment by recruiting pro-tumor immune cells (276,277).

Generally, type 2 immunity is considered to be pro-tumorigenic as it favors M2 polarization of macrophages, which produce various growth factors that promote tumor growth and generate immunosuppressive microenvironment (278). Considering the ability of ILC2s to potentially produce type 2 cytokines, they are likely pro-tumor. However, ILC2 research in tumor

immunity is still in its infancy and mostly focused on correlations between ILC2 numbers or activation status and cancer progression. Hence, direct evidence regarding pro- or anti-tumor role of ILC2s is lacking. ILC2s are elevated in patients with various tumors including APL and prostate (190), gastric (279), breast (280) and lung cancers (281), while their frequency is reduced in patients with non-small cell lung carcinoma (282). Similarly, pro-tumor effects of ILC2s have been shown in mouse melanoma (283), whereas anti-tumor roles have been described in mouse models of lung and prostate cancers (284).

More recently, anti-tumor role of ILC2s have been demonstrated in mouse models of pancreatic ductal adenocarcinoma (PDAC) and PDAC patients. Moral et al. showed that ILC2s were elevated in tumor tissues of long-term PDAC survivors and PDAC-bearing mice. Anti-tumor immunity provided by ILC2s was IL-33 dependent, where IL-33-activated ILC2s produced chemokines recruiting DCs, which, in turn, activated CD8<sup>+</sup> cytotoxic T cells (285). The immune checkpoint PD-1 was upregulated in ILC2s upon IL-33 treatment and co-injection of anti-PD-1 and activated ILC2s were effective in controlling tumor burden of established tumors, suggesting their potential as therapeutic targets.

#### **1.4 Thesis objective**

Asthma prevalence is higher among boys than girls, while the trend switches after adolescence (248). Although the role of sex steroid hormones is suspected, the underlying mechanism is yet to be determined. Given the known pathologic roles of ILC2s in airway inflammation, lung ILC2s appeared to be a logical candidate to investigate in order to understand the mechanism behind sex bias in asthma prevalence. This led to the first objective of this thesis, which is to examine the sex related differences in lung resident ILC2s. Based on the age-related

sex bias in asthma prevalence, I hypothesized that sex steroid hormones regulate ILC2 proliferation and type 2 inflammation in the lung upon stimulation. While I worked on this project, multiple papers were published reporting negative regulatory effects of androgen signaling on ILC2Ps and ILC2s, uncovering the mechanism behind sex difference in asthma prevalence (214–216). Therefore, I focused on intrinsic differences between female and male lung resident ILC2s and the effect of sex on epithelium-derived cytokines. The results are presented in Chapter 3.

ILC2s are considered to be tissue resident at steady state and during inflammatory conditions such as systemic autoimmunity and parasitic infection (86). In agreement with their tissue residency, very few ILC2s are found circulating in naïve mouse PB. In contrast, ILC2s are detected in human PB (25) and elevated in asthmatic patients' PB (236), suggesting that ILC2s may be able to leave the lung and circulate once activated. This observation led to the second objective of this thesis, which is to determine the roles of migratory ILC2s induced upon activation. I hypothesized that a subset of lung ILC2s enter circulation, migrate to and settle in another organ and alter immune environment. By following ILC2s after activation in the lung, I have found that a subset of migratory ILC2s circulated through PB and reached the liver, and thus, I have focused my studies on the liver. This part of the thesis is separated into two chapters: characterization of lung resident and migratory ILC2s are presented in Chapter 4 and the effects of lung-derived ILC2s in the liver are presented in Chapter 5.

## Chapter 2: Materials and Methods

### 2.1 Materials

#### 2.1.1 Mice

C57BL/6J (B6), B6.SJL-*Ptprc<sup>a</sup>Pepc<sup>b</sup>*/BoyJ (Pep3b), B6.129P2(Cg)-*Rorc<sup>tm2Litt</sup>*/J (*Rorc<sup>-/-</sup>*) and B6.129S7-*RagI<sup>tm1Mom</sup>*/J (*RagI<sup>-/-</sup>*) mice were bred in the British Columbia Cancer Research Centre (BCCRC) and Biomedical Research Centre (BRC) animal facilities from breeder mice purchased from the Jackson Laboratory. *Il33<sup>tm1(KOMP)Vlbg</sup>* (*Il33<sup>-/-</sup>*) mice were obtained from the Knockout Mouse Project and bred in the BCCRC animal facility. CD127 cKO mice were generated in house as follows. B6.*Rora-IRES-Cre* (286) mice were re-derived in BCCRC Animal Resource Centre (ARC) by in vitro fertilization of albino C57BL/6J (B6(Cg)-*Tyr<sup>c-2J</sup>*/J) mouse eggs with B6.*Rora-IRES-Cre* mouse sperms obtained from Dr. O’Leary (The Salk Institute). CD127 conditional KO (cKO) mice were generated by crossing re-derived B6.*Rora-IRES-Cre* mice and *Il7ra<sup>fl/fl</sup>* mice (287), which were kind gifts from Dr. Ninan Abraham (University of British Columbia) with Dr. Singer’s approval.

All animal use was approved by the animal care committee of the University of British Columbia and were maintained in specific pathogen-free facilities and euthanized in accordance with the guidelines of the Canadian Council on Animal Care. Briefly, mice were housed in static cages (4 mice maximum per cage) with cotton or crinkle paper nesting materials and a hiding place. They were fed low fat diet and water was provided per cage. To minimize animal suffering and distress, mice were anesthetized by isoflurane inhalation during i.n. injections and monitored until they were fully recovered from anesthesia in a separate cage with heating mat underneath it. The mice were monitored daily during treatment period and after the treatment as indicated in the protocol. Their health status was assessed by their behaviour, appearance,

hydration status, respiration, and presence/absence of any obvious pain. Their health and well-being were monitored daily by facility staff based on their appearance and behaviour. At the time of harvest, mice were anesthetized by isoflurane inhalation until they were unconscious and euthanized by carbon dioxide asphyxiation. Mice were treated at the ages indicated in the text (Chapter 3) or between 6-26 weeks of age (Chapters 4 & 5). For Chapter 3, female and male mice were used as indicated in the text, while for Chapters 4 & 5, female mice were used for most experiments and a mixture of male and female mice were used for Figures 4.3, 5.2, 5.3A and Appendices B.1, B.3A and C.1.

### **2.1.2 Parabiosis**

Parabiosis mice were prepared in the BRC animal facility using female B6 and Pep3b mice as previously described (288). Briefly, weight matched female mice were co-housed for 1 week prior to the surgery. The two mice were juxtaposed and the hindlimbs, bodies and forelimbs were joined together, while being maintained in a surgical plane of anesthesia by isoflurane inhalation. Both mice were given subcutaneous injections of 1 mL saline twice a day and 0.03 mg/mL of Buprenorphine analgesic for the first 3 days post-surgery. Mice were monitored twice a day during the first week and once a day after that for a total of 3 weeks post-surgery, and the monitoring was extended if mice did not recover well. The health status was assessed based on pain, hydration and body weight loss. Mice were used between 5-6 weeks after the surgery.

### 2.1.3 Antibodies and flow cytometry

Antibodies used for flow cytometric analyses are listed in Table 2.1. BD FACS (fluorescence-activated cell sorting) Aria was used for cell sorting and BD LSRFortessa was used for flow cytometric analyses. Flowjo version 10.0.7r2 was used for data analyses.

<b>Antigen</b>	<b>Cells detected</b>	<b>Fluorophore</b>	<b>Clone</b>	<b>Vendor</b>
<b>Armenian Hamster IgG isotype control</b>	isotype control for CXCR3, CD103	Allophycocyanin (APC)	HTK888	BioLegend
	isotype control for CD103	Brilliant Violet (BV) 711		
<b>CCR1</b>	monocytes (Mo), T cells, DCs and neutrophils, NK cells	Phycoerythrin (PE)	S15040E	BioLegend
<b>CCR2</b>	Mo	Fluorescein isothiocyanate (FITC)	SA203G11	BioLegend
<b>CCR3 (CD193)</b>	eosinophils, basophils, T cells, airway epithelial cells	Alexa Fluor 647	83103	BD Biosciences
<b>CCR4 (CD194)</b>	Th2 cells, Tregs	PECy7	2G12	BioLegend
<b>CCR7</b>	B cells, DCs, naïve T cells, Tregs, central memory T cells	APC	4B12	Thermo Fisher Scientific
<b>CCR9</b>	intestinal T cells and ILCs	APC	CW-1.2	Thermo Fisher Scientific
<b>CD103 (ITGαE)</b>	cDC1, intraepithelial T cells, Tregs	APC	2E7	Thermo Fisher Scientific
		BV711		BioLegend
<b>CD11b</b>	Mo, granulocytes, some NK cells	FITC, eFluor 450	M1/70	Thermo Fisher Scientific
		PE		BD Biosciences
<b>CD11c</b>	some macrophages (Macs) & Mo	Alexa Fluor 700, eFluor 450	N418	Thermo Fisher Scientific
<b>CD117 (C-kit)</b>	hematopoietic stem cells & progenitors, mast cells	PerCP-eFluor 710	2B8	Thermo Fisher Scientific
<b>CD127</b>	T cells, ILCs, some DCs	PE, PECy7, Alexa Fluor 700	A7R34	Thermo Fisher Scientific

<b>Antigen</b>	<b>Cells detected</b>	<b>Fluorophore</b>	<b>Clone</b>	<b>Vendor</b>
<b>CD19</b>	B cells	FITC, PerCP-Cy5.5, eFluor 450	1D3	Thermo Fisher Scientific
		PE		BD Biosciences
		BV711	6D5	BioLegend
<b>CD2</b>	B cells, NK cells, T cells	APC	RM2-5	BioLegend
<b>CD206</b>	Macs, LSECs	PECy7	C068C2	BioLegend
<b>CD218a (IL-18R)</b>	NK cells, NKT cells, Th1 cells, B cells, ILC1s, ILC3s	PerCP-eFluor 710	P3TUNYA	Thermo Fisher Scientific
<b>CD24</b>	B cells, DCs, some granulocytes	PECy7	M1/69	Thermo Fisher Scientific
<b>CD25</b>	Tregs, ILC2s, ILC3s	PerCP-Cy5.5	PC61.5	Thermo Fisher Scientific
<b>CD3ε</b>	T cells	FITC, PerCP-Cy5.5, eFluor 450	145-2C11	Thermo Fisher Scientific
		APC		BD Biosciences
<b>CD4</b>	CD4 <sup>+</sup> T cells, some ILC3s, some DCs	eFluor 450	RM4-5	Thermo Fisher Scientific
		PECy7	GK1.5	BioLegend
		APC, BV650		BioLegend
<b>CD45</b>	leukocytes	V500	30-F11	BD Biosciences
<b>CD45.1</b>	Ly5.1 <sup>+</sup> leukocytes from Pep3b mice	Alexa Fluor 700	A20	BioLegend
<b>CD45.2</b>	Ly5.2 <sup>+</sup> leukocytes from B6 mice	Alexa Fluor 700	104	Thermo Fisher Scientific
		V500		BD Biosciences
<b>CD45R (B220)</b>	B cells	eFluor 450	RA3-6B2	Thermo Fisher Scientific
<b>CD49a</b>	ILC1s, some γδT cells	BV711	Ha31/8	BD Biosciences
<b>CD49b</b>	NK cells, basophils	Alexa Fluor 647	DX5	BioLegend
<b>CD5</b>	T cells	BV421	53-7.3	BioLegend
<b>CD64</b>	Mo, Macs	APC	X54-5/7.1	BioLegend
<b>CD69</b>	activated T cells and NK cells	PerCP-Cy5.5	H1.2F3	Thermo Fisher Scientific
<b>CD8</b>	CD8 <sup>+</sup> T cells, CD8 <sup>+</sup> DCs, some γδT cells	APC	53-6.7	Thermo Fisher Scientific
<b>CD80</b>	DCs, activated B cells, Mo, Macs	PE	16-10A1	Thermo Fisher Scientific
<b>CD90.2 (Thy1.2)</b>	T cells, NKT cells, ILCs	BV605	53-2.1	BD Biosciences
<b>CX3CR1</b>	T cells, DCs, some Mo, microglia, NK cells	PE	SA011F11	BioLegend



<b>Antigen</b>	<b>Cells detected</b>	<b>Fluorophore</b>	<b>Clone</b>	<b>Vendor</b>
<b>CXCR3 (CD183)</b>	Th1 cells, CD8 <sup>+</sup> T cells, NK cells	APC	CXCR3-173	BioLegend
<b>CXCR4</b>	B cells, T cells, DCs, NK cells	PE	2B11	Thermo Fisher Scientific
<b>CXCR6 (CD186)</b>	ILC1, some NK cells, NKT cells, activated T cells	PerCP-eFluor 710	DANID2	Thermo Fisher Scientific
<b>EOMES</b>	CD8 <sup>+</sup> T cells, NK cells, some $\gamma\delta$ T cells	PerCP-eFluor 710	Dan11mag	Thermo Fisher Scientific
<b>F4/80</b>	Macs, Mo, eosinophils	BV650	BM8	BioLegend
<b>FcεR1a</b>	mast cells, basophils	FITC, APC	MAR.1	Thermo Fisher Scientific
<b>GATA3</b>	Th2 cells, ILC2s	eFluor 660, PE	TWAJ	Thermo Fisher Scientific
<b>Gr-1 (Ly6C &amp; Ly6G)</b>	plasmacytoid DCs, Mo, some NK cells, neutrophils	eFluor 450	RB6-8C5	Thermo Fisher Scientific
<b>IFN<math>\gamma</math></b>	NK cells, NKT cells, Th1 cells, CD8 <sup>+</sup> T cells	FITC	XMG1.2	BD
<b>IL-13</b>	activated Th2 cells, ILC2s, mast cells, basophils, eosinophils, NKT cells	PE, PECy7	eBio13A	Thermo Fisher Scientific
<b>IL-17RB (IL-25R)</b>	some ILC2s, Th2 cells	PE	MUNC33	Thermo Fisher Scientific
		Alexa Fluor 700	752101	R&D Systems
<b>IL-5</b>	activated Th2 cells, ILC2s, mast cells, basophils, eosinophils, NKT cells	APC	TRFK5	BD Biosciences
<b>IL-6</b>	Mo, Macs, some DCs, mast cells, basophils, ILC2s	PE	MP5-20F3	Thermo Fisher Scientific
<b>ITGa4 (CD49d)</b>	lymphocytes, Mo, eosinophils, neutrophils, non- immune cells	APC	R1-2	BioLegend
<b>ITGaL (CD11a)</b>	lymphocytes, DCs, neutrophils	PerCP-Cy5.5	M17/4	BioLegend
<b>ITGav (CD51)</b>	ILCs, some T cells, some Macs, some Mo	PE	RMV-7	BioLegend
<b>ITGβ1 (CD29)</b>	lymphocytes, Mo, eosinophils,	PerCP-Cy5.5	HMβ1-1	BioLegend

<b>Antigen</b>	<b>Cells detected</b>	<b>Fluorophore</b>	<b>Clone</b>	<b>Vendor</b>
	neutrophils, non-immune cells			
<b>ITGβ2 (CD18)</b>	lymphocytes, DCs, neutrophils, Mo, Macs	PE	M18/2	BioLegend
<b>ITGβ3 (CD61)</b>	some T cells, NKT cells, eosinophils, basophils, ILCs	APC	2C9.G2 (HMβ3-1)	BioLegend
<b>ITGβ7</b>	lymphocytes, some DCs, some Macs, Mo, eosinophils, basophils	PE	FIB27	BioLegend
<b>Ki67</b>	proliferating cells	FITC	SolA15	Thermo Fisher Scientific
<b>KLRG1</b>	CD8 <sup>+</sup> T cells, NK cells, some ILC2s	APC	2F1	Thermo Fisher Scientific
		BV711		BD Biosciences
<b>Ly6B.2 (7/4)</b>	neutrophils, inflammatory Mo	FITC	7/4	Abcam
<b>Ly6C</b>	plasmacytoid DCs, Mo, some NK cells	PerCP-Cy5.5	AL-21	BD Biosciences
<b>Ly6G</b>	neutrophils	BV605	1A8	BioLegend
<b>MHCII</b>	DCs, Macs, B cells	eFluor 450	M5/114-15-2	Thermo Fisher Scientific
<b>Mouse IgG2a, κ isotype control</b>	isotype control for CCR9	APC	eBM2a	Thermo Fisher Scientific
<b>NK1.1</b>	NK cells, NKT cells, ILC1s	PerCP-Cy5.5, eFluor 450, PECy7	PK136	Thermo Fisher Scientific
		FITC		BD Biosciences
<b>NKp46</b>	NK cells, NKT cells, ILC1s, some ILC3s	FITC	29A1.4	BioLegend
		eFluor 450		Thermo Fisher Scientific
<b>Rat IgG1, κ isotype control</b>	isotype control for IL-5	APC	R3-34	BD Biosciences
	isotype control for ITGαv, IL-6, IL-13	PE	RTK2071	BioLegend
<b>Rat IgG2a, κ isotype control</b>	isotype control for Ki67	FITC	eBR2a	Thermo Fisher Scientific
	isotype control for CXCR6	PerCP-eFluor 710		
<b>Rat IgG2b, κ</b>	isotype control for CCR2	FITC	RTK4530	BioLegend

<b>Antigen</b>	<b>Cells detected</b>	<b>Fluorophore</b>	<b>Clone</b>	<b>Vendor</b>
<b>isotype control</b>	isotype control for CCR1	PE	A95-1	BD Biosciences
<b>ROR<math>\gamma</math>t</b>	some $\gamma\delta$ T cells, ILC3s, Th17	PE	B2D	Thermo Fisher Scientific
<b>SiglecF</b>	eosinophils, alveolar macrophages	PE	E50-2440	BD Biosciences
<b>T1/ST2 (IL-33R)</b>	ILC2s, eosinophils, Tregs, mast cells, basophils	PerCP-eFluor 710	RMST2-2	Thermo Fisher Scientific
		FITC	DJ8	MD Bioproducts
<b>T-bet</b>	NK cells, ILC1s, Th1, some ILC3s & NKT	PECy7	4B10	Thermo Fisher Scientific
<b>TCR<math>\beta</math></b>	$\alpha\beta$ T cells	FITC	H57-597	BD Biosciences
		eFluor 450		Thermo Fisher Scientific
		APC		BioLegend
<b>TCR<math>\gamma\delta</math></b>	$\gamma\delta$ T cells	FITC	GL3	BD Biosciences
		eFluor 450		Thermo Fisher Scientific
		APC		BioLegend
<b>Ter119</b>	erythrocytes	eFluor 450	TER-119	Thermo Fisher Scientific
<b>TNF<math>\alpha</math></b>	Mo, Macs, neutrophils, NK cells, CD4 <sup>+</sup> T cells	PE	MP6-XT22	Thermo Fisher Scientific

**Table 2.1: Table of antibodies used in this study**

A complete list of antibodies used in this study, the antigens they detect, fluorophores to which they are conjugated, clones and vendors.

#### 2.1.4 Reagents

eFluor 780 fixable viability dye and recombinant mouse TSLP were purchased from Thermo Fisher Scientific. Recombinant mouse IL-25, IL-33 and IL-7 were purchased from BioLegend. Recombinant human IL-2 was purchased from Peprotech. Concanavalin A from *Canavalia ensiformis*, papain from *Carica papaya*, phorbol 12-myristate 13-acetate (PMA) and ionomycin were purchased from Sigma. Brefeldin A (Golgi Plug) was purchased from BD Biosciences.

## **2.2 Methods**

### **2.2.1 In vivo stimulation**

Mice were anesthetized by isoflurane inhalation and i.n. injections were given. Mice were given 3 daily i.n. administrations of 0.25 µg IL-33 (BioLegend) or 0.218U papain (Sigma) in 40 µL phosphate-buffered saline (PBS). For Concanavalin A (ConA) treatment, mice were intravenously injected with 7 mg/kg of ConA at 5 mL/kg (in PBS).

### **2.2.2 Primary leukocyte preparation**

Single cell suspensions of lung, mediastinal lymph nodes (medLN), BALF, BM, liver, SI and mLN were prepared as previously described (289). For data presented in Appendix B.1, mice were perfused with plain PBS until the livers appeared blanched before collecting the livers. For analyses of liver Kupffer cells and macrophages, mouse livers were mashed through 40 µm strainers in 10 mL Dulbecco's Modified Eagle's Medium (DMEM) containing 10% fetal bovine serum (FBS), 100 U/mL penicillin/streptomycin (P/S) and 50 µM 2-mercaptoethanol (2-ME), and washed twice with 15 mL of the same media. Hepatocytes were sedimented by centrifugation (4 °C, 3 mins, 30 xg) and discarded. The supernatant was collected and centrifuged (4 °C, 5 mins, 300 xg), after which the cell pellet was washed once with 10 mL DMEM + 10% FBS + 100 U/mL P/S + 50 µM 2-ME (4 °C, 5 mins, 300 xg). Red blood cells (RBCs) were lysed using 150 mM ammonium chloride solution. To prepare single cell suspension from PB, cardiac blood was collected in PBS containing 25 mM ethylenediaminetetraacetic acid (EDTA) and cells were pelleted by centrifugation (4 °C, 5 min, 600 xg). RBCs were lysed with 150 mM ammonium chloride solution twice.

For spleen, samples were mashed through 70  $\mu$ m strainers in 5 mL PBS + 2% FBS. Strainers were washed with 5 mL of the same buffer and cells were pelleted by centrifugation (4 °C, 5 min, 400 xg). RBCs were lysed using 150 mM ammonium chloride solution. For single cell suspension of skin cells, both ears were collected from mice and split into dorsal and ventral halves with forceps. Ear tissues were digested in 5 mL PBS + 2% FBS containing 420 U/mL type IV collagenase (37 °C, 40 mins, 250 rpm shaker). Digested tissues were mashed through 70  $\mu$ m strainers, which were washed with 5 mL PBS + 2% FBS. Cells were collected by centrifugation (4 °C, 5 min, 400 xg) and washed again with 10 mL PBS + 2% FBS.

For microarray analyses, lung and liver samples were processed as previously described (289), with two additional washes with 10 mL DMEM + 10% FBS + 100 U/mL P/S + 50  $\mu$ M 2-ME before (lung) or after (liver) Percoll density gradient separation.

Isolated leukocytes were counted using a hemocytometer. Samples were incubated in 2.4G2 monoclonal antibody to block Fc receptors prior to cell surface staining with fluorochrome-conjugated antibodies for flow cytometry analyses.

### **2.2.3 BM transplantation**

Recipient mice (Pep3b) were lethally irradiated with 10 Gray radiation, followed by i.v. injection (5 mL/kg) of 10 million BM cells isolated from donor mice (B6). Chimerism test was performed to confirm donor cell reconstitution before mice were treated for analyses. Irradiated mice were provided with water supplemented with Ciprofloxacin and hydrochloric acid for the first 4 weeks post irradiation.

#### 2.2.4 Intracellular staining

Leukocytes were incubated at 37 °C for 3 hours in 500 µL Roswell Park Memorial Institute (RPMI) 1640 media containing 10% FBS, 100 U/mL P/S, 50 µM 2-ME, Brefeldin A (Golgi Plug), PMA (30 ng/mL) and ionomycin (500 ng/mL). Intracellular cytokine staining was performed after the incubation, Fc receptor blocking and cell surface staining, using Cytofix/Cytoperm Fixation/Permeabilization Solution kit (BD Biosciences) according to manufacturer's protocol. Intracellular CD80 and CD206 staining was performed as above but without pre-incubation. Transcription factor and Ki67 staining was performed without pre-incubation using Foxp3/Transcription Factor Staining Buffer Set (Thermo Fisher Scientific) according to manufacturer's protocol.

#### 2.2.5 Immune cell identification

Samples were first gated on live cells using eFluor 780 fixable viability dye. ILC2s were identified as CD45<sup>+</sup> Lin A (CD3ε, CD4, CD11b, CD11c, CD19, TCRβ, TCRγδ, Ter119, Gr-1, NK1.1 (CD2, CD5 for Figure 4.2 and Appendix B.2))<sup>-</sup> Thy1<sup>+</sup> ST2<sup>+</sup> CD127<sup>+</sup> cells (Figure 2.1A) based on surface markers. SI and mLN ILC2s were identified as CD45<sup>+</sup> Lin A<sup>-</sup> Thy1<sup>+</sup> CD127<sup>+</sup> Gata3<sup>+</sup> cells (Figure 2.1B) and skin ILC2s were identified as CD45<sup>+</sup> Lin A<sup>-</sup> Thy1<sup>+</sup> CD127<sup>+</sup> CD103<sup>+</sup> cells (Figure 2.1C). The gating strategies used to identify each lymphoid population in the liver are shown in Figure 2.1D. ILC2s: CD45<sup>+</sup> Lin A<sup>-</sup> Thy1<sup>+</sup> Gata3<sup>+</sup> ST2<sup>+</sup>, ILC3s: CD45<sup>+</sup> Lin A (CD4 excluded)<sup>-</sup> Thy1<sup>+</sup> RORγt<sup>+</sup>, NK cells: CD45<sup>+</sup> T/B (CD19, TCRβ, TCRγδ, CD3ε)<sup>-</sup> T-bet<sup>+</sup> EOMES<sup>+</sup> RORγt<sup>-</sup> CD49a<sup>-</sup> CD49b<sup>+</sup> NK (NK1.1, NKp46)<sup>+</sup>, ILC1s: CD45<sup>+</sup> T/B<sup>-</sup> T-bet<sup>+</sup> EOMES<sup>-</sup> RORγt<sup>-</sup> CD49a<sup>+</sup> CD49b<sup>-</sup> NK<sup>+</sup>, B cells: CD45<sup>+</sup> B220<sup>+</sup> T (TCRβ, TCRγδ, CD3ε)<sup>-</sup> NK<sup>-</sup> CD19<sup>+</sup>,

NKT: CD45<sup>+</sup> B220<sup>-</sup> T<sup>+</sup> NK<sup>+</sup>, Tregs: CD45<sup>+</sup> B220<sup>-</sup> T<sup>+</sup> NK<sup>-</sup> CD25<sup>+</sup>, T cells: CD45<sup>+</sup> B220<sup>-</sup> T<sup>+</sup> NK<sup>-</sup> CD25<sup>-</sup>.

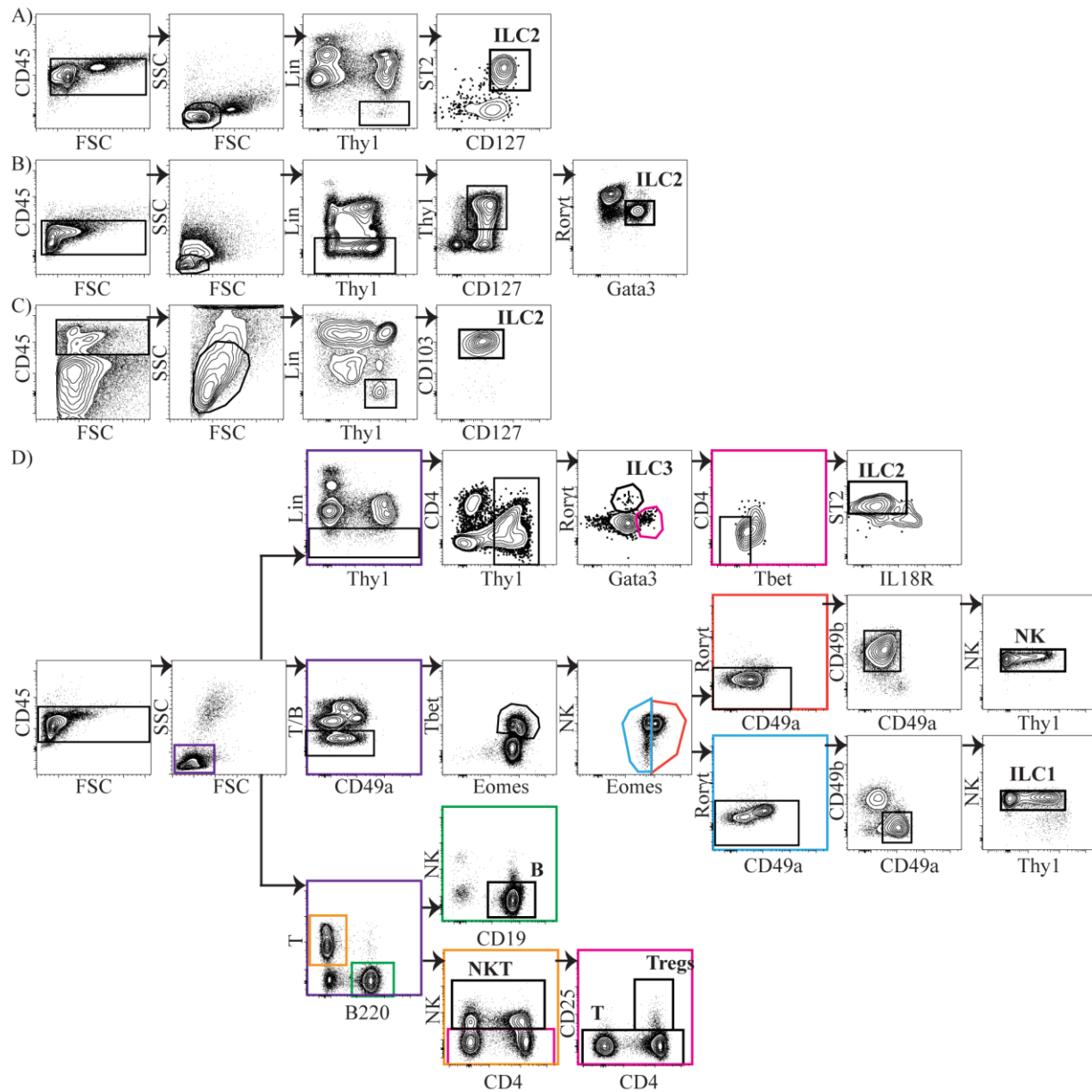


**Figure 2.1: Gating strategies used to identify various lymphoid populations**

(A) ILC2 gating strategy based on surface markers. (B, C) ILC2 gating strategies used for SI and mLN (B) and skin (C) analyses. (D) Gating strategies used for identification of various lymphocyte populations in Chapter 5. Samples were first gated on live cells using eFluor 780 fixable viability dye. Lin cocktail contains CD3ε, CD4, CD19, TCRβ, TCRγδ, CD11b, CD11c, NK1.1, Ter119 and Gr-1 (CD2 and CD5 included for data shown in Figure 4.2 and Appendix B.2, CD4 excluded for D), NK cocktail contains NK1.1 and NKp46, T cocktail contains TCRβ, TCRγδ and CD3ε, T/B cocktail contains CD19, TCRβ, TCRγδ and CD3ε. Tregs=regulatory T cells.

Eosinophils were identified as  $CD45^+ Lym (CD3\epsilon, CD19, NK1.1)^- Ly6B^- SiglecF^+ CD11c^-$  in Chapter 3 and Appendix B.1 (Figure 2.2A). The gating strategies used to identify each myeloid cell population in Chapter 5 are shown in Figure 2.2B. Neutrophils:  $CD45^+ Ly6G^+$ , eosinophils:  $CD45^+ Ly6G^- SiglecF^+$ , type 1 conventional DCs (cDC1):  $CD45^+ Ly6G^- MHCII^+ CD64^- CD24^+ CD103^+ CD11b^-$ , type 2 conventional DCs (cDC2):  $CD45^+ Ly6G^- MHCII^+ CD64^- CD24^+ CD103^- CD11b^+$ ,  $Ly6C^+$  monocytes (Mo):  $CD45^+ Ly6G^- MHCII^- CD64^+ CD11b^+ Ly6C^+ CD11c^-$ ,  $Ly6C^-$  Mo:  $CD45^+ Ly6G^- MHCII^- CD64^+ CD11b^+ Ly6C^- CD11c^+$ , liver monocyte-derived macrophages (Macs):  $CD45^+ Ly6G^- MHCII^+ CD64^+ CD11b^+ F4/80^{lo}$ , Kupffer cells (KC):  $CD45^+ Ly6G^- MHCII^+ CD64^+ CD11b^{lo} F4/80^+$ , basophils:  $CD45^+ Lin B (CD3\epsilon, NK1.1, CD11c, Ter119, CD5, CD19, Gr-1)^- Fc\epsilon R1a^+ CD11b^+ CD49b^+ Ckit^-$ , mast cells:  $CD45^+ Lin B^- Fc\epsilon R1a^+ CD11b^- CD49b^- Ckit^+$ . The gating strategies used to identify lung macrophage populations are shown in Figure 2.2C. Alveolar macrophages (AMacs):  $CD45^+ Ly6G^- CD11c^+ SiglecF^+$ , interstitial macrophages (IMacs):  $CD45^+ Ly6G^- MHCII^+ F4/80^+ CD11c^- SiglecF^-$ , monocyte-derived macrophages (MoMacs):  $CD45^+ Ly6G^- MHCII^+ F4/80^+ CD11c^+$ .





### **2.2.6 ILC/ILC2 enrichment**

For FACS sorting of ILC2s prior to in vitro stimulation or RNA extraction, primary leukocyte cell suspension was enriched for ILC2s using EasySep mouse ILC2 enrichment kit (STEMCELL Technologies) or for ILCs using EasySep mouse pan-ILC enrichment kit (STEMCELL Technologies) according to manufacturer's protocol with the following modification: normal rat serum (STEMCELL Technologies) was added to samples at 50  $\mu$ L/mL together with pan-ILC or ILC2 enrichment cocktail to optimize enrichment.

### **2.2.7 In vitro stimulation**

ILC2s were FACS-sorted from lung and liver after ILC or ILC2 enrichment and cell surface staining. 1000 cells were cultured in 200  $\mu$ L RPMI-1640 media + 10% FBS + 100 U/mL P/S + 50  $\mu$ M 2-ME, containing cytokines IL-33 (BioLegend) and IL-2 (Peprotech), IL-7 (BioLegend), IL-25 (BioLegend) or TSLP (Thermo Fisher Scientific) (10 ng/mL for Chapter 4, 5 ng/mL for Chapter 3), or 30 ng/mL PMA (Sigma) and 500 ng/mL ionomycin (Sigma). Culture supernatant was collected 48 or 72 hours later. For whole lung leukocytes cultures, single cell suspensions were prepared from B6 and *Rag1*<sup>-/-</sup> mice and 5 x 10<sup>5</sup> cells were cultured in 200  $\mu$ L volume as described above for 72 hours in the presence of 10 ng/mL (B6) or 5 ng/mL (*Rag1*<sup>-/-</sup>) IL-33 and TSLP.

### **2.2.8 Tissue homogenate preparation**

Lungs and livers were collected from naïve and IL-33 treated mice and homogenized in Hank's Balanced Salt Solution (HBSS) with EDTA and Halt protease inhibitor cocktail (Thermo Fisher

Scientific) at 200 mg/mL, following manufacturer's protocol. Total protein content was quantified using Protein quantification kit-rapid (Sigma) according to manufacturer's protocol.

### **2.2.9 Quantification of cytokines**

BALF samples and in vitro culture supernatants were analyzed for IL-5 and IL-13 using Thermo Fisher Scientific enzyme-linked immunosorbent assay (ELISA) kits according to the manufacturer's protocol. Lung and liver culture supernatants were analyzed for granulocyte-macrophage colony-stimulating factor (GM-CSF), IL-2, IL-4, IL-6, IL-9, IL-10 and TNF $\alpha$  by U-plex assay platform (Meso Scale Discovery), IL-5 and IL-13 by ELISA (Thermo Fisher Scientific). The tissue homogenate samples were analyzed for cytokines using IL-33 (Thermo Fisher Scientific), TSLP (Thermo Fisher Scientific) and IL-7 (Abcam) ELISA kits according to manufacturer's protocols.

### **2.2.10 IL-33 immunohistochemistry**

Lungs were inflated with 1 mL of 4% paraformaldehyde solution. Fixed lungs were embedded in paraffin and 4  $\mu$ m sections were prepared by the Centre for Translational and Applied Genomics (Vancouver, Canada). Immunohistochemical staining of lung sections were performed using a polyclonal goat anti-mouse IL-33 IgG (R&D systems) at 5  $\mu$ g/mL in normal serum (Vector Labs) as described before (83). IL-33 quantification was performed using ImmunoRatio (290).

### **2.2.11 Liver histology**

Median lobe of the liver was fixed in 10% formalin for >72 hours and later stored in 70% ethanol. Formalin fixed paraffin embedded sections (5  $\mu$ m thickness) were prepared and stained

with Hematoxylin and Eosin (H&E) staining by Wax-it Histology Services Inc (Vancouver, Canada). Sections were also stained for collagen fibers by picrosirius red stain kit (Abcam) according to manufacturer's protocol.

#### **2.2.12 RNA extraction**

For microarray analyses, ILC2s were FACS-purified after ILC or ILC2 enrichment and cell surface staining. Total ribonucleic acid (RNA) was extracted from purified ILC2s using TRIzol reagent (Thermo Fisher Scientific) according to manufacturer's protocol. For Real-time quantitative polymerase chain reaction (RT-qPCR) analyses, 15 – 35 mg of median lobe of the liver was homogenized using a pestle and total RNA was extracted as above.

#### **2.2.13 Microarray**

RNA quality check, complementary deoxyribonucleic acid (cDNA) preparation and microarray hybridization were performed at The Centre for Applied Genomics (Toronto, Canada). Briefly, RNA quality was assessed using Agilent 2100 Bioanalyzer and the samples with RNA integrity number (RIN) above 6 were selected for microarray analyses. RNA amplification and cDNA preparation were performed using GeneChip WT Pico Kit (Thermo Fisher Scientific). cDNA samples were hybridized to Affymetrix GeneChip Mouse Gene 2.0ST Array. Two (Chapter 4) or three (Chapter 3) samples per group were analyzed for gene expression profile by Flex Array 1.6.3 (Genome Quebec) after normalization using robust multi-array average (RMA) algorithm.

#### **2.2.14 Genes set enrichment analysis**

Gene set enrichment analysis (GSEA) was performed using GSEA v2.2.4 software available at <http://software.broadinstitute.org/gsea/index.jsp> (291). Briefly, genes were ranked in descending order based on the fold differences of expression values between two data sets and analyzed for the gene set collection C7: immunologic signatures (292) using default parameters.

#### **2.2.15 Visualization of Cytoscape network analyses**

In Chapter 3, differentially expressed gene sets ( $p < 0.05$ , no fold difference cut-off was applied) were analyzed using Cytoscape (v3.6.1) plugin BiNGO (Biological Network Gene Ontology tool) (v.3.0.3) to identify over-represented “Gene Ontology (GO) biological process” terms (293). The hypergeometric test was used to measure the statistical significance of the enrichments and the Benjamini & Hochberg method ( $p < 0.05$ ) was used to correct p-values. Resulting BiNGO output files were then visualized as functional overlapping networks using the Cytoscape plugin Enrichment Map (v.3.1.0) with the following parameters: P-value cut-off of 0.001, Q-value cut-off of 0.05, and Jaccard Coefficient cut-off of 0.25 (294). The nodes comprising the network were then clustered using the plugin Autoannotate (v.1.2) and the clusters were labelled manually by revising labels generated by the plugin.

#### **2.2.16 Reactome pathway analyses**

In Chapter 4, genes that are more than 1.5 fold differentially expressed in various comparisons were analyzed for over-represented *Mus musculus* pathways by reactome pathway database (<https://reactome.org>) without using the projection to human (295,296).

### 2.2.17 cDNA synthesis

For RT-qPCR analyses, cDNA was prepared from 1.5 µg RNA using high-capacity cDNA reverse transcription kit (Thermo Fisher Scientific) according to manufacturer's protocol.

### 2.2.18 RT-qPCR

RT-qPCR was carried out by StepOnePlus system (Thermo Fisher Scientific) using TaqMan fast universal PCR master mix (Thermo Fisher Scientific). Seventy-five ng of cDNA was used per reaction and the sets of probe/primers (Integrated DNA Technologies) summarized in Table 2.2 were used for detection. Changes in gene expression were analyzed relative to naïve samples using  $2^{-\Delta\Delta C_T}$  method (297). *Tbp* was used as a housekeeping gene for normalization.

Gene	Assay ID	Probe/primer	Sequence
<i>Colla1</i>	Mm.PT.58.7562513	Probe	5'-/56-FAM/CCGGAGGTC/ ZEN/CACAAAGCTGAACA/ 3IABkFQ/-3'
		Primer 1	5'-CGCAAAGAGTCTACATGTCTAGG- 3'
		Primer 2	5'-CATTGTGTATGCAGCTGACTTC-3'
<i>Acta2</i>	Mm.PT.58.16320644	Probe	5'-/56-FAM/CCGCTGACT/ ZEN/CCATCCCAATGAAAGA/ 3IABkFQ/-3'
		Primer 1	5'-GAGCTACGAACTGCCTGAC-3'
		Primer 2	5'-CTGTTATAGGTGGTTTCGTGGA-3'
<i>Timp1</i>	Mm.PT.58.30682575	Probe	5'-/56-FAM/AATCAACGA/ ZEN/GACCACCTTATACCAGCG/ 3IABkFQ/-3'
		Primer 1	5'-AGACAGCCTTCTGCAACTC-3'
		Primer 2	5'-CAGCCTTGAATCCTTTTAGCATC- 3'
<i>Tbp</i>	Mm.PT.39a.22214839	Probe	5'-/56-FAM/ACTTGACCT/ ZEN/AAAGACCATTGCACTTCGT/ 3IABkFQ/-3'
		Primer 1	5'-TGTATCTACCGTGAATCTTGGC-3'
		Primer 2	5'-CCAGAACTGAAAATCAACGCAG- 3'

Table 2.2: Table of probes/primers used for RT-qPCR analyses

### **2.2.19 Statistics**

GraphPad Prism 7 was used for data analyses. Unpaired or paired two-tailed t test, one-way ANOVA (analysis of variance) with Bonferroni correction, Kruskal-Wallis test followed by Dunn's multiple comparison test (where a population does not follow a normal distribution), or two-way ANOVA with Bonferroni correction was used to determine statistical significance, with a P value <0.05 being significant, as indicated in each figure. Data in graphs represent the mean  $\pm$  SEM (standard error of the mean). \*P<0.05, \*\*P<0.01, \*\*\*P<0.001, \*\*\*\*P<0.0001, n.s, not significantly different [P>0.05].

## **Chapter 3: Female and male mouse lung ILC2s differ in gene expression profiles and cytokine production**

### **3.1 Introduction**

Epidemiological studies have shown sex- and age- related disparities in the prevalence of asthma. At pre-pubertal ages, boys have a higher prevalence of wheezing and diagnosed asthma compared to girls (298–302). However, the trend switches at puberty, where females have increased incidence of asthma and its symptoms compared to males (303–307). It has also been shown that the sex-specific differences in the incidence of asthma is more pronounced in non-allergic asthma than in allergic asthma during reproductive age (308). These patterns of sex- and age- related differences in prevalence of asthma coincide with the fluctuation in female and male sex steroid hormones at various ages, suggesting their involvement. Multiple studies have also described more pronounced type 2 immune responses in females compared to males in OVA-induced mouse models of asthma (309–311).

Recent studies have shown sex-related differences in mouse ILC2 development and responsiveness. Warren et al. reported that ILC2s isolated from female mouse lungs were more responsive upon ex vivo cytokine stimulation compared to male ILC2s (312). Laffont et al. reported that male mice had reduced ILC2 progenitors in the BM and mature ILC2s in peripheral tissues compared to female mice due to inhibitory effects of androgen signaling on ILC2 differentiation. The percentages of proliferating ILC2 progenitors and mature ILC2s, determined by Ki67 expression, were also lower in male than female mice (214). Cephus et al. also found that post-pubertal female mice have higher numbers of ILC2s in the lung than male mice, whereas they did not see sex differences in ILC2 numbers in younger mice. They also reported



that male ILC2s have reduced sensitivity towards IL-2 stimulation due to negative regulation of CD25 (IL-2R $\alpha$ ) expression by androgen signaling (215). Interestingly, Kadel et al. demonstrated that there was a KLRG1 negative population of ILC2s in females that increased with age and partly contributed to the higher number of ILC2s in female lungs compared to male lungs in which this population was largely absent. They also showed that androgen signaling inhibited differentiation of BM ILCP into ILC2s (216). In contrast, Bartemes and colleagues reported a role of estrogen in the regulation of uterine but not lung ILC2s, demonstrating tissue-dependent effects of sex steroid hormones on ILC2s (313).

To further understand the ILC2 intrinsic and lung environmental effects on sex differences in ILC2 functions, I have investigated age-dependent functional differences in ILC2s in female and male lung as well as lung-draining medLN before and after IL-33 stimulation. Moreover, I have analyzed gene expression profiles of naïve and activated ILC2 and age-dependent changes in the amounts of ILC2-activating cytokines in the lung of male and female mice. Here, I show that there is no significant difference in the numbers of ILC2s between naïve male and female mouse lungs, contradicting previous reports (214–216), whereas female ILC2s respond more vigorously to IL-33 stimulation than male ILC2s. Overall, my results suggest female lung ILC2s are more prone to be activated by IL-33 than male ILC2s due to intrinsic differences in gene expression at naïve state.

## **3.2 Results**

I gave three daily i.n. injections of IL-33 (Figure 3.1A) into 8 week-old male and female mice and found greater numbers of ILC2s (2.7 fold) and eosinophils (3.3 fold) in female than male lungs (Figure 3.1B). Female ILC2s also expanded more significantly compared to male

ILC2s in the lung-draining medLN upon IL-33 stimulation (3.3 fold, Figure 3.1C). In contrast, the numbers of ILC2s and eosinophils in naïve male and female lungs or medLN were not significantly different, contradicting the recent reports by Laffont et al., Cephus et al. and Kadel et al. The amounts of IL-5 and IL-13 in BALF from the IL-33 treated 8 week-old female mice were also significantly higher compared to age-matched treated male mice (Figure 3.1D), while there was no difference in the percentages of intracellular IL-5<sup>+</sup> and/or IL-13<sup>+</sup> ILC2s between female and male lungs (Figure 3.1E) or medLN (Figure 3.1F). As ILC2s are thought to be regulated by Tregs, which express the IL-33 receptor ST2 (195,203), and differences between female and male Tregs have also been reported (314,315), I tested *Rag1*<sup>-/-</sup> mice, which are deficient in T and B cells. I.n. injections of IL-33 into 8 week-old *Rag1*<sup>-/-</sup> mice resulted in significant differences in the numbers of ILC2s and eosinophils between female and male lungs (Figure 3.1G), similar to WT mice, indicating that the ILC2 difference between sexes is independent of Tregs. These results were confirmed by in vitro IL-33 and TSLP stimulation of whole lung leukocytes from B6 (Figure 3.1H) and *Rag1*<sup>-/-</sup> (Figure 3.1I) mice.

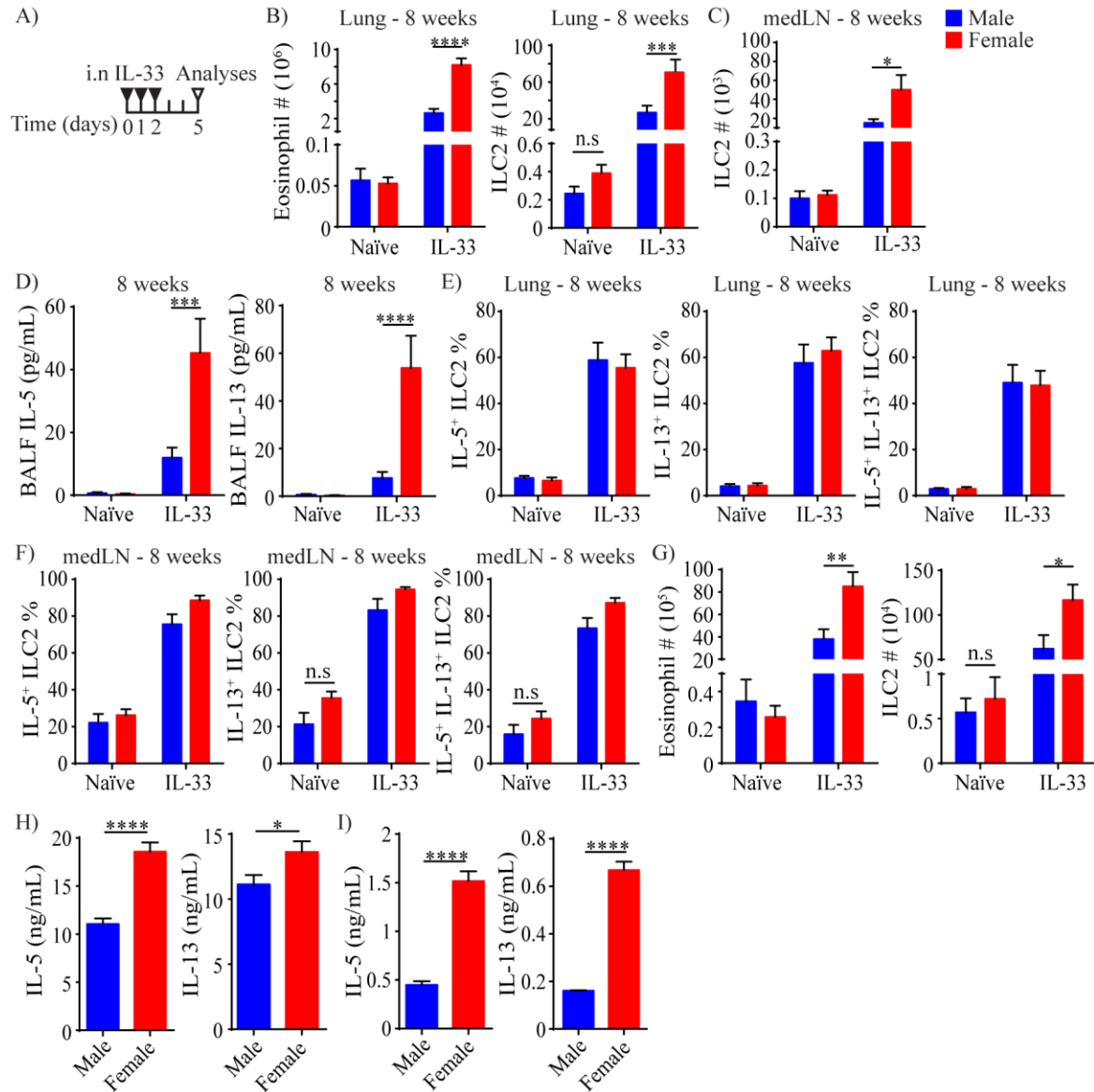


**Figure 3.1: Post-pubertal female lung ILC2s are more responsive to IL-33 than male ILC2s**

(A) Treatment scheme for in vivo experiments shown in B-G. (B-F) Lung eosinophil and ILC2 numbers (B), medLN ILC2 numbers (C), BALF cytokines (D) and percentages of intracellular IL5<sup>+</sup> and/or IL-13<sup>+</sup> lung (E) or medLN (F) ILC2s in untreated and IL-33 treated 8 week-old mice 3 days after 3 consecutive IL-33 injections. (G) Eosinophil and ILC2 numbers in untreated and IL-33 treated 8 week-old *Rag1*<sup>-/-</sup> mice 3 days after 3 consecutive IL-33 administrations. (H, I) Amounts of IL-5 and IL-13 in supernatant collected from male and female B6 (H) or *Rag1*<sup>-/-</sup> (I) whole lung leukocytes cultures stimulated with 10 ng/mL (H) or 5 ng/mL (I) IL-33 and TSLP for 72 hours. Red=female, blue=male. Data represented are mean  $\pm$  SEM. n=5-12;  $\geq 3$  independent experiments (B-F), n=3-7; 2 independent experiments (G), n=7-10; 1 experiment (H), n=4-5; 1 experiment (I). Two-way ANOVA with Bonferroni correction was used to assess statistical significance, with a P value <0.05 being significant. \*P<0.05, \*\*P<0.01, \*\*\*P<0.001, \*\*\*\*P<0.0001, n.s, not significantly different [P>0.05].

To test the effects of age on sex differences in ILC2 responsiveness, I gave three daily i.n injections of IL-33 into pre-pubertal mice. Unlike 8 week-old mice, there was no significant difference in eosinophil or ILC2 numbers between female and male lungs or medLN of 3 (Figures 3.2A, B) or 4 (Figures 3.2C, D) week-old mice upon IL-33 treatment. Similar to 8 week-old mice, there was no sex difference in the numbers of eosinophils or ILC2s in naïve lungs or medLN of 3 or 4 week-old mice. Moreover, there was no difference in the amounts of BALF cytokines (Figure 3.2E) or the percentages of intracellular cytokine positive ILC2s in the lungs (Figure 3.2F) or medLN (Figure 3.2G) between females and males.

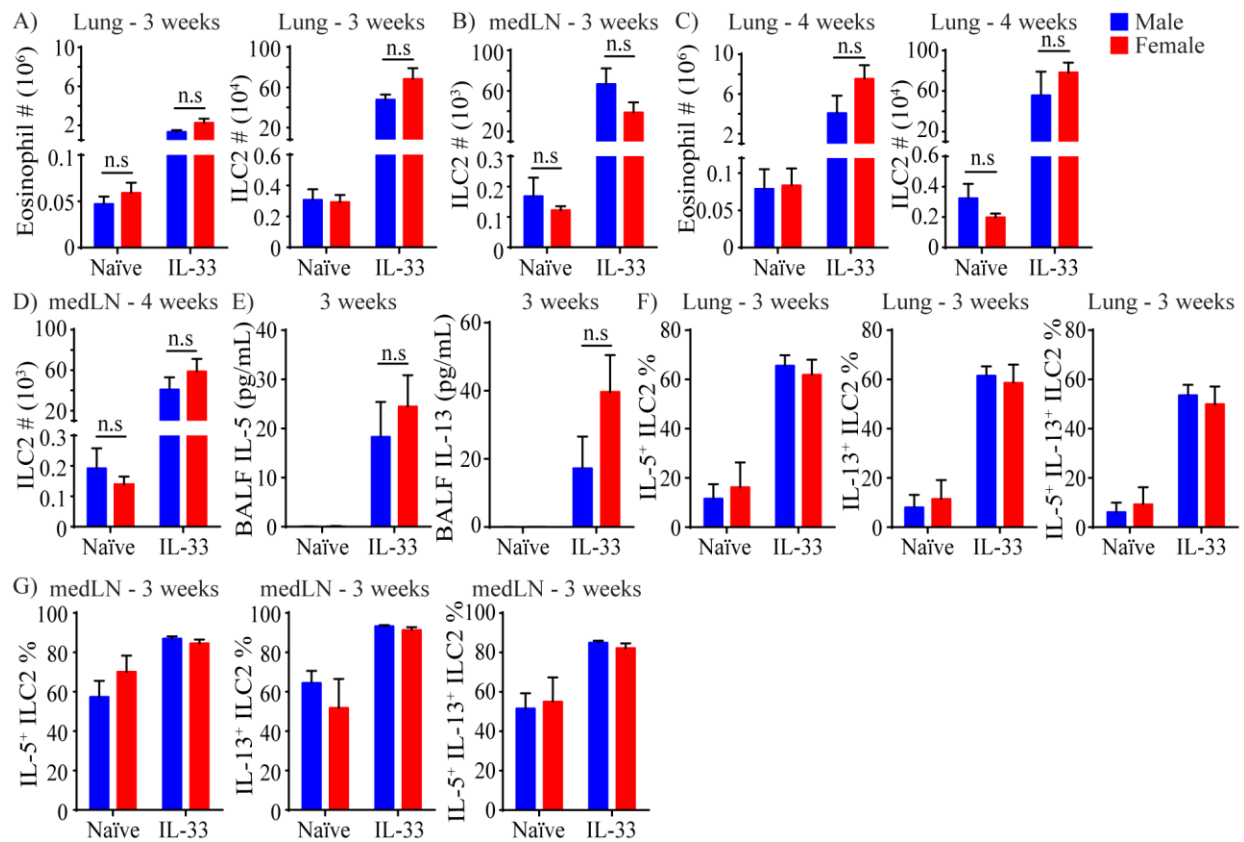


**Figure 3.2: Pre-pubertal female and male lung ILC2s respond similarly to IL-33 stimulation**

(A-D) Lung eosinophil and ILC2 numbers in 3 (A) or 4 (C) week-old mice and medLN ILC2 numbers in 3 (B) or 4 (D) week-old mice before and 3 days after IL-33 administrations (treatment scheme in Figure 3.1A). (E-G) BALF cytokines (E) and percentages of intracellular IL-5<sup>+</sup> and/or IL-13<sup>+</sup> lung (F) and medLN (G) ILC2s in untreated and IL-33 treated 3 week-old mice 3 days after the treatment. Red=female, blue=male. Data represented are mean  $\pm$  SEM. n=5-10; 3 independent experiments (A, B, E-G), n=4-6; 2 independent experiments (C-D). Two-way ANOVA

with Bonferroni correction was used to assess statistical significance, with a P value <0.05 being significant. n.s, not significantly different [P>0.05].

To determine whether female and male ILC2s have different kinetics of activation, I analyzed lungs and BALF of 8 week-old female and male mice at various time points after i.n IL-33 administration (Figure 3.3A). Both female and male eosinophils and ILC2s showed similar kinetics of expansion, although male eosinophil numbers peaked on day 7 whereas female eosinophils peaked on day 5 (Figure 3.3B). The amounts of IL-5 and IL-13 in BALF also increased similarly between females and males (Figure 3.3C), indicating that the kinetics of activation is similar. I also analyzed the expression of the proliferation marker Ki67 in naïve and IL-33 treated male and female ILC2s one day after three consecutive injections (day 3 in Figure 3.3A) to investigate whether female and male ILC2s differ in their ability to proliferate. Interestingly, significantly higher percentages of naïve female lung ILC2s expressed Ki67 compared to male lung ILC2s. However, once they were stimulated with IL-33, the difference was no longer present (Figure 3.3D), suggesting that both female and male ILC2s have similar ability to proliferate upon stimulation.

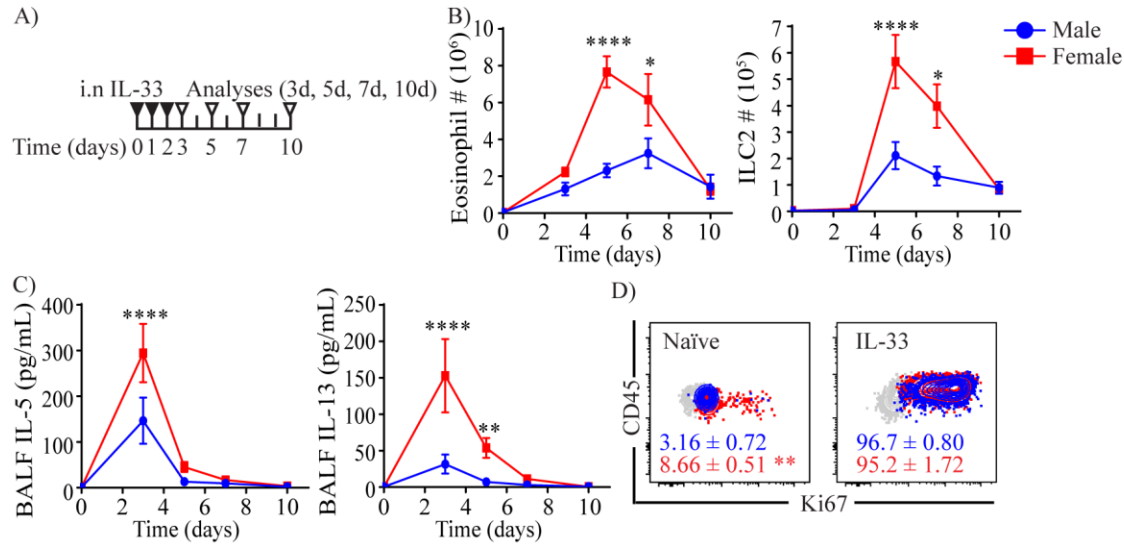


**Figure 3.3: Kinetics of ILC2 activation in female and male lungs**

(A) Treatment scheme for in vivo time-course analyses shown in B and C. (B, C) Eosinophil and ILC2 numbers (B) and BALF cytokines (C) were quantified at day 0 (naïve) and 1 day (day 3), 3 days (day 5), 5 days (day 7) and 8 days (day 10) after 3 consecutive IL-33 injections into 8 week-old mice. (D) Ki67 staining of male and female ILC2s before (left) and 1 day after (right) IL-33 injections (day 3 in A). Red=female, blue=male, grey=isotype control. Data represented are mean ± SEM. n=6-19; ≥2 independent experiments for all time points except d10, where n=4; 1 experiment (B, C), n=5; 1 experiment (D). Two-way ANOVA with Bonferroni correction was used to assess statistical significance, with a P value <0.05 being significant. \*P<0.05, \*\*P<0.01, \*\*\*\*P<0.0001.

Cephus et al. recently reported that IL-33 and TSLP are negatively regulated by male hormones in *A. alternata* stimulated mice (215). Because these cytokines are known to activate ILC2s, I measured the amounts of IL-33, TSLP and IL-7 in whole lung homogenate prepared from naïve male and female B6 mice at different ages. In young mice, the amount of IL-33 was similar in male and female lungs. Strikingly, the IL-33 levels increased at 6 weeks of age in female lungs, resulting in significantly higher amounts of endogenous IL-33 compared to male lungs (Figure 3.4A). Immunohistochemical analyses of naïve lung sections also showed more IL-33 positive cells in 8 week-old female than male lungs (Figure 3.4B). The expression of IL-7 (Figure 3.4C) and TSLP (Figure 3.4D) also showed similar age dependent changes. I have also measured IL-7 and TSLP amounts after IL-33 injections to determine whether IL-33 induces differential expression of IL-7 and TSLP in male and female lungs. To this end, I selected 6

week-old mice as there is no significant difference in IL-7 and TSLP amounts between naïve male and female lungs at this age, and the effects of IL-33 on the amounts of IL-7 and TSLP can be directly assessed. I.n. injections of IL-33 into 6 week-old mice caused the amount of IL-33 in male and female lungs to increase as expected (Figure 3.4E), while there was no significant change in the amount of IL-7 and TSLP both in male and female mice (Figures 3.4F, G). IL-7 and TSLP levels were also similar in WT and *Il33<sup>+/-</sup>* lungs (Figure 3.4H), further confirming that IL-33 does not induce IL-7 or TSLP expression. To test whether the differences in the amount of endogenous IL-33 in naïve mice are responsible for the differences between female and male ILC2s in their responses to i.n injections of IL-33, I compared female and male *Il33<sup>-/-</sup>* mice. Similar to WT mice, there was no difference in the numbers of ILC2s in post-pubertal male and female *Il33<sup>-/-</sup>* lungs before stimulation, while *Il33<sup>-/-</sup>* female lungs had less eosinophils compared to male lungs (Figure 3.4I). Three daily i.n. injections of IL-33 into post-pubertal male and female *Il33<sup>-/-</sup>* mice revealed statistically significant differences in the numbers of ILC2s and eosinophils between the sexes. Therefore, the differences in ILC2 responsiveness between male and female lungs are independent of endogenous IL-33.

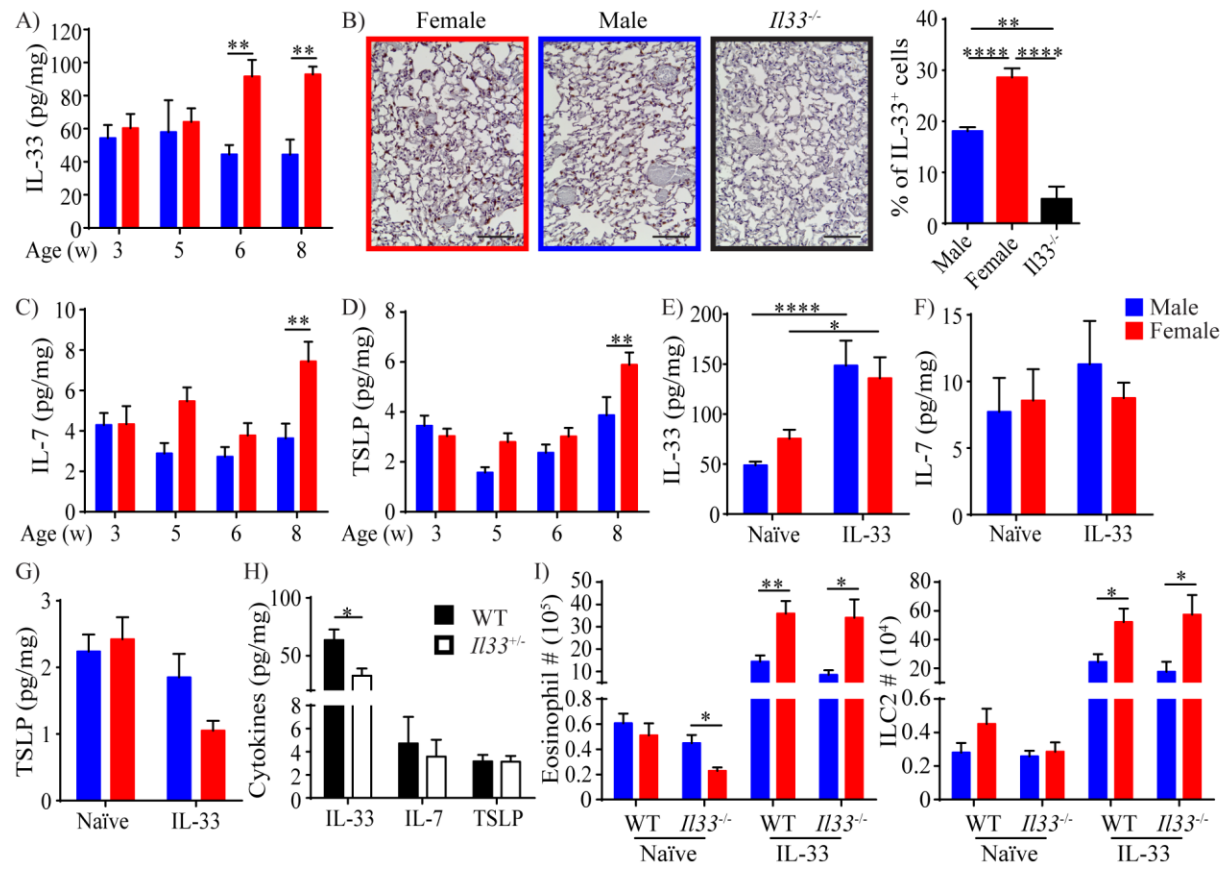


**Figure 3.4: IL-33, IL-7 and TSLP are differentially expressed in naïve female and male lungs**

(A) The amounts of IL-33 in naïve mouse whole lung homogenates were measured using ELISA at different ages. (B) Immunohistochemical analysis and quantification of IL-33 in naïve 8 week-old lungs (scale bar=100  $\mu$ m). (C, D) The amounts of IL-7 (C) and TSLP (D) in naïve mouse whole lung homogenates were measured as in A. (E-G) The amounts of IL-33 (E), IL-7 (F) and TSLP (G) in 6 week-old mouse whole lung homogenates were measured by ELISA one day after three daily i.n. injections of IL-33. (H) The amounts of IL-33, IL-7 and TSLP were quantified in the whole lung homogenates prepared from WT (black bars) and *Il33*<sup>+/-</sup> (heterozygous, white bars) mice. (I) Eosinophil and ILC2 numbers in post-pubertal WT (*Il33*<sup>+/+</sup>) and *Il33*<sup>-/-</sup> male and female mouse lungs before and 3 days after 3 consecutive IL-33 administrations. Red=female, blue=male. Data represented are mean  $\pm$  SEM. n=6-8;  $\geq 2$  litters (A, C-D), n=4; 4 pictures per lung (B), n=4-11;  $\geq 2$  independent experiments (E-G), n=3; 2 independent experiments (H), n=7-17;  $\geq 3$  independent experiments (I). Two-way ANOVA with Bonferroni correction (A, C-G, I), one-way ANOVA with Bonferroni correction (B) or unpaired two-tailed t-test (H) was used to assess statistical significance, with a P value <0.05 being significant. \*P<0.05, \*\*P<0.01, \*\*\*\*P<0.0001.

In vitro stimulation of ILC2s purified from 8 week-old naïve male and female lungs demonstrated that female ILC2s produced more type 2 cytokines than male ILC2s (Figure 3.5A), demonstrating that female and male ILC2s differ in their ability to produce cytokines upon stimulation. The result also suggested a cell intrinsic difference between male and female ILC2s.



To further investigate intrinsic sex differences in ILC2s, I performed microarray analyses of purified 8 weeks old naïve male and female lung ILC2s. Overall, 4% of the genes were differentially expressed, the majority of which were autosomal rather than sex-linked genes (Figures 3.5B, C). Detailed analyses demonstrated no significant differences in the expression of *Il2ra* encoding CD25, *Il1rl1* encoding ST2, *Gata3*, *Rora*, *Il7r* encoding CD127, which are known to be important for ILC2 development and functions (Figure 3.5D). GSEA of the naïve ILC2 microarray data set showed that female ILC2s were enriched for a gene signature of memory T cells, with leading edge genes including *Lck*, *Car5b*, *Manea*, and *Cmcl* (Figure 3.5E). To further understand the gene expression data, the set of genes that were differentially expressed between male and female ILC2s were analyzed for over-represented GO terms using BiNGO plugin for Cytoscape network analysis platform and visualized as interaction networks using Cytoscape and Enrichment Map (293,294). Naïve female ILC2s showed an over-representation of cellular metabolism-related networks, including protein metabolic process and electron transport chain (Figure 3.5F). This implies that female ILC2s are more metabolically active than male ILC2s at naïve state, in line with the increased levels of basal proliferation in naïve female lung ILC2s.

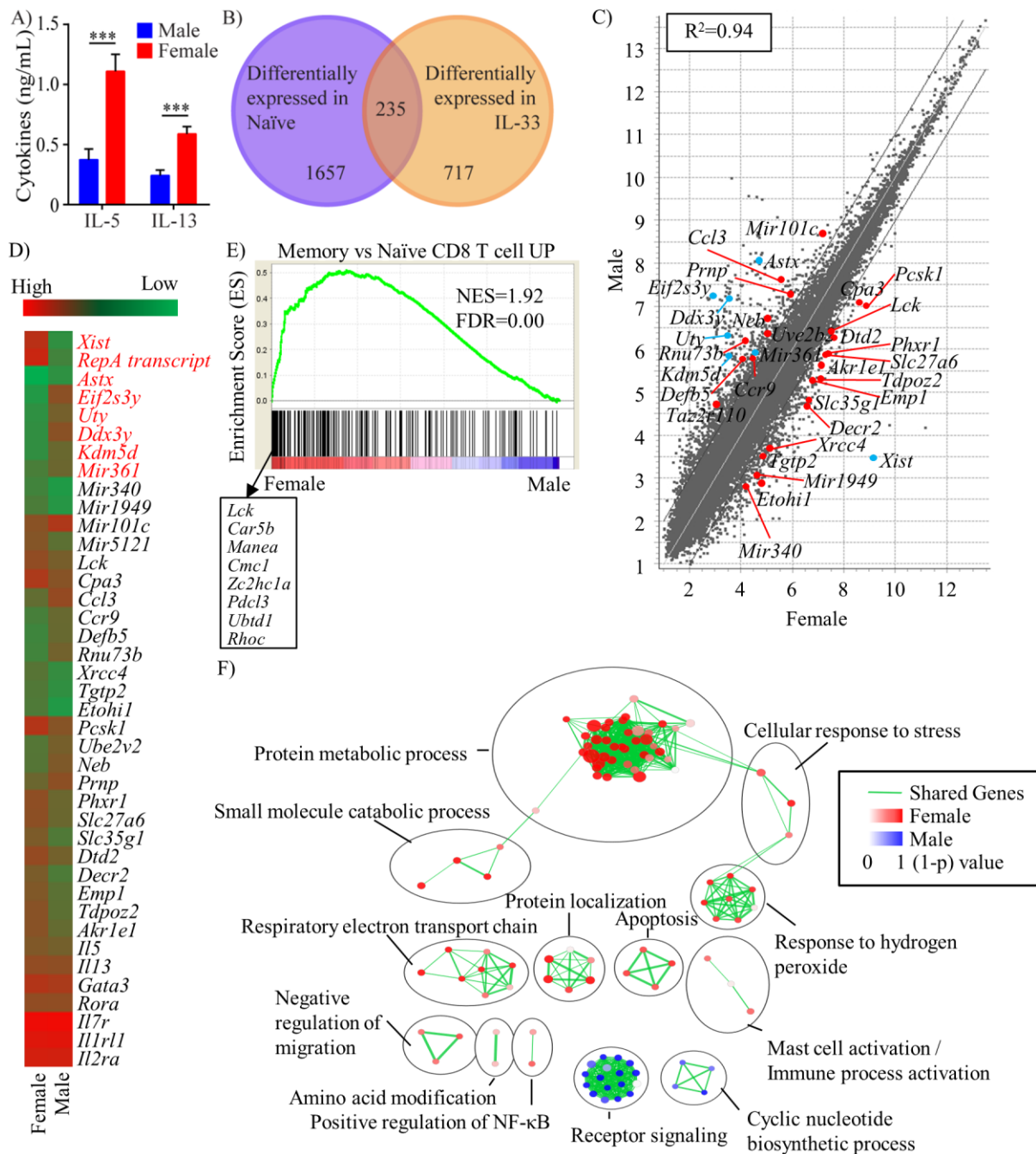


**Figure 3.5: Gene expression analyses of naïve female and male lung ILC2s**

(A) The amounts of IL-5 and IL-13 produced by purified naïve 8 week-old male and female ILC2s stimulated with 5 ng/mL IL-33 and TSLP for 48 hours. Red=female, blue=male. Data represented are mean  $\pm$  SEM.  $n=10-15$ ; 2 independent experiments. Unpaired two-tailed t-test was used to determine statistical significance, with a P value  $<0.05$  being significant. \*\*\* $P<0.001$ . (B) A Venn diagram showing numbers of differentially expressed genes. Purple=naïve female and male comparison, orange=IL-33 treated female and male comparison (see Figure 3.6). (C) Scatter plot of 8 week-old naïve male and female mouse lung ILC2 gene expression in log2 scale.  $R^2$  value demonstrates the similarities between male and female ILC2s (1=identical). Grey lines show fold change=2. Blue=sex-linked genes, red=autosomal genes.  $n=5-14$  mice per sample, 3 samples per group. (D) Relative expression levels of selected genes in 8 week-old naïve male and female mouse lung ILC2s. Annotated genes were

selected if they were expressed at intermediate to high levels ( $>5.0$  in log2 scale) in at least one sex and were more than 2 fold differentially expressed between male and female. Genes highlighted in red are sex-linked genes. (E) GSEA of naïve male and female lung ILC2 microarray data is shown in (C). Leading edge genes are shown in the box. (F) BiNGO analyses comparing naïve female and male mouse lung ILC2 gene expression. Cytoscape and Enrichment Map were used for visualizing the functional clusters enriched in each sex. Nodes represent enriched GO terms. Node size is proportional to total number of genes in each gene set, and node colour to the 1-p value. Edges depict gene set overlap between nodes and thickness represents fraction of shared genes.

I also compared the gene expression profiles of ILC2s purified from IL-33 injected male and female lungs (8 week-old) and found that they were remarkably similar to each other (Figure 3.6A). The number of differentially expressed genes between activated male and female ILC2s was much less than that between naïve male and female ILC2s (Figure 3.5B). Similar to naïve male and female ILC2s, there was no significant difference in the expression of *Il2ra*, *Il1rl1*, *Gata3*, *Rora*, and *Il7r*. However, in agreement with cytokine quantification in BALF (Figure 3.1D) and purified ILC2 culture (Figure 3.5A), *Il5* was more highly expressed in activated female than male ILC2s (Figure 3.6B). Analyses of the differentially expressed gene sets for over-represented GO terms showed that female ILC2s isolated after IL-33 injections were characterized by activation-related networks, namely leukocyte activation, signal transduction and MyD88-dependent signaling pathway (Figure 3.6C). Unexpectedly, activated male ILC2s were defined by cell proliferation-related networks, which may indicate that it takes a greater upregulation of proliferation-related genes in male ILC2s than female ILC2s due to their “more naïve” state before stimulation (Figure 3.5E). These results suggested that ILC2 intrinsic differences in gene expression may make naïve female ILC2s more prone to be activated and proliferate than naïve male ILC2s.

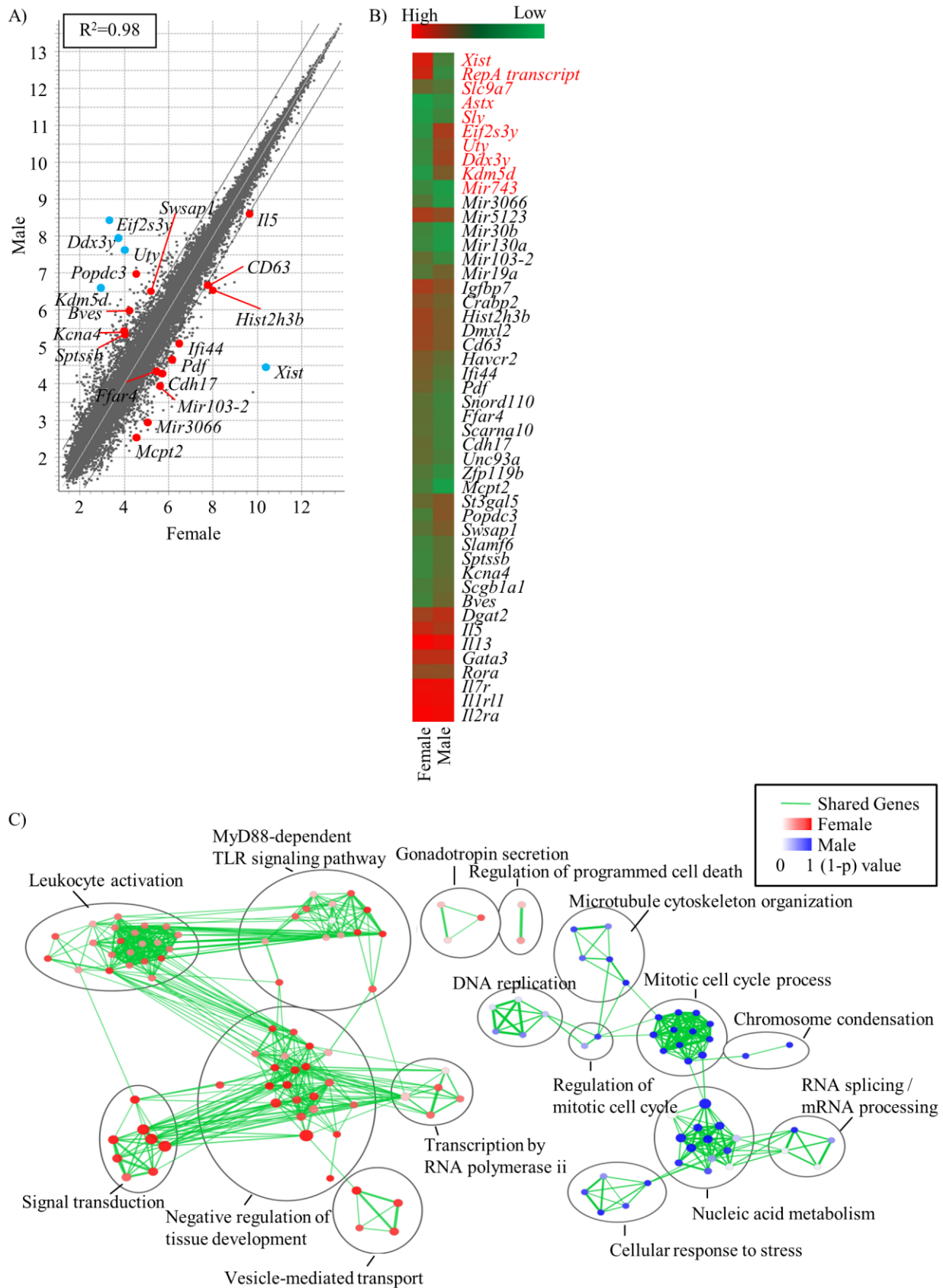


**Figure 3.6: Gene expression analyses of activated female and male lung ILC2s**

(A) Scatter plot of gene expression in male and female ILC2s purified from 8 week-old mouse lungs one day after three consecutive injections of IL-33. Gene expression values are in log<sub>2</sub> scale. R<sup>2</sup> value demonstrates the similarities between male and female ILC2s (1=identical). Grey lines show fold change=2. Blue=sex-linked genes, red=autosomal genes. n=2 mice per sample, 3 samples per group. (B) Relative expression levels of selected genes in 8 week-old activated male and female mouse lung ILC2s. Genes highlighted in red are sex-linked genes. (C) BiNGO analyses comparing activated female and male mouse lung ILC2 gene expression. Cytoscape and Enrichment Map were used for visualizing the functional clusters enriched in each sex. Nodes represent enriched GO terms. Node size is proportional to total number of genes in each gene set, and node colour to the 1-p value. Edges depict gene set overlap between nodes and thickness represents fraction of shared genes.

### 3.3 Discussion

I have shown that post-pubertal female ILC2s are more responsive to cytokine stimulation than their male counterparts using in vivo animal models and in vitro cell cultures. Although transcriptome analysis of naïve male and female lung ILC2s identified differentially expressed genes, I was not able to find individual genes that are associated with ILC2 functions or development. On the other hand, GSEA of the same data set showed that the genes that are more highly expressed by naïve female than male ILC2s are enriched in a set of genes more highly expressed in memory than naïve T cells. These results suggest that female ILC2s are more responsive to stimulation than male ILC2s, resembling the relationship between memory and naïve T cells. BiNGO analyses of differentially expressed genes also suggest that female ILC2s may be more metabolically active than male ILC2s at naïve state, consistent with the idea that female lung ILC2s are more prone to be activated, similar to memory T cells. Gene expression analyses of activated male and female ILC2s did not reveal specific genes that may play a role in determining the differences in male and female ILC2 responsiveness. However, the notion that activated female ILC2s are enriched for activation-related genes, whereas those from male are enriched for proliferation-associated genes is interesting. As percentages of Ki67<sup>+</sup> ILC2s in naïve male lungs are lower than female lungs, while they are comparable upon IL-33 treatment, this

implies that a greater proportion of male than female ILC2s requires upregulation of cell cycle-related genes.

Recent reports by Laffont et al., Cephus et al. and Kadel et al. showed that ILC2 development and their CD25 expression are negatively regulated by male sex hormones (214–216), explaining a potential mechanism behind epidemiologically observed sex-related differences in asthma prevalence. However, contradictory to those previous reports, I did not find a significant difference in lung ILC2 numbers at any ages or strains tested, or the expression of *Il2ra* encoding CD25 (Figure 3.5D) between naïve male and female lung ILC2s. Moreover, I also did not find any differences in the numbers of ILC2s in the lung, SI, skin or liver of naïve male and female mice (Appendix A.1), indicating that ILC2 development is not likely regulated by sex. Differences in mouse strains, models and animal facilities, possibly including the microbial environment, may be responsible for the discrepancy in our results. It is also important to note that the number of ILC2s detected in mouse lungs in these studies is noticeably higher than that shown here, which suggest that tissue processing protocols or identification of ILC2s may also contribute to the discrepancy in our results. It should also be noted that most ILC2s in adult mouse lungs are tissue resident, and very few ILC2s develop from BM progenitors in adult mice (87). Therefore, it is unlikely that differences in ILC2 development from BM progenitors between male and female mice significantly contribute to the lung ILC2 population.

Transplantation of female and male BM cells into irradiated female recipients did not result in any sex-related differences in ILC2 or eosinophil numbers (Appendix A.2). These data indicate that ILC2 intrinsic differences are overridden by environmental differences, including sex steroid hormones and cytokines, after long-term exposure, suggesting the importance of environmental contribution to ILC2 responsiveness. The role of sex steroid hormones in ILC2

regulation was not investigated here as others demonstrated that androgen negatively regulates lung ILC2s while female hormones have no effects by using slow-release hormone pellets and/or gonadectomy models (214–216). Instead, I have shown age-dependent differences in the expression of IL-33, IL-7 and TSLP between naïve male and female lungs (Figure 3.4A-D). However, there is no significant difference in the amount of IL-33 in male and female lungs after IL-33 injections (Figure 3.4E). Furthermore, WT and *Il33*<sup>-/-</sup> mice showed similar sex-related differences in ILC2 expansion and eosinophilia (Figure 3.4I), indicating that the differences in the levels of endogenous IL-33 in naïve male and female lungs were not responsible for the disparity in responsiveness between male and female ILC2s. Therefore, the significance of the differences in the amounts of IL-33, IL-7 and TSLP in naïve male and female lungs in terms of ILC2 function is unclear. As activation of purified ILC2s by IL-33 in vitro requires an additional stimulus, which can be provided by IL-7 or TSLP (26), it seems likely that higher amounts of these cytokines in female than male mouse lungs may contribute to enhanced ILC2 activation in IL-33-injected female mice. It is interesting to note that i.n. IL-33 injections did not cause upregulation of IL-7 (Figure 3.4F) or TSLP (Figure 3.4G) and reduced amounts of endogenous IL-33 did not affect the amounts of IL-7 or TSLP in *Il33*<sup>+/-</sup> mice (Figure 3.4H). These results indicate that IL-7 and TSLP expression is independent of IL-33 and higher levels of endogenous IL-7 and TSLP in female than male lungs at steady state may together contribute to increased responsiveness of female lung ILC2s compared to male lung ILC2s. As the levels of these epithelium-derived cytokines increase with age in female lungs, I have also investigated the effects of short-term exposure to estrogen and progesterone via intraperitoneal or subcutaneous routes, but they did not induce increase in the amounts of these cytokines (data not shown).

These results indicate that epithelium-derived cytokines are not regulated by female sex steroid hormones or long-term exposure is required to observe any effects.

This study suggested that multiple factors including ILC2 intrinsic and lung environmental components differ in male and female lungs. It is likely that sex differences in ILC2 responses and type 2 inflammation involve multiple mechanisms, and the effect of each component in isolation may not be significant. Overall, I have shown that post-pubertal female ILC2s produce more cytokines upon stimulation than male ILC2s. It remains to be determined whether this is due to differences in gene expression potentially driven by the effects of sex hormones on ILC2s or the lung environment.

While investigating the sex difference in ILC2 numbers in various tissues, I detected expansion of ILC2s in circulation after i.n. IL-33 administration. This goes against the idea of ILC tissue residency (86), suggesting migratory potential of lung ILC2s. The migration of tissue resident lung ILC2s is investigated in the next chapter.



## Chapter 4: Activation-induced migration of lung ILC2s to the liver

### 4.1 Introduction

Many lymphocytes, including T, B and NK cells, constantly circulate through blood and lymphoid organs. These cells patrol throughout our body until they encounter antigens, providing systemic protection against invading pathogens. In contrast, some lymphocytes reside in non-lymphoid tissues, mainly at barrier sites such as the skin and mucosal tissues, providing tissue specific local protection as an immune sentinel. They are also important in sensing perturbations and maintaining tissue homeostasis. Tissue resident lymphocytes include unconventional T cells such as NKT cells and  $\gamma\delta$  T cells (316).

ILCs, including ILC2s, have previously been shown to be tissue resident. Gasteiger et al. used parabiosis models to show that more than 95% of ILCs are tissue resident at steady state for at least 3 months after parabiosis surgery, with a minimal renewal from precursors or mature ILCs in circulation. Moreover, ILCs remained largely tissue resident even during systemic autoimmunity and parasitic infections, although they did detect increase in ILC2s originating from paired parabionts (donor-derived) during the chronic phase of parasite infection, suggesting some degree of recruitment from hematogenous sources (86). More recently, Schneider et al. used fate-mapping system to demonstrate that adult-derived ILC2s largely remain tissue resident for a long time and are rarely replenished by circulating progenitors in most tissues (87).

On the contrary, there are accumulating numbers of reports suggesting migratory potential of ILC2s. Stier et al. found egress of ILC2 progenitors out of the BM upon intravenous (i.v.) injections of IL-33 and i.n. injections of fungal allergen *A. alternata* (317). Karta et al. demonstrated that ILC2s ( $\text{Lin}^- \text{Thy1}^+$  cells) are recruited from the BM to the lung in mice receiving i.n. *A. alternata* injections (318). They also showed that this process was mediated by

$\beta 2$  ITG. Huang et al. reported that i.p. injections of IL-25 induced migration of KLRG1<sup>+</sup> ST2<sup>-</sup> iILC2s from the intestine to the lung and differentiation into natural ILC2s (129,130). This was through S1P-mediated chemotaxis (130). More recently, Ricardo-Gonzalez et al. described the ability of intestinal and lung ILC2s to circulate upon parasite *N. brasiliensis* infection, demonstrating that ILC2s can mediate transition of local immune response to systemic type 2 responses (319).

Despite these reports, the fate of lung resident ILC2s upon activation is largely unknown. As our group has previously detected increase in ILC2 numbers in lung draining medLN (76) and PB after i.n. IL-33 administrations (unpublished data), I hypothesized that lung ILC2s exit the lung, enter circulation and reach other tissues upon activation. To test this hypothesis, I analyzed ILC2s in various mouse tissues after i.n. IL-33 administration aiming to investigate interorgan trafficking of ILC2s. Here, I show that activation of lung ILC2s by IL-33 induces upregulation of CD103 by lung ILC2s and CD103<sup>-</sup> ILC2s migrate out of the lung, circulate through PB and reach the liver. The migratory ILC2s are phenotypically and functionally different from the tissue-resident subset that remains in the lung after activation.

## 4.2 Results

We have previously shown that i.n. administrations of the protease allergen papain cause expansion of lung ILC2s (76). The papain treatment (Figure 4.1A) also increased the number of ILC2s in PB from less than 100 cells/mL in naïve mice to almost 800 cells/mL (Figure 4.1B, left), while liver ILC2s also increased by about 6 fold upon i.n. papain administration (Figure 4.1B, right). As the activation of lung ILC2s by papain is mediated by IL-33 released by epithelial cells (30), I tested the effects of i.n. administration of recombinant IL-33. I gave three

daily i.n. injections of IL-33 into B6 mice and analyzed different tissues at various time points (Figure 4.1C). In agreement with our previous report (76), ILC2s in the lung expanded by almost 175 fold upon i.n. IL-33 treatment, underwent a contraction phase, but remained high in number for 2 months post injections (Figure 4.1D). The number of ILC2s in PB and spleen similarly increased in the IL-33 treated mice and declined to the naïve mouse levels in 2-4 weeks (Figures 4.1E, F). In the liver, ILC2 numbers peaked on day 5, then quickly decreased but remained higher than those in naïve liver for 2 months (Figure 4.1G). I also quantified ILC2s in the SI and mLN on day 7. The number of intestinal and mLN ILC2s did not significantly increase upon i.n. IL-33 injections (Figure 4.1H). For the following sections, I have mostly focused on liver ILC2s as they undergo significant expansion, the numbers remain higher than those in naïve liver for a long time, and ILC2s have previously been implicated in hepatic fibrosis (65).

To determine whether intranasally administered IL-33 entered circulation and caused systemic activation of ILC2s, I measured IL-33 in tissue homogenate prepared from the lung and liver as well as serum of the IL-33 treated mice one day after three daily i.n. injections. The amount of IL-33 increased in the lung after the IL-33 treatment as expected but did not increase in the liver and was undetectable in serum (Figure 4.1I, data not shown). These results suggest that the expansion of the ILC2 populations in PB, spleen and the liver in the i.n. IL-33 administered mice was unlikely due to systemic activation of ILC2s.

It is worth noting that the liver tissues used in this study were not perfused because percentages of ILC2s and eosinophils in perfused liver were higher than in non-perfused livers, most likely due to the elimination of circulating cells by perfusion. Thus, that the proportion of ILC2s/eosinophils in circulation does not make a significant contribution to the quantification of liver ILC2s/eosinophils (Appendix B.1).

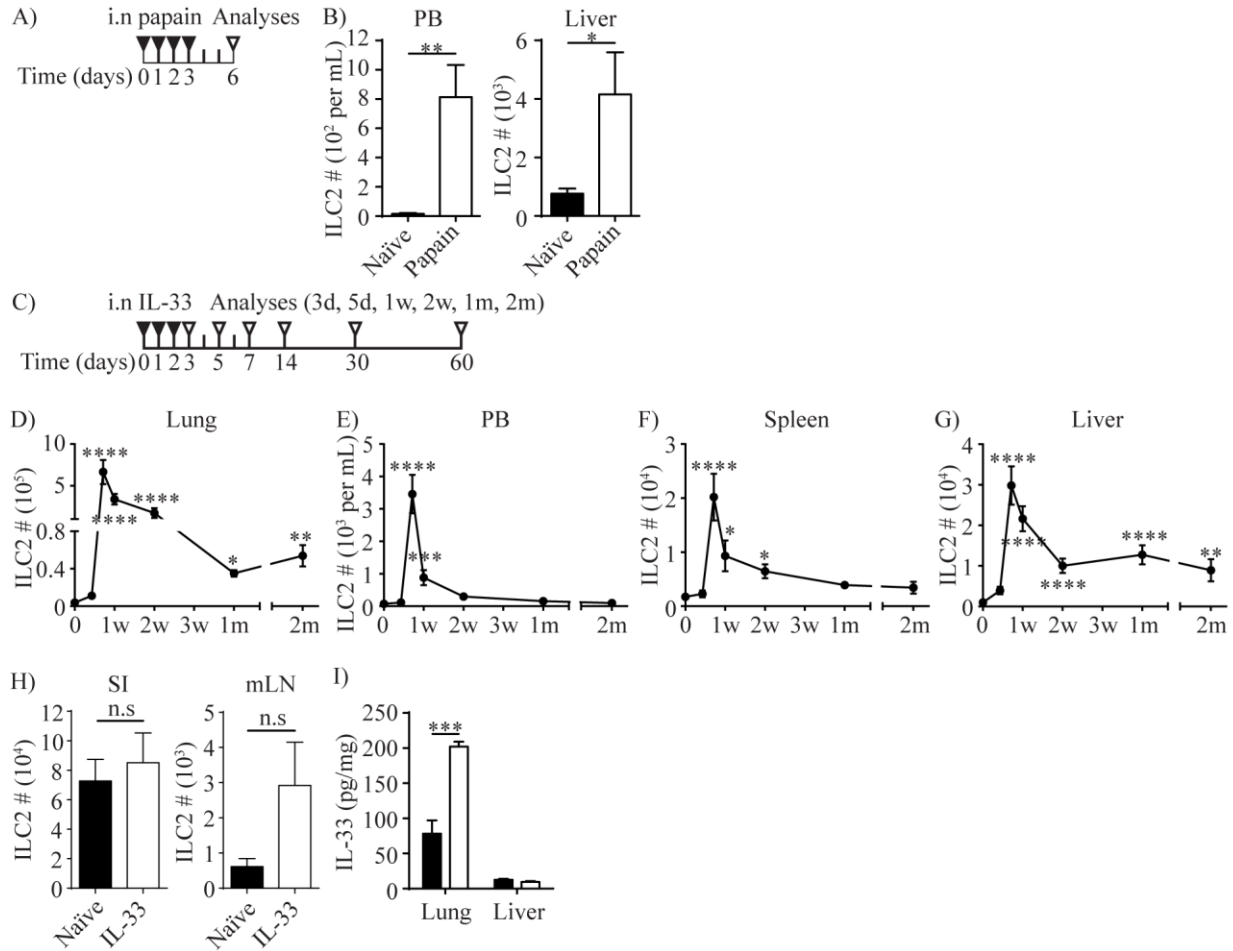


**Figure 4.1: ILC2s expand in peripheral tissues after stimulation in the lung**

(A) Female mice received four daily i.n. papain injections and were analyzed on day 6. (B) ILC2s were quantified in PB and liver. Black=naïve, white=papain treated. (C) Female mice received three daily i.n. injections of IL-33 and were analyzed at various time points. d=day, w=week, m=month. (D-G) The number of ILC2s in the lung (D), PB (E), spleen (F) and liver (G) after i.n. IL-33 administrations. Day 0 is naïve, w=week, m=month. Asterisks indicate significant differences from naïve. (H) Female mice received three daily i.n. injections of IL-33 and were analyzed on day 7 (see C). ILC2s were quantified in the SI and mLN. (I) Female mice received three daily i.n. injections of IL-33 and the amount of IL-33 was measured in lung and liver homogenate on day 3 (see C). Black=naïve, white=IL-33 treated. Data represented are mean  $\pm$  SEM. n=5-10; 1 (PB) or 2 (liver) independent experiments (B), n=4-48;  $\geq 3$  independent experiments (D-G), n=6; 2 independent experiments (H), n=4; 1 experiment (I). Unpaired two-tailed t test (B, H and I) or Kruskal-Wallis test followed by Dunn's multiple comparison test (D-G) was used to determine statistical significance, with a P value  $<0.05$  being significant. \*P $<0.05$ , \*\*P $<0.01$ , \*\*\*P $<0.001$ , \*\*\*\*P $<0.0001$ . n.s, not significantly different [P $>0.05$ ].

To determine whether i.n. administration of IL-33 induces proliferation of lung-resident ILC2s and their migration to the liver through PB, we generated parabiotic mice by conjoining CD45.2<sup>+</sup> B6 and CD45.1<sup>+</sup> Pep3b mice. Five to six weeks after the surgery, we gave three daily

i.n. administrations of IL-33 (or PBS for control) into B6 mice and analyzed various tissues from both the B6 and Pep3b mice on day 7 (Figure 4.2A). In PBS treated control mice, most (more than 92%) ILC2s in the lung, BM and SI were of host origin in both B6 and Pep3b mice as previously reported (86), whereas smaller fractions of ILC2s in PB and spleen were host-derived although the percentages varied due to small numbers of ILC2s in PBS control mice (Figures 4.2B-G). Upon i.n. IL-33 administration into B6 mice, both CD45.1<sup>+</sup> and CD45.2<sup>+</sup> ILC2s expanded in the lung of B6 mice while their ratio remained unchanged from control mice, indicating an expansion of lung resident ILC2s rather than recruitment from other tissues. In the Pep3b partners, the number of lung ILC2s slightly increased due to an increase in CD45.2<sup>+</sup> cells while CD45.1<sup>+</sup> ILC2 numbers did not significantly change (Figure 4.2B). ILC2 numbers in PB and spleen also increased in both B6 and Pep3b mice, and the increases were almost entirely accounted for by the expansion of CD45.2<sup>+</sup> ILC2s (Figures 4.2C, D). In the liver of B6 mice, ILC2 numbers significantly increased by the IL-33 treatment due to a large increase in CD45.2<sup>+</sup> ILC2s while the percentage of CD45.1<sup>+</sup> cells decreased. In Pep3b liver, CD45.2<sup>+</sup>, but not CD45.1<sup>+</sup>, ILC2 numbers significantly increased (Figure 4.2E). IL-33 administration had little effect on ILC2s in the BM and SI of both B6 and Pep3b mice (Figures 4.2F, G). The i.n. IL-33 had no effect on the total numbers of B cells in the lung or liver (data not shown) and the ratio between CD45.1<sup>+</sup> and CD45.2<sup>+</sup> remained 1:1 as expected for circulating cells (Figures 4.2H, I). To exclude the possibility that genetic differences between B6 and Pep3b mice might contribute to those results, we also administered i.n. IL-33 into Pep3b, instead of B6, mice. The results were very similar to those with IL33 treatment into B6 mice (Appendix B.2). These results together demonstrate that lung resident ILC2s locally expand upon i.n. IL-33 treatment rather than being

recruited from elsewhere, and some activated lung ILC2s leave the lung, circulate in blood and mostly settle in the liver.

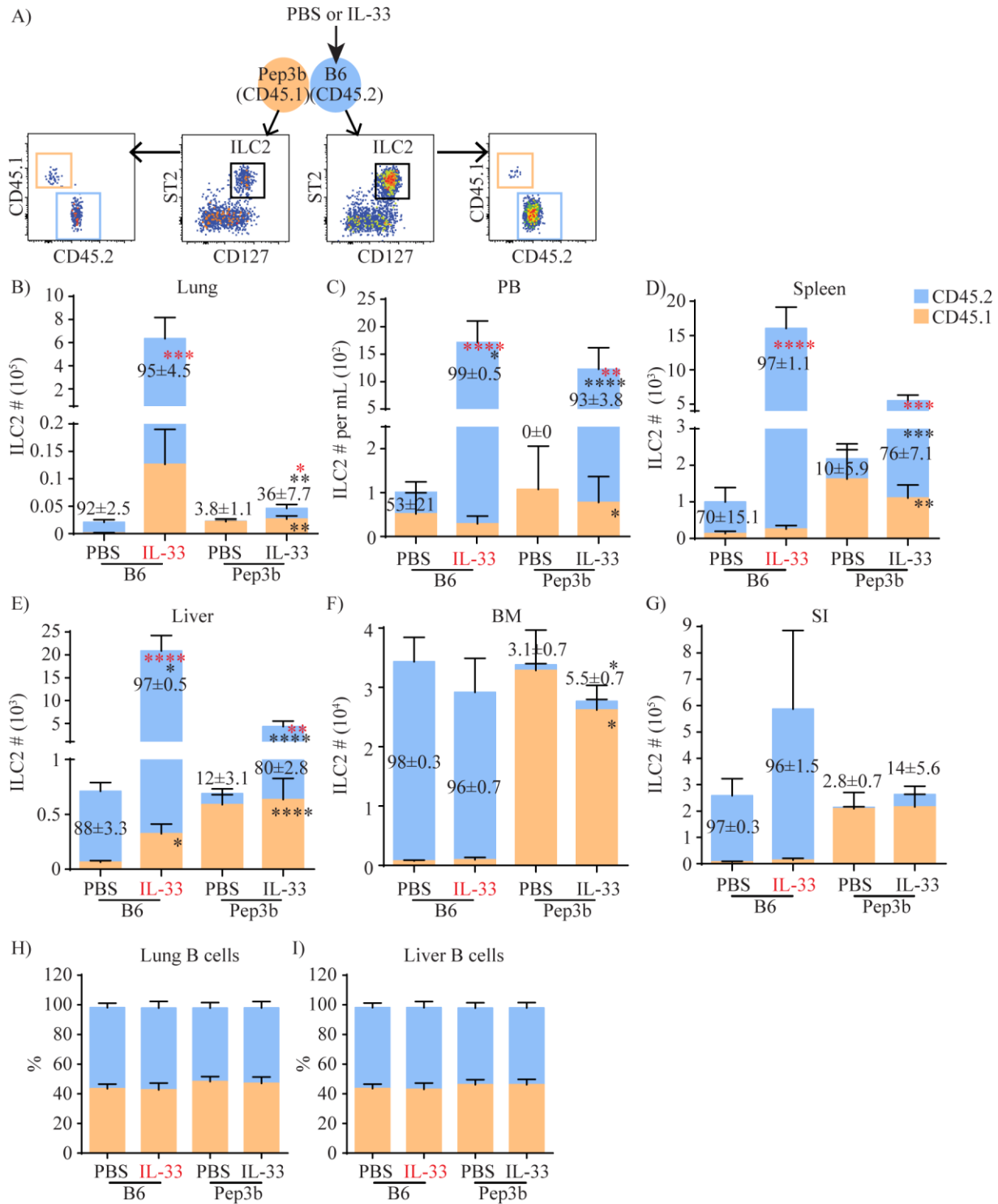


**Figure 4.2: Activated lung ILC2s migrate to the liver: analysis of parabiosis mice**

(A) Female B6 and Pep3b mice were conjoined by parabiosis surgery. B6 mice were given three daily i.n. injections of PBS or IL-33 and both B6 and Pep3b mice were analyzed on day 7 (see Figure 4.1C). (B-G) CD45.1<sup>+</sup> (orange) and CD45.2<sup>+</sup> (blue) ILC2s were quantified in the lung (B), PB (C), spleen (D), liver (E), BM (F) and SI (G). (H and I) Percentages of CD45.1<sup>+</sup> (orange) and CD45.2<sup>+</sup> (blue) B cells in the lung (H) and liver (I) were calculated. The x-axes show the strains of mice analyzed (B6 or Pep3b) and treatment groups (PBS or IL-33). IL-33 highlighted in red indicates the mouse that received IL-33 injections. Numbers within graphs indicate the percentages of CD45.2<sup>+</sup> ILC2s. Black and red asterisks indicate statistical significance of percentages and cell numbers, respectively, of CD45.2<sup>+</sup> (within blue bars) and CD45.1<sup>+</sup> (within orange bars) ILC2s compared to PBS treated pairs. Data represented are mean  $\pm$  SEM. n=6-7 (except SI, where n=3-4);  $\geq 3$  independent experiments. Two-way ANOVA with Bonferroni correction was used to determine statistical significance, with a P value  $<0.05$  being significant. \*P $<0.05$ , \*\*P $<0.01$ , \*\*\*P $<0.001$ , \*\*\*\*P $<0.0001$ .

We have previously found that i.n. administration of IL-33 resulted in a large increase in ILC2 numbers in the lung draining medLN (76), suggesting that activated lung ILC2s migrate to the lymph node (LN). As T cell migration involves their trafficking between blood and lymphatics through LNs (320), I next analyzed the migration of lung ILC2s in *Rorc*<sup>-/-</sup> mice that lack LNs (321) to determine whether LNs were required for ILC2 migration. The numbers of ILC2s in the naïve lung and liver were slightly higher in *Rorc*<sup>-/-</sup> than WT mice, while they were similar in PB (Figure 4.3). Upon IL-33 treatment, ILC2 numbers in the lung, liver and PB increased in both WT and *Rorc*<sup>-/-</sup> mice, and ILC2 numbers in the lung and liver, but not PB were higher in *Rorc*<sup>-/-</sup> mice than WT mice, indicating that LNs are not required for migration of ILC2s from the lung to the liver. Of note, the elevated numbers of ILC2s in *Rorc*<sup>-/-</sup> mice is most likely due to the inability of ILC progenitors to differentiate into ILC3s in the absence of Ror $\gamma$ t, which skews their development towards ILC2s. These results suggest that activated lung ILC2s exit the lung and enter the blood independent of LNs and preferentially settle in the liver.

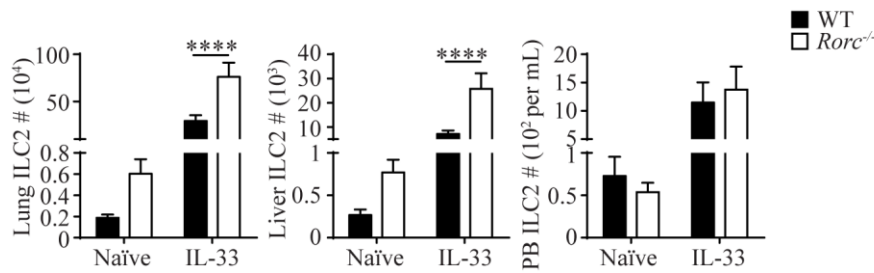


**Figure 4.3: LNs are not required for ILC2 migration from the lung to the liver**

ILC2s were quantified in female or male WT and *Rorc*<sup>-/-</sup> lung, liver and PB before and 5 days after three daily i.n. IL-33 injections (day 7 in Figure 4.1C). Black=WT, white=*Rorc*<sup>-/-</sup>. Data represented are mean  $\pm$  SEM. n=5-19;  $\geq 3$  independent experiments. Two-way ANOVA with Bonferroni correction was used to determine statistical significance, with a P value  $<0.05$  being significant. \*\*\*\*P $<0.0001$ .

To investigate functions of lung-derived ILC2s in the liver, I analyzed intracellular cytokine expression in ILC2s isolated from the lung and liver of naïve and IL-33 treated mice at various time points after the treatment. Unlike naïve lung ILC2s, which were mostly negative for IL-5 and IL-13, approximately 33% of naïve liver ILC2s were positive for these cytokines, indicating that some liver ILC2s constitutively express intracellular IL-5 and IL-13 (Figure 4.4A). After IL-33 administration, the percentage of cytokine positive lung ILC2s increased significantly until day 5 and quickly decreased, reaching a similar level as in naïve ILC2s by two weeks after the IL-33 treatment. In contrast, the percentages of IL-5 and IL-13 double positive liver ILC2s peaked on day 5, plateaued and remained high until 2 months after the treatment (Figure 4.4A). I purified ILC2s from the lung and the liver 14 days after the initial IL-33 treatment and stimulated ex vivo with PMA + ionomycin or various combinations of cytokines known to activate ILC2s, and the culture supernatants were analyzed for IL-5 and IL-13 (Figure 4.4B). Strikingly, in most conditions tested, ILC2s isolated from the liver produced greater amounts of IL-5 and IL-13 compared to those from the lung (Figure 4.4C). Interestingly, ILC2s isolated from the liver produced small amounts of IL-5 and IL-13 upon stimulation with IL-33 only, which did not stimulate lung ILC2s. The amounts of Areg, a growth factor known to be



produced by ILC2s (28), were very low, although ILC2s isolated from the liver produced significantly more Areg than lung ILC2s (Figure 4.4D). The supernatants collected from PMA + ionomycin and IL-33 + IL-25 + IL-7 + IL-2 conditions were also analyzed by multiplex cytokine assay to determine cytokine profiles of the lung-derived liver ILC2s. Upon stimulation by PMA + ionomycin, both lung and liver ILC2s produced detectable amounts of GM-CSF, IL-10, IL-2, IL-4 and IL-6 (Figure 4.4E, top). When stimulated with IL-33 + IL-25 + IL-7 + IL-2, both lung and liver ILC2s produced GM-CSF and IL-9, while only small amounts of IL-10, IL-2, IL-4 and TNF $\alpha$  were detected. Unexpectedly, ILC2s isolated from the liver produced large amounts of IL-6 (Figure 4.4E, bottom). Intracellular cytokine staining also showed greater percentages of liver ILC2s expressing IL-6 after IL-33 treatment compared to the lung ILC2s (Figure 4.4F). Co-staining of lung and liver ILC2s before and after IL-33 treatment with IL-5, IL-13 and IL-6 showed that the majority of lung and liver ILC2s in naïve mice were negative for IL-6, and most liver ILC2s that became IL-6<sup>+</sup> by the IL-33 treatment co-expressed IL-5 or IL-13 (Figure 4.4G). In summary, lung-derived liver ILC2s produce more type 2 cytokines, Areg and IL-6 than lung ILC2s.

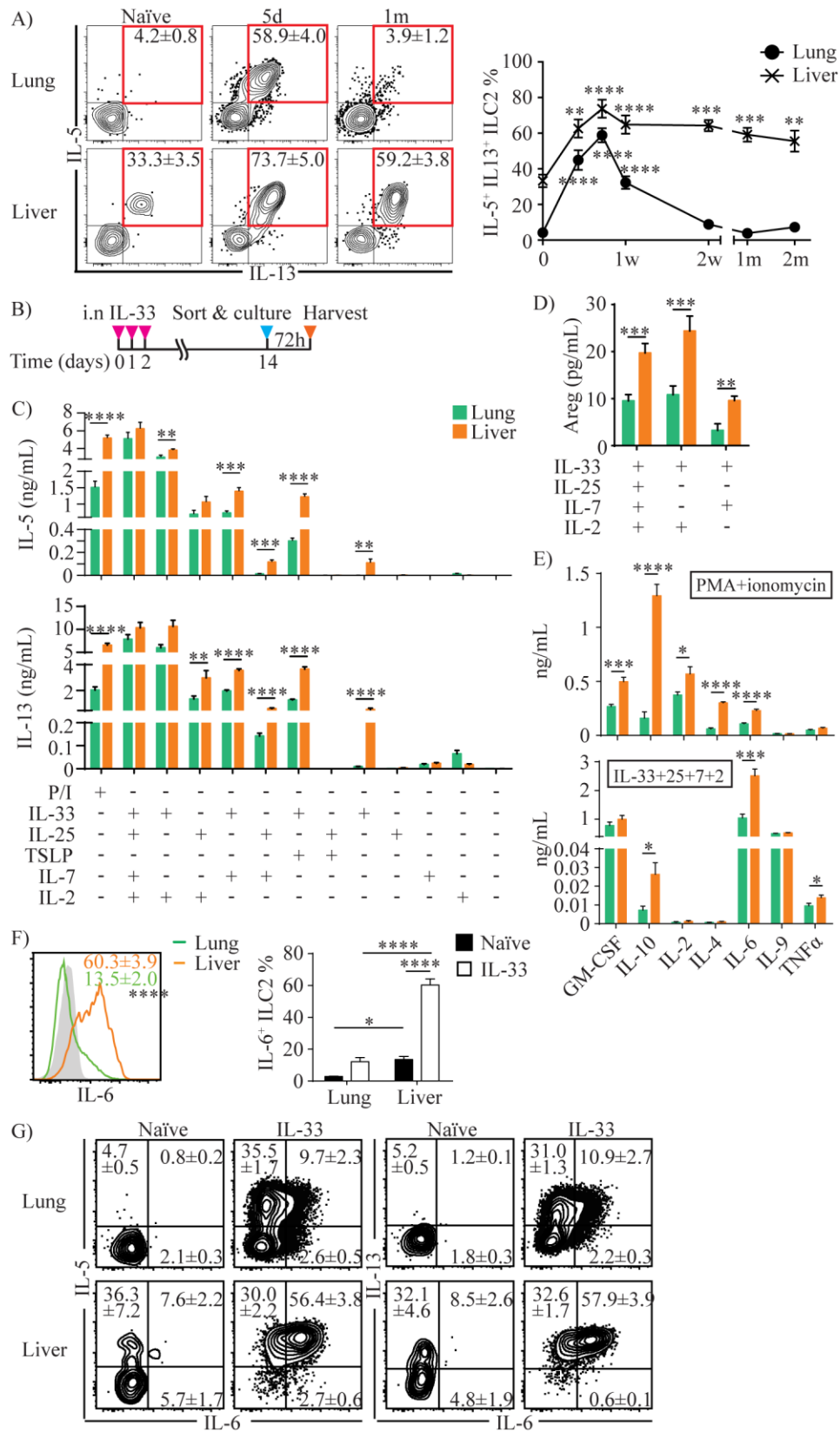


**Figure 4.4: Lung-derived liver ILC2s produce more IL-5, IL-13 and IL-6 than lung ILC2s**

(A) Female mice received three daily i.n injections of IL-33 and lung and liver ILC2s were analyzed for intracellular IL-5 and IL-13 expression at various time points as shown in Figure 4.1C. The contour plots show the expression of IL-5 (y axis) and IL-13 (x axis) in the lung (top) and liver (bottom) ILC2 at three selected time points. Boxes indicate IL-5<sup>+</sup> IL-13<sup>+</sup> ILC2s and the numbers show mean  $\pm$  SEM percentages of IL-5<sup>+</sup> IL-13<sup>+</sup> ILC2s. The graph shows the percentages of IL-5<sup>+</sup> IL-13<sup>+</sup> lung (filled circle) and liver (cross) ILC2. d=day, w=week, m=month. Asterisks indicate significant differences compared to naïve. (B) Treatment scheme of the ex vivo culture experiment shown in C-E. Female mice received three daily i.n injections of IL-33 and ILC2s were purified on day 14. Purified ILC2s were cultured for 72 hours before supernatants were harvested. (C-E) The amounts of IL-5 (C, top), IL-13 (C, bottom), Areg (D) and various cytokines (E) in conditions indicated below graphs (C and D), P/I (E, top) or IL-33 + IL-25 + IL-7 + IL-2 (E, bottom) conditions. P/I=PMA + ionomycin, “+” =present, “-” =absent. Green=lung, orange=liver. (F and G) Lung and liver ILC2s isolated from female mice were stained for intracellular IL-5, IL-6 and IL-13 before and 5 days after IL-33 treatment (day 7 in Figure 4.1C). (F) Histograms (left) show IL-6 expression in IL-33 treated lung (green) and liver (orange) ILC2s. Shaded=isotype. Graphs (right) show percentages of IL-6<sup>+</sup> ILC2s in naïve (black) and IL-33 treated (white) lung and liver. (G) Contour plots showing IL-5, IL-6 and IL-13 expression in the lung (top) and liver (bottom) ILC2s in naïve (left) and IL-33 treated (right) mice. Numbers indicate percentages of ILC2s in cytokine positive quadrants. Data represented are mean  $\pm$  SEM. n=4-22;  $\geq 2$  independent experiments except 2w lung, where n=3; 3 independent experiments (A). n=9-15;  $\geq 2$  independent experiments except n=5 for lung cultures with IL-7 or TSLP and IL-2 only conditions, n=4 for liver cultures with TSLP or IL-7, n=3 for liver IL-7 or IL-2 only conditions; 1 experiment (C and D). n=7; 2 independent experiments (E), n=6; 2 independent experiments (F and G). One-way ANOVA with Bonferroni correction (A), unpaired two-tailed t test (C-E) or two-way ANOVA with Bonferroni correction (F) was used to determine statistical significance, with a P value <0.05 being significant. \*P<0.05, \*\*P<0.01, \*\*\*P<0.001, \*\*\*\*P<0.0001.

To characterize lung-derived migratory ILC2s and gain insight into the mechanism of migration, I compared the expression of ILC2-related surface markers, chemokine receptors and integrin molecules on ILC2s in the lung and liver before and after i.n. IL-33 administration (Table 4.1). Similar to the lung ILC2s, most naïve liver ILC2s expressed CD25, a marker commonly used for ILC2 identification (Table 1.1) (22–24,26,28,61,65), while it was decreased after i.n IL-33 treatment (Figure 4.5A). KLRG1, a marker known to be expressed by intestinal ILC2s (78), was expressed at low levels on naïve lung and liver ILC2s but the percentages of KLRG1<sup>+</sup> ILC2s increased in both tissues after i.n IL-33 injections (Figure 4.5B). IL-25R is highly expressed on intestinal ILC2s (75) and iILC2s (129). Expression of IL-25R on naïve lung ILC2s is low, but it is upregulated upon ILC2 activation (76). In contrast, some liver resident ILC2s expressed IL-25R and its expression also increased after i.n IL-33 treatment, resulting in most ILC2s being positive for the marker (Figure 4.5C).

Naïve lung and liver ILC2s did not express most of the chemokine receptors tested, including CCR7, CCR3, CCR4, CCR2, CXCR3, and CCR1 (Table 4.1). The majority of lung ILC2s did not express CCR9, while approximately 30% of naïve liver ILC2s expressed the receptor, although most of them became negative upon IL-33 injections. Some naïve lung ILC2s expressed CXCR4, but the majority of other populations tested showed low expression of the marker.

I have also analyzed the expression of some ITGs that were found to be expressed by ILC2s at the transcript levels in previously generated microarray data (76). The majority of lung and liver ILC2s expressed ITG $\beta$ 7, ITG $\alpha$ L, ITG $\beta$ 3, ITG $\alpha$ v and ITG $\beta$ 2. Most ILC2s in naïve lung and liver expressed ITG $\beta$ 1, but its expression was increased after i.n IL-33 treatment. ITG $\alpha$ 4 expression also showed a similar pattern as ITG $\beta$ 1, although the percentage of ITG $\alpha$ 4<sup>+</sup> cells was slightly lower than ITG $\beta$ 1<sup>+</sup> cells.

Among the markers analyzed, the chemokine receptor CXCR6 and CD103 (ITG $\alpha$ E) were of particular interest. In naïve mice, CXCR6, which is required for some lymphocytes to enter the liver (322), was highly expressed on ~25% of lung ILC2s, ~45% of PB ILC2s and ~70% of liver ILC2s. After i.n. IL-33 administration, the majority of ILC2s in the lung and PB became positive for CXCR6, while its expression on liver ILC2s remained largely unchanged (Figure 4.5D). CD103 paired with the ITG $\beta$ 7 chain is known to bind E-cadherin and mediate the localization of intraepithelial lymphocytes (323). Almost all lung ILC2s in naïve mice were CD103<sup>lo</sup>. About 65% of IL-33 activated lung ILC2s highly expressed CD103 while ~35% remained CD103<sup>lo</sup>. In contrast, PB and liver ILC2s were mostly CD103<sup>lo</sup> regardless of the i.n. IL-33 treatment (Figure 4.5E). These results suggested that CD103 is involved in maintenance of activated ILC2s in the lung while CD103<sup>-</sup> ILC2s migrate out of the lung. To further investigate

this possibility, we purified CD103<sup>+</sup> and CD103<sup>-</sup> lung ILC2s as well as liver and PB ILC2s after i.n IL-33 administration and carried out transcriptome analyses by Affymetrix microarrays.

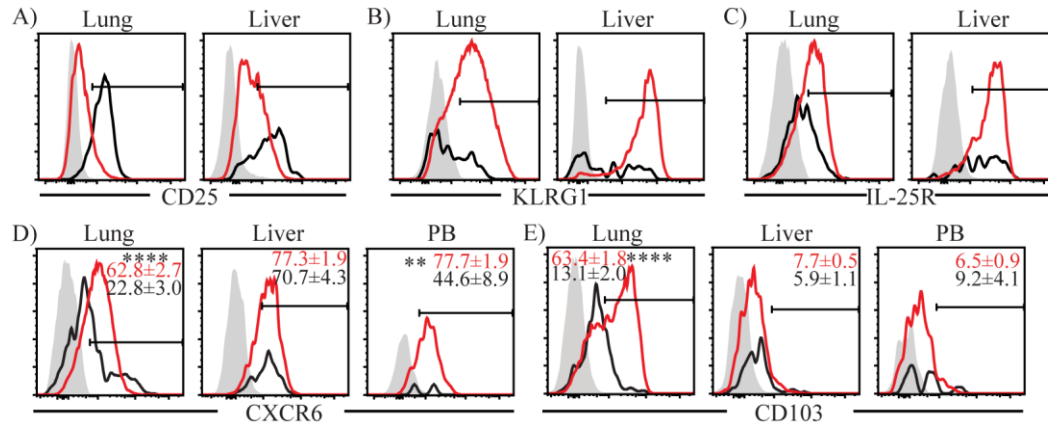


**Figure 4.5: Surface marker expression on ILC2s in the lung, liver and PB**

(A) Female mice received i.n IL-33 and CD25 expression was analyzed before and 5 days after IL-33 injections (day 7 in Figure 4.1C). (B-E) Female mice were treated as in A and KLRG1 (B), IL-25R (C), CXCR6 (D) and CD103 (E) expression was analyzed before and 3 days after IL-33 injections (day 5 in Figure 4.1C). Histograms show representative expression of each marker (A-E), while numbers show percentages of CXCR6<sup>+</sup> (D) and CD103<sup>+</sup> (E) ILC2s. Black lines/letters=naïve, red lines/letters=IL-33 treated, shaded=isotype. (A-C) Histograms are representative of n=5-7; 2 independent experiments except KLRG1 expression on IL-33 treated lung ILC2s, where n=3; 1 experiment (B, left, red). (D, E) Data represented are mean ± SEM. n=6-15 (D) or n=5-23 (E); ≥2 independent experiments. Unpaired two-tailed t test was used to determine statistical significance (D, E), with a P value <0.05 being significant. \*\*P<0.01, \*\*\*\*P<0.0001.

	Lung		Liver	
	Naïve	+IL-33 <sup>a</sup>	Naïve	+IL-33
<b>CD25</b>	Mostly + <sup>b</sup>	Mostly - <sup>c</sup>	Mostly +	Decreased
<b>KLRG1</b>	~35% +	~70% +	~40% +	Mostly +
<b>IL-25R</b>	low	Increased	~60% +	Mostly +
<b>CX3CR1</b>	-	-	-	-
<b>CCR7</b>	-	-	-	-
<b>CCR3</b>	-	-	~10% +	-
<b>CCR4</b>	~10% +	-	>10% +	-
<b>CXCR4</b>	<20% +	Decreased	<10% +	-
<b>CCR2</b>	-	-	-	-
<b>CXCR3</b>	>5% +	-	-	-
<b>CCR1</b>	-	-	-	-
<b>CXCR6</b>	~25% +	>60% +	Mostly +	Mostly +
<b>CCR9</b>	~5% +	-	~30% +	Mostly -
<b>ITGαE</b>	>10% +	~65% +	Mostly -	Mostly -
<b>(CD103)</b>				
<b>ITGβ7</b>	Mostly +	Increased	Mostly +	Increased
<b>ITGαL</b>	Mostly +	Increased	Mostly +	Increased
<b>ITGβ1</b>	>60% +	Increased	~80% +	Slightly increased
<b>ITGβ3</b>	Mostly +	+	Mostly +	+
<b>ITGαv</b>	Mostly +	+	Mostly +	+
<b>ITGβ2</b>	+	+	+	+
<b>ITGα4</b>	>40% +	~80% +	~60% +	~90% +

**Table 4.1: Phenotype of naïve and IL-33 treated lung and liver ILC2s**

A summary table showing expression of surface markers on naïve and IL-33 treated lung and liver ILC2s.

<sup>a</sup>. +IL-33 mice were given three daily i.n. injections of IL-33 and analyzed on day 5 or 7 (see Figure 4.1C).

<sup>b</sup>. “+” indicates positive expression of the indicated markers.

<sup>c</sup>. “-” indicates no expression of the indicated markers.

The gene expression profiles of individual ILC2 populations in various combinations were compared by scatter plots and  $R^2$  values, which show how close the data are to the linear regression line and demonstrate the similarities between the two data sets being compared (representative figure in Figure 4.6A). CD103<sup>+</sup> and CD103<sup>-</sup> lung ILC2s most closely correlated to each other (Table 4.2). Liver and PBs ILC2s also showed strong correlations, followed by CD103<sup>-</sup> lung ILC2s vs. liver ILC2s while CD103<sup>+</sup> lung and liver ILC2s were less similar. Reactome pathway analyses (295,296) of the genes upregulated in specific dataset in various

comparisons demonstrated that CD103<sup>-</sup> lung ILC2s expressed higher levels of genes related to DNA replication (324–328), including *E2f3*, *Gins3*, *Orc4*, *Orc2*, *Fbxo5*, *Hist2h2ab*, *Hist2h3b* and *Hist1h4m*, compared to CD103<sup>+</sup> lung ILC2s, suggesting that CD103<sup>-</sup> subset may be undergoing replication to a greater degree than the CD103<sup>+</sup> subset (Figure 4.6B). Liver and PB ILC2s had a higher expression of genes related to cell cycle and mitosis (324,326,327,329–333), including *Orc*, *Mcm*, *Gins*, *E2f* and *Ccnb* genes, compared to CD103<sup>+</sup> lung ILC2s, also suggesting that liver and PB ILC2s are more proliferative than CD103<sup>+</sup> lung ILC2s. *Mki67*, which is a commonly used proliferation marker, was also more highly expressed by liver and PB ILC2s in comparison to CD103<sup>+</sup> lung ILC2s. These results are consistent with the idea that CD103<sup>-</sup> lung ILC2s may leave the lung, circulate in PB and settle in the liver, but further investigation is necessary.

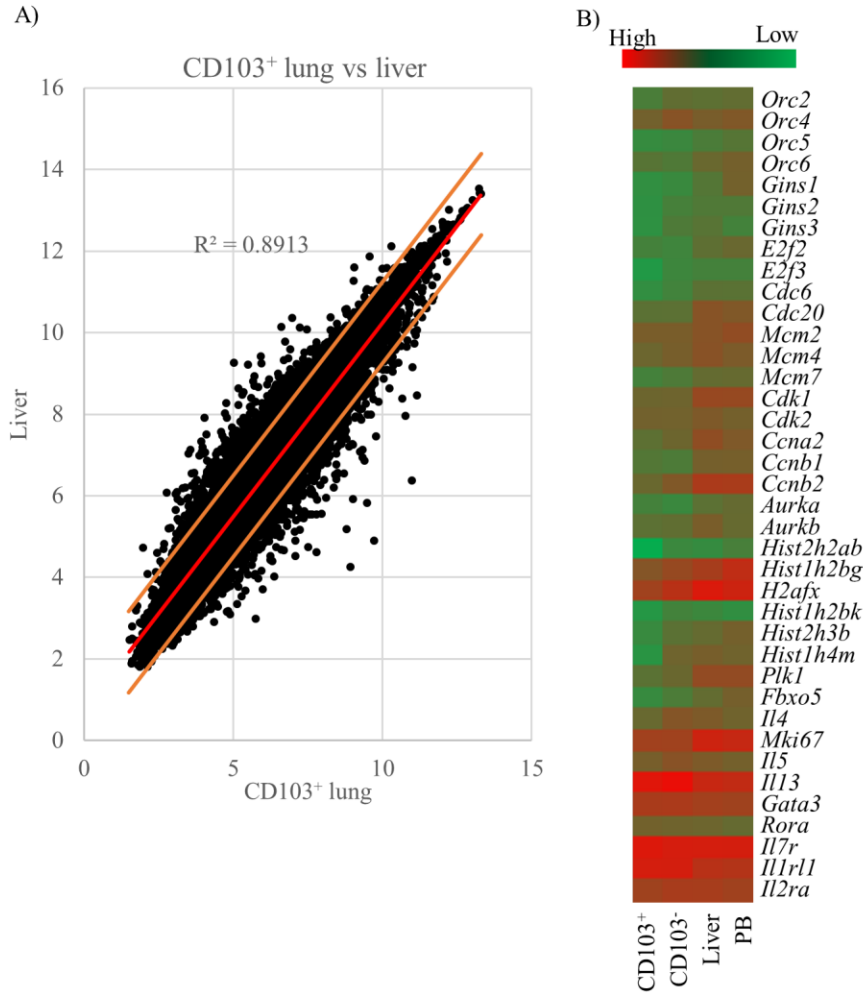


**Figure 4.6: Gene expression analyses of CD103<sup>+</sup> and CD103<sup>-</sup> lung, liver and PB ILC2s**

(A, B) ILC2s were purified from the lung, liver and PB of female mice three days after i.n IL-33 administration (day 5 in Figure 4.1C). Lung ILC2s were separated into CD103<sup>+</sup> and CD103<sup>-</sup> subsets. RNA was extracted from these populations and analyzed by Affymetrix microarray analyses. (A) A representative scatter plot of two datasets.  $R^2$  values for various comparisons are listed in Table 4.2. Gene expression values are in log<sub>2</sub> scale. Orange lines show fold change=2, red line=linear regression line. (B) A heatmap showing relative expression of selected genes. CD103<sup>+</sup>=CD103<sup>+</sup> lung, CD103<sup>-</sup>=CD103<sup>-</sup> lung samples. Data are representative of 2 samples per group, with 3-4 mice per sample.

Dataset comparisons	$R^2$ values
Lung CD103 <sup>+</sup> vs. Lung CD103 <sup>-</sup>	0.926
Lung CD103 <sup>+</sup> vs. Liver	0.891
Lung CD103 <sup>+</sup> vs. PB	0.864
Lung CD103 <sup>-</sup> vs. Liver	0.918
Lung CD103 <sup>-</sup> vs. PB	0.891
Liver vs. PB	0.922

**Table 4.2: Table of  $R^2$  values for each microarray dataset comparison**



### 4.3 Discussion

The results presented here indicate that i.n. administration of IL-33 induces localized activation and proliferation of lung resident ILC2s rather than recruitment from the BM as previously reported (86). Although ILC2 numbers in PB, spleen and liver also increased following i.n. IL-33 administration, the parabiosis experiments showed that the increases in ILC2 numbers are due to migration of activated lung ILC2s to those tissues. While activated lung ILC2s circulated in PB, they preferentially migrated to the liver, and migration to other tissues, including the SI and BM, was negligible. The majority of lung-derived liver ILC2s expressed the chemokine receptor CXCR6, while they were negative for ITG CD103. CD103<sup>-</sup> lung, PB and liver ILC2s shared similarities in that they expressed more transcripts of cell cycle-related genes compared to CD103<sup>+</sup> lung ILC2s, the majority of which remained in the lung after IL-33 administration. Moreover, lung-derived liver ILC2s maintained intracellular cytokine expression and produced greater amounts of type 2 cytokines ex vivo.

Since the emergence of the idea of ILC tissue residence (86), multiple reports have shown the ability of ILC2s to traffic between different organs. Stier et al. reported migration of ILC2s out of the BM to the lung upon systemic IL-33 injections, while Karta et al. demonstrated  $\beta$ 2 ITG-mediated recruitment of ILC2s from the BM to the lung upon allergen stimulation (317,318). A recent report by Huang et al. also demonstrated S1P-dependent trafficking of iILC2s from the intestine to the lung (130). Our parabiosis results agree with the reports by Gasteiger et al. in terms of expansion of the tissue resident ILC2s in the lung upon i.n. IL-33 treatment (86). While the reports by Stier et al. and Karta et al. showed that ILC2s can be mobilized from the BM upon i.v. injections of IL-33 and i.n. injections of *A. alternata* (317,318), the parabiosis analyses shown in this chapter indicate no sign of ILC2 egress from the BM or

recruitment from other organs. The discrepancy between the results presented here and reports by Karta et al. is likely due to differences in the ways ILC2s are defined. Karta et al. defined ILC2s as Lin<sup>-</sup>Thy1<sup>+</sup>. In my hands, the majority of Lin<sup>-</sup>Thy1<sup>+</sup> lung lymphocytes are GATA3<sup>-</sup> non-ILC2s (Appendix B.3A) and are not tissue resident as they are mixtures of CD45.1<sup>+</sup> and CD45.2<sup>+</sup> cells in our parabiotic mice (Appendix B.3B). In the analyses shown in this chapter, ILC2s were defined by Lin<sup>-</sup>Thy1<sup>+</sup>CD127<sup>+</sup>ST2<sup>+</sup>, and they were predominantly GATA3<sup>+</sup> (Appendix B.3A). It is also possible that tissue residency and migration potential of ILC2s are model-dependent. The model used here, IL-33, is relatively specific to ILC2s although it can stimulate other ST2 expressing cells such as mast cells and Tregs (334), whereas allergens such as *A. alternata* act by inducing oxidative stress in epithelium (335,336) and can induce more global changes in the lung environment followed by activation of many other cell types. This, in turn, can result in secretion of various soluble mediators that induce recruitment of ILC2s from the BM into the lung.

Parabiosis data shown here do not provide direct evidence that the liver ILC2s come from the lung and it is possible that they originate elsewhere. However, as IL-33 was locally administered, stimulation of ILC2s in organs other than the lung would require IL-33 to enter circulation or other soluble signals to be released. In parabiosis settings, where B6 and Pep3b mice share the circulatory system, these signals would equally stimulate ILC2s in both mice, resulting in 1:1 ratio of CD45.1<sup>+</sup> and CD45.2<sup>+</sup> ILC2s. In contrast, only CD45.2<sup>+</sup> ILC2s expanded in B6 and Pep3b livers upon IL-33 injections into B6 mice, while the majority were CD45.1<sup>+</sup> when IL-33 was administered to Pep3b mice, suggesting that the liver ILC2s are derived from the lung. Furthermore, it has been shown that IL-33 is quickly oxidized into an inactive form upon release (337). Considering that it takes 3 daily i.n. injections of IL-33 at the dosage used

here to induce strong activation of ILC2s in the lung, it is very unlikely that the amount of bioactive IL-33 that may enter circulation is sufficient to induce significant proliferation of ILC2s outside of the lung. Overall, it is most likely that the liver ILC2s induced upon i.n. IL-33 administration originate from the lung.

Lung-derived liver ILC2s shown here phenotypically resemble iILC2s described by Huang et al. as they highly express IL-25R and KLRG1 (129). It is conceivable that iILC2s originating in the SI may migrate into the liver upon activation considering their anatomical locations. However, unlike iILC2s, lung-derived liver ILC2s express the IL-33R, ST2 and are induced by IL-33 stimulation. Moreover, while iILC2 most likely migrate through LNs (130), both lung and lung-derived liver ILC2s lack the expression of a LN homing marker CCR7 (338), implicating that their migration may not involve LNs. Indeed, in *Rorc*<sup>-/-</sup> mice, which lack LNs, ILC2s were still able to migrate out of the lung into the liver, suggesting that this process does not require the LNs. However, it is important to note that lung ILC2s may migrate through the lymphatic system and enter blood circulation through the thoracic duct as other lymphocytes do (320) since *Rorc*<sup>-/-</sup> mice do have lymphatic vessels despite their lack of LNs (321). Alternatively, ILC2s may enter blood vasculature directly from the lung in a process called reverse transendothelial migration as shown in various leukocytes including neutrophils and monocytes (339,340).

Chemokine receptors and ITGs play important roles in cell migration as they sensitize cells towards chemokine gradient and mediate firm adhesions during migration, respectively. I have investigated expression of various chemokine receptors and ITGs on ILC2s. ILC2s did not express many of the chemokine receptors investigated before or after IL-33 stimulation. Therefore, the exact mechanisms by which activated lung ILC2s migrate out of the lung,

circulate through PB and settle in the liver are still under investigation. However, CD103 and CXCR6 likely play roles.

Most ILC2s in PB and liver express the chemokine receptor CXCR6, which is expressed by hepatic lymphocytes including NK cells, CD4<sup>+</sup> and CD8<sup>+</sup> T cells and mediates migration of NKT cells to the liver (322). This suggests that CXCR6 may also mediate the migration of lung ILC2s to the liver, where its ligand CXCL16 is highly expressed (341,342).

Because the majority of activated lung ILC2s express CD103 whereas ILC2s in PB and liver in the same mice are CD103<sup>-</sup>, it seems likely that a CD103<sup>-</sup> subset of activated ILC2s migrates out of the lung, circulates through PB and settles in the liver. The  $\alpha$ E $\beta$ 7 ITG, formed by pairing of CD103 with the  $\beta$ 7 chain, binds E-cadherin on epithelial cells (323), and CD103 KO mice have greatly reduced numbers of intraepithelial lymphocytes (343). Thus, activated lung ILC2s expressing CD103 may be retained in the lung by the interaction between CD103 and E-cadherin while CD103<sup>-</sup> ILC2s migrate out of the lung. Although ILC2s also expressed high levels of other ITGs, it is difficult to draw conclusions regarding their roles in migration as ITG molecules are required to be in active conformation in order to efficiently execute their functions (344) and therefore, presence or absence of expression does not indicate their functional involvement. The finding that the gene expression profiles are similar between CD103<sup>-</sup> lung, liver and PB ILC2s further supports the idea that CD103<sup>-</sup> lung ILC2s migrate out of the lung into the liver. Further experiments with KO mouse models will be necessary to elucidate the roles of CD103 and CXCR6 in ILC2 migration.

The results presented here suggested that once activated, some lung ILC2s circulate in PB, migrate to and persist in the liver. Asthma patients have been reported to have high numbers of ILC2s in PB (236), but their origin has been unknown. Those PB ILC2s likely derive from

allergen-stimulated lung of the patients. The idea of ILC2 migration upon stimulation has broad applications as it implies that disease-causing ILC2s in one organ may have been primed in another, and the inhibition of their migration may allow us to prevent inflammation in another tissue. To achieve this, further studies will be necessary to 1) identify markers to distinguish between lung-derived liver ILC2s and liver resident ILC2s and 2) elucidate the mechanism by which activated lung ILC2s migrate.

In the next chapter, I aim to investigate the reasons behind ILC2 migration by focusing on the roles of lung-derived ILC2s in liver inflammation.

## Chapter 5: Lung-derived liver ILC2s induce changes in the liver immune environment

### 5.1 Introduction

The pathogenesis of liver fibrosis is mediated primarily by ECM producing cells such as myofibroblasts as discussed in Chapter 1. However, activation and differentiation of HSCs (hepatic stellate cells) to myofibroblasts are dependent on the environmental cues such as the cytokine milieu in the liver, which is often provided by immune cells. From an immunological perspective, fibrosis is mediated by type 2 immune response as demonstrated by the contribution of type 2 cytokines, IL-5 and IL-13 to the development of fibrosis, although evidence of the involvement of type 3 immunity also exists (345,346).

IL-13 has been shown to be pro-fibrotic using an IL-13 transgenic mouse model (223). Although IL-4 and IL-13 share IL-4R $\alpha$  as a component of their receptor complex, IL-13 inhibition but not IL-4 deficiency reduces fibrogenesis in a model of *Schistosoma mansoni* (*S. mansoni*)-mediated hepatic fibrosis, demonstrating a dominant role of IL-13 in the development of fibrosis (347). IL-13 directly stimulates HSCs to produce pro-fibrotic factors such as collagen (348) and connective tissue growth factor (349), which regulate liver fibrogenesis. The roles of IL-5 in fibrosis are more controversial. Pro-fibrotic roles of IL-5 were demonstrated in the lungs using antibody neutralization of IL-5 (350) and IL-5 deficient mice (351). Similarly, IL-5 deficiency also results in attenuation of liver fibrosis upon *S. mansoni* infection, suggesting its pro-fibrotic effects in the liver (352). In contrast, although it has been shown that IL-5 and eosinophils promote lung fibrosis by using IL-5 transgenic mice, and eosinophil instillation, respectively, IL-5 is not necessary to induce fibrosis as lung fibrosis can still develop in the

absence of IL-5 (353). This suggests that the role of IL-5 is of an accessory cytokine that enhances a fibrotic phenotype rather than a causative cytokine.

Macrophages are also known as major modulators of fibrogenesis. Specifically, M2 type macrophages produce proline as a product of arginine metabolism, and proline is a critical building block of collagen (354). They also produce MMP12, which suppresses ECM degrading MMPs, including MMP2, MMP9 and MMP13, thus augmenting fibrotic response (355). Considering the roles of type 2 cytokines in macrophage skewing towards an M2 type, and the roles type 2 cytokines and M2 macrophages play in fibrogenesis, it was no surprise that ILC2s, which are potent producers of type 2 cytokines, became a major effector cell culprit in pathogenesis of fibrosis.

The function of ILC2s in the liver was first described in 2013 by Mchedlidze et al. The authors reported that IL-33 was elevated in the serum of liver cirrhosis patients, and liver resident ILC2s mediated development of carbon tetrachloride and thioacetamide-induced fibrosis. This was dependent on ILC2-derived IL-13, which activated HSCs, resulting in fibrosis (65). Subsequently, ILC2s were shown to be involved in the development of ConA-induced immune-mediated hepatitis (356) while they provided mild protection from adenovirus-induced viral hepatitis (237). In the human liver, the number of liver ILC2s is increased proportionally to the severity of the disease in fibrosis patients (81,82). Additionally hepatic ILC2s of fibrosis and cirrhosis patients expressed higher amounts of the activation marker CD69, compared to healthy liver ILC2s (82).

ConA, a plant lectin, binds to carbohydrates on cell surface glycoproteins (357). In vitro, ConA induces polyclonal activation of murine T cells (358,359) whereas i.v. injections into mice cause acute and severe hepatitis (360). ConA-induced hepatitis is a well-established mouse

model of autoimmune and viral hepatitis. ConA-induced hepatitis is mediated by T cells as T cell deficient mice have significantly reduced sign of hepatitis upon ConA treatment (360,361).

Whereas CD4 antibody provides protection, CD8 antibody fails to do so, suggesting it is specifically mediated by CD4<sup>+</sup> T cells (360,361). Moreover, macrophage depletion also confers protection from the development of hepatitis, suggesting their significant contribution (360).

Intravenously injected ConA first binds to LSECs, inducing their death followed by disruption of endothelial integrity (360,362). This allows ConA to enter the parenchyma, where it sticks to hepatocytes (362). Subsequently, T cells recognize MHCII bound with ConA on hepatocytes, resulting in T cell differentiation into Th1 cells, which produce IFN $\gamma$  and TNF $\alpha$ . This series of events happens very quickly and the levels of these cytokines start rising within the first few hours after ConA administration (361,363,364). By 8 hours after ConA treatment, hepatocytes damage becomes apparent (360), which progresses further and eventually results in liver failure. While IFN $\gamma$  has been shown to be necessary for ConA-induced hepatocytes apoptosis, which leads to liver injury (363–365), the role of TNF $\alpha$  is controversial. Although TNF $\alpha$  blocking studies demonstrated significant contribution of this cytokine to hepatic cell death and liver damage (361,364,366,367), TNF $\alpha$  deficiency has no effects (365). Another study showed that TNF $\alpha$  and IFN $\gamma$  regulate each other, suggesting signaling from both cytokines are necessary (363).

In Chapter 4, I have shown that a subset of lung ILC2s that does not express CD103 migrates to the liver upon i.n. IL-33 treatment and potently produces type 2 cytokines as well as IL-6. In this chapter, I investigate the impact of lung-derived ILC2s in the liver in the context of immune environment and disease relevance to further understand the significance of lung ILC2 migration to the liver. Here, I show that lung-derived ILC2s induce alteration in myeloid cell



populations, causing type 2 skewing in the liver. Moreover, I demonstrate pro- and anti-fibrotic effects of lung-derived ILC2s in the liver, using two different mouse models.

## **5.2 Results**

To investigate the effects of lung ILC2 migration to the liver, I analyzed various lymphocytes and myeloid cells in the liver before and 5 days after i.n IL-33 treatment. Flow cytometric analyses showed that ILC2s were the only lymphocyte population that expanded in the liver upon i.n. IL-33 treatment. (Figure 5.1A). Eosinophils expanded greatly, suggesting that lung-derived liver ILC2s actively produced IL-5 (Figure 5.1B). The numbers of neutrophils, CD11b<sup>+</sup> cDC2, Ly6C<sup>+</sup> monocytes and basophils also slightly increased. The number of monocyte-derived macrophages (CD11b<sup>+</sup> F4/80<sup>lo</sup>) remained unchanged before and after IL-33 stimulation. However, the percentage of monocyte-derived macrophages expressing the mannose receptor CD206 (M2 phenotype) significantly increased after the IL-33 treatment, likely due to IL-13 produced by lung-derived liver ILC2s (Figure 5.1C). These results suggest that lung-derived ILC2s actively produce type 2 cytokines in the liver, inducing type 2 skewing of the immune environment in the liver.

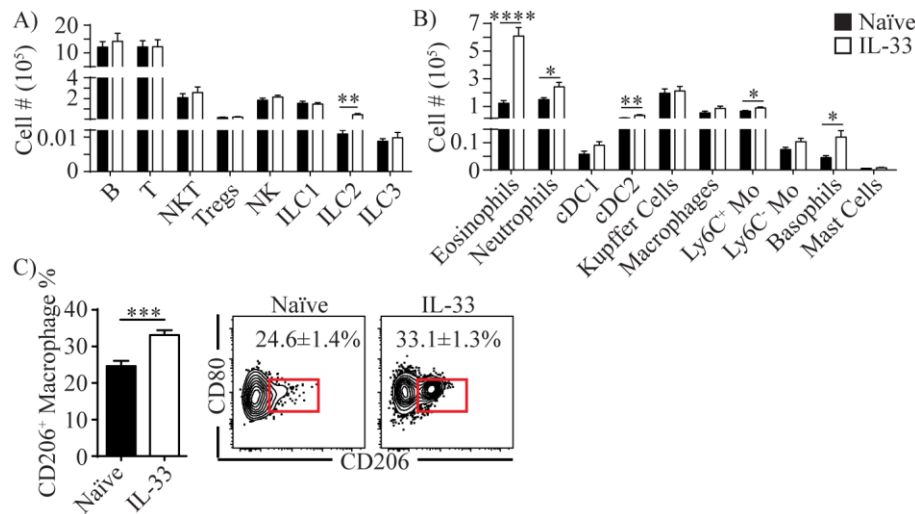


**Figure 5.1: Lung-derived liver ILC2s induce changes in the liver immune environment**

Female mice received three daily injections of i.n. IL-33 and liver was analyzed 5 days later (day 7 in Figure 4.1C). Various lymphocytes (A) and myeloid populations (B), and CD206<sup>+</sup> macrophages (C) were quantified in naïve (black bars) and IL-33 treated (white bars) livers. Contour plots in C show CD206<sup>+</sup> macrophages (red boxes) in naïve and IL-33 treated livers and the numbers show mean ± SEM percentages of CD206<sup>+</sup> macrophages. Gating strategies for identification of each population are shown in Figures 2.1 and 2.2. Mo=monocytes. Data represented are mean ± SEM. n=6-17; ≥2 independent experiments. Unpaired two-tailed t test was used to determine statistical significance, with a P value <0.05 being significant. \*P<0.05, \*\*P<0.01, \*\*\*P<0.001, \*\*\*\*P<0.0001.

RORα is a transcription factor that is required for ILC2 development and highly expressed by ILC2s (60,78,99), while CD127 or IL-7Rα is a cytokine receptor that is also required for ILC2 development (99,105). Our laboratory has generated ILC2 deficient mice (CD127 cKO) by crossing *Rora-IRES-Cre* (286) and *Il7ra<sup>fl/fl</sup>* (287) mice. Comparison of the frequencies of various lymphoid and myeloid cell populations in the lung showed that ILC2s were reduced by almost 80% in CD127 cKO mice compared to WT (Figure 5.2A). B cells, NKT cells, ILC1s and monocyte-derived macrophages were slightly reduced while Tregs and Ly6C<sup>-</sup> monocytes were slightly increased in CD127 cKO mice (Figures 5.2A, B). In the liver, ILC2s were the only cells that were reduced, whereas NK cells, ILC3s and Ly6C<sup>-</sup> monocytes were slightly increased in CD127 cKO mice (Figures 5.2A, B). In the SI, ILC1s and ILC2s were reduced by about 75%, B cells, Tregs, NKT cells and ILC3s were reduced by about 50% while NK cells were increased in

CD127 cKO (Appendix C.1). In the spleen, NKT cells and ILC2s were the only two populations that were reduced in the CD127 cKO mice, whereas T cells, Tregs and NK cells were slightly increased in CD127 cKO mice (Appendix C.1). B cells and NK cells were increased, while ILC1s and ILC2s were reduced in the BM (Appendix C.1). Despite alterations in the composition of immune cells in CD127 cKO compared to WT mice, ILC2s were the only population that was significantly reduced in all tissues analyzed, indicating that CD127 cKO is a useful ILC2 deficient mouse model. Therefore, I used this newly-generated strain in the following analyses.

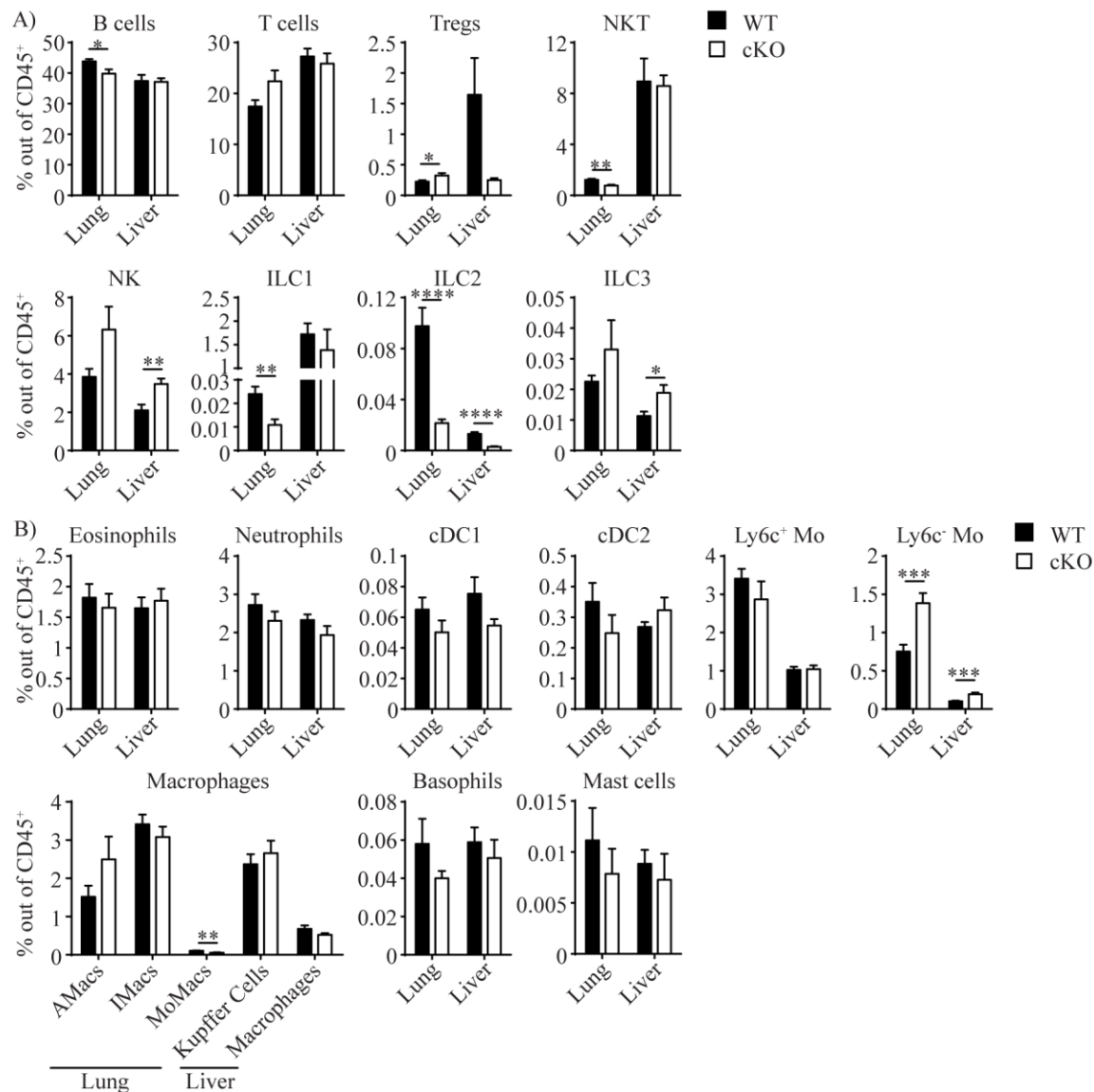


**Figure 5.2: Characterization of CD127 cKO mice**

Percentages of various lymphocytes (A) and myeloid cells (B) within CD45<sup>+</sup> cells were quantified in the lung and liver of naïve female or male WT (black bars) and CD127 cKO (white bars) mice. Gating strategies used for identification of each population are shown in Figures 2.1 and 2.2. Tregs=regulatory T cells, cDC1= type 1 conventional DCs, cDC2= type 2 conventional DCs, AMacs=alveolar macrophages, IMacs=interstitial macrophages, MoMacs=monocyte-derived macrophages, Mo=monocytes. Data represented are mean  $\pm$  SEM. n=6-21;  $\geq 2$  independent experiments. Unpaired two-tailed t test was used to determine statistical significance, with a P value <0.05 being significant. \*P<0.05, \*\*P<0.01, \*\*\*P<0.001, \*\*\*\*P<0.0001.

As shown above (Figure 5.2, Appendix C.1), the numbers of lung and liver ILC2s in the CD127 cKO mice were about 10% of those in the WT mice (Figure 5.3A). Upon IL-33

treatment, the residual ILC2s in CD127 cKO mice expanded, but the numbers of ILC2s in the

liver of CD127 cKO mice remained about 10% of those in the WT mice (Figure 5.3B), further supporting the use of these mice as an ILC2 deficient mouse model to study the contribution of ILC2s in immune responses. To determine whether changes in immune populations in the liver are due to lung-derived ILC2s, various myeloid cell populations were quantified in the liver of CD127 cKO mice before and 5 days after three daily i.n IL-33 injections. I.n. IL-33 induced mild eosinophilia in CD127 cKO mouse liver, likely due to IL-5 produced by residual ILC2s, while there was no increase in other myeloid populations (Figure 5.3C), indicating that ILC2s induce changes in myeloid populations in the liver upon IL-33 administration. Similarly, the percentages of monocyte-derived macrophages expressing CD206 were no longer significantly different (Figure 5.3D). These results indicate that lung-derived liver ILC2s are responsible for the type 2 skewing seen in the liver after i.n. IL-33 treatment.

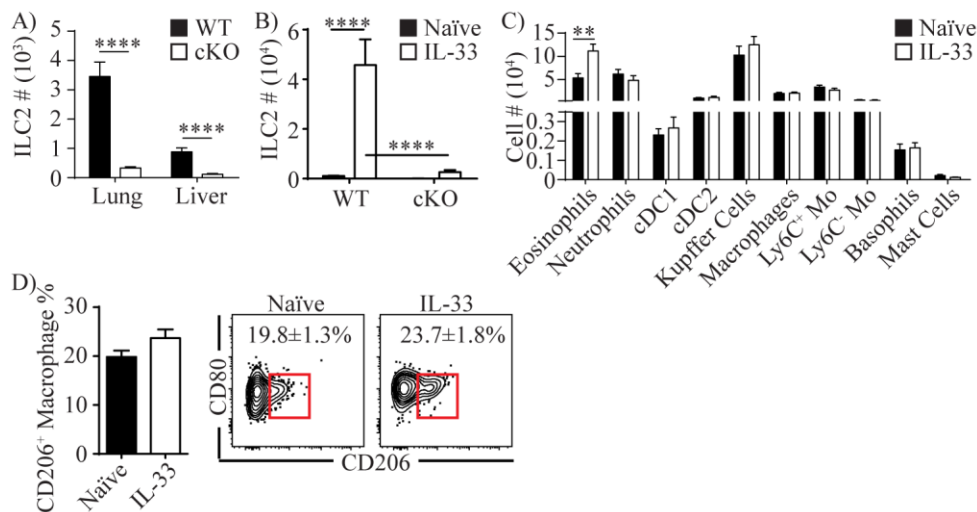


**Figure 5.3: Liver inflammation is diminished in ILC2 deficient mice**

(A) Numbers of ILC2s in the lung and liver of naïve female or male WT (black bars) and CD127 cKO (white bars) mice. (B) Female WT (black bars) or CD127 cKO (white bars) mice received three daily injections of IL-33 and liver ILC2s were quantified 5 days later (day 7 in Figure 4.1C). (C, D) Female CD127 cKO mice were treated as in B and various myeloid populations (C) and CD206<sup>+</sup> macrophages (D) were quantified in naïve (black bars) and IL-33 treated (white bars) livers. Contour plots show CD206<sup>+</sup> macrophages (red boxes) in naïve and IL-33 treated livers and the numbers show mean ± SEM percentages of CD206<sup>+</sup> macrophages (D). Gating strategies used to identify each myeloid population are shown in Figure 2.2. Data represented are mean ± SEM. n=17-21; ≥3 independent experiments (A), n=6; 2 independent experiments (B), n=9-14; ≥3 independent experiments (C), n=9-10; 3

independent experiments (D). Unpaired two-tailed t test (A, C, D) or two-way ANOVA with Bonferroni correction (B) was used to determine statistical significance, with a P value <0.05 being significant. \*\*P<0.01, \*\*\*\*P<0.0001.

ILC2s have previously been implicated in liver fibrosis (65). Therefore, I analyzed the expression of the fibrosis-related genes *Colla1*, *Acta2* and *Timp1*, which encode  $\alpha 1$  chain of type 1 collagen, smooth muscle  $\alpha$  actin and TIMP1, respectively, in the liver by RT-qPCR. The expression of these genes was significantly increased by i.n. IL-33 administration into WT mice, although the increase was relatively mild, and the levels of these genes returned to those in naïve liver by 2-4 weeks after the treatment (Figure 5.4A). These results indicate that lung-derived ILC2s induce type 2 inflammation in the liver and may be involved in the development of liver fibrosis.

To mimic chronic type 2 inflammation in the lung, I gave two sets of i.n. IL-33 administrations into WT mice one month apart (Figure 5.4B). Three days after the last administration, ILC2 numbers in the lung, liver and PB of the mice treated with two sets of IL-33 (+IL33/+IL33) were much higher than those in the mice treated with one set of IL-33 (-IL33/+IL33, +IL33/-IL33) or naïve mice (-IL33/-IL33) (Figure 5.4C). Similarly, IL-5, IL-6 and IL-13 expressing ILC2s also expanded significantly in the lung and liver of +IL33/+IL33 mice compared to -IL33/+IL33, +IL33/-IL33 or -IL33/-IL33 mice (Figure 5.4D). Analyses of myeloid cell populations in the liver revealed that eosinophils, neutrophils, cDC1, cDC2, Ly6C<sup>+</sup> monocytes, basophils and mast cells were all increased in +IL33/+IL33 treatment group compared to other groups (Figure 5.4E). Interestingly, the tissue resident Kupffer cells (CD11b<sup>lo</sup> F4/80<sup>+</sup>) were slightly decreased in +IL33/+IL33 treatment group in comparison to +IL33/-IL33 group, although it is not clear whether this is due to the change in their phenotype or decrease in their numbers. The IL-33 challenge also caused an increase in the frequency of CD206<sup>+</sup>

monocyte-derived macrophages (Figure 5.4F). Strikingly, the +IL33/+IL33 treatment greatly enhanced the expression of *Colla1* gene compared to naïve or single treatment groups, reaching 5 fold increase in relative expression compared to the naïve liver, whereas *Acta2* or *Timp1* gene expression was comparable to single treatment groups (-IL33/+IL33 or +IL33/-IL33) (Figure 5.4G). Picrosirius red staining of type 1, 2 and 3 collagen fibers (368,369) showed collagen deposits in some of the sections of +IL33/+IL33 treated livers, indicating mild fibrosis (Figure 5.4H). Interestingly, H&E staining showed large cell clusters containing eosinophils in the +IL33/+IL33 liver (Figure 5.5I). These clusters were much smaller and less frequent in naïve mouse livers compared to +IL33/+IL33 livers. These results indicate that lung-derived ILC2s induce eosinophilic inflammation and mild fibrosis in the liver.

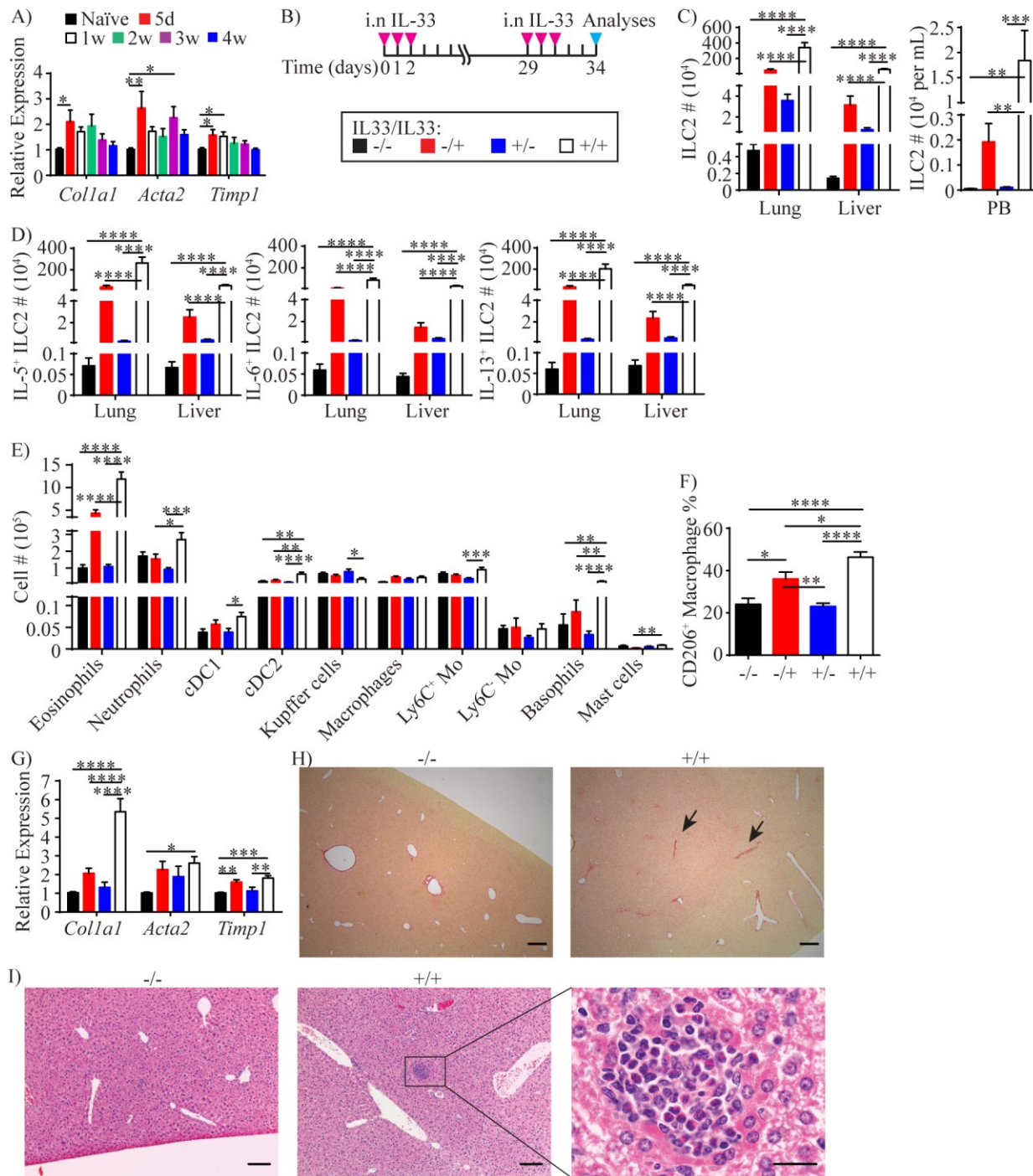


**Figure 5.4: Repeated i.n. IL-33 injections cause eosinophilic hepatitis and mild fibrosis**

(A) Female WT mice received three daily i.n. injections of IL-33 and liver was collected at various time points (treatment scheme in Figure 4.1C) for RT-qPCR analyses of *Coll1a1*, *Acta2* and *Timp1* genes. Day 0 is naïve, d=day, w=week. Black=naïve, red=5d, white=1w, green=2w, purple=3w, blue=4w. (B) Treatment scheme for the data presented in C-I. Female mice received three daily i.n. administration of IL-33 and challenged with another set of IL-33 injections a month later. Mice were analyzed three days after the last injection. (C-G) ILC2s were quantified in the lung, liver and PB (C), IL-5<sup>+</sup>, IL-6<sup>+</sup> and IL-13<sup>+</sup> ILC2s were quantified in lung and liver (D), and various



myeloid populations (E) and CD206<sup>+</sup> macrophage (F) were quantified in the liver. Liver was analyzed for expression of *Colla1*, *Acta2* and *Timp1* genes (G). Gating strategies used for identification of each population are shown in Figure 2.2. “+/-” indicates the presence and absence of the first and second treatments, respectively. (H) Picrosirius red staining of naïve (left) and +IL33/+IL33 treated (right) liver. Scale bar=200 µm. Arrows indicate collagen fiber staining. (I) H&E staining of naïve (left, scale bar=100 µm) and +IL33/+IL33 treated liver at low (middle, scale bar=100 µm) and high (right, scale bar=20 µm) magnifications. Data represented are mean ± SEM. n=4-6; ≥2 independent experiments except d5, where n=4; 1 experiment (A), n=6-12; ≥2 independent experiments (C-G), n=5; 2 independent experiments (H, I). One-way ANOVA with Bonferroni correction (A) or two-way ANOVA with Bonferroni correction (C-G) was used to determine statistical significance, with a P value <0.05 being significant. \*P<0.05, \*\*P<0.01, \*\*\*P<0.001, \*\*\*\*P<0.0001.

Repeated i.n. IL-33 administration into CD127 cKO mice (+IL33/+IL33) caused expansion of ILC2s in the lung and liver of these mice, although the numbers were approximately 9 and 7 times less compared to WT mice, respectively (Figure 5.5A). As a result, most of the differences seen in the myeloid cell populations in WT mice were diminished in CD127 cKO mice, except eosinophils, which expanded significantly after IL-33 challenge compared to naïve (-IL33/-IL33) or single treatment groups (-IL33/+IL33 or +IL33/-IL33) (Figure 5.5B). The numbers of monocyte-derived macrophages increased in the liver of +IL-33/+IL33 mice compared to other groups, although the levels of increase were minor. Interestingly, the increase in the percentages of CD206<sup>+</sup> macrophages was not affected by decreased numbers of ILC2s in CD127 cKO mice, as CD206<sup>+</sup> macrophage percentage in +IL33/+IL33 treated mice was similar to that in WT mice (Figure 5.5C), indicating that the number or activation levels of ILC2s in CD127 cKO mice was sufficient to induce macrophage differentiation into M2 type. Finally, although a single set of IL-33 injections did not cause any increase in fibrosis related genes (-IL33/-IL33 vs. -IL33/+IL33), a second set of IL-33 injections resulted in mild increase in the relative expression of these genes (Figure 5.5D). However, the changes in the relative expression levels were much lower than in WT mice.

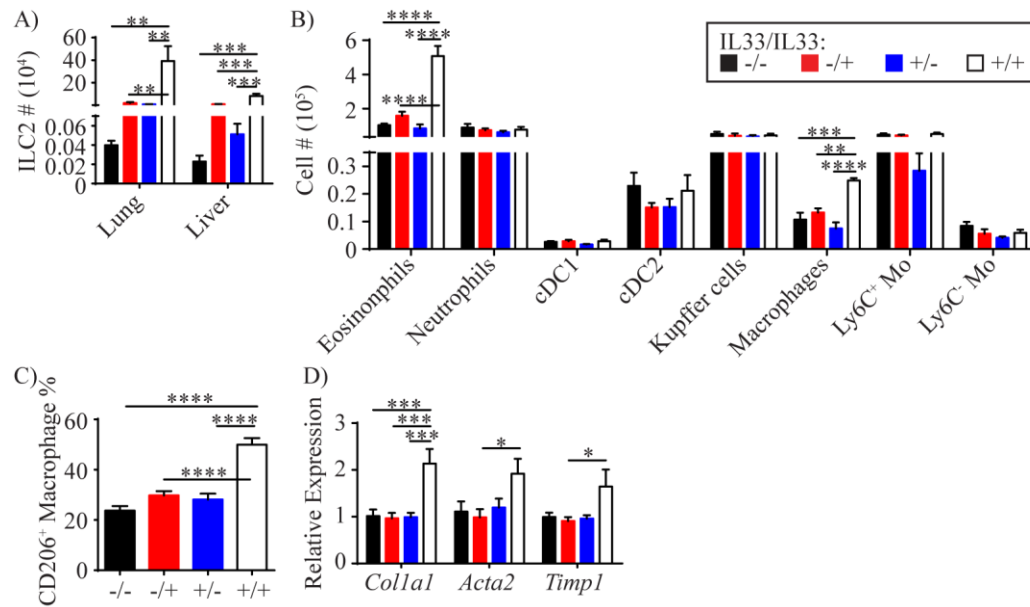


**Figure 5.5: Hepatic inflammation upon IL-33 challenge is attenuated in CD127 cKO mice**

Female CD127 cKO mice received three daily i.n. administration of IL-33 and challenged with another set of IL-33 injections a month later. Mice were analyzed three days after the last injection (treatment scheme in Figure 5.4B). ILC2s were quantified in the lung and liver (A), and various myeloid populations (B), CD206<sup>+</sup> macrophage (C) and expression of *Colla1*, *Acta2* and *Timp1* genes (D) were quantified in the liver. Gating strategies used for identification of each population are shown in Figure 2.2. “+/-” indicates the presence and absence of the first and second treatments, respectively. Data represented are mean ± SEM. n=5; 2 independent experiments. Two-way ANOVA with Bonferroni correction was used to determine statistical significance, with a P value <0.05 being significant. \*P<0.05, \*\*P<0.01, \*\*\*P<0.001, \*\*\*\*P<0.0001.

To further investigate the functional role of lung-derived ILC2s in the liver, I tested their effects on ConA-induced acute hepatitis. WT mice were given three consecutive days of i.n. IL-33 injections followed by i.v. injection of ConA one month later (Figure 5.6A). Both IL-33 pre-treated and untreated mice lost weight in a similar manner during the first 24 hours after ConA injection. However, IL-33 pre-treated mice started gaining weight within 2 days post-treatment and recovered more quickly than untreated mice (Figure 5.6B). At the time of sacrifice, the liver of IL-33 pre-treated mice appeared smooth and healthy, while the liver of mice treated with ConA without IL-33 pre-treatment had discoloured regions indicative of cirrhosis (Figure 5.6C). The IL-33 pre-treated mice had higher numbers of liver ILC2s compared to naïve mice whereas

ConA treatment had no effects on liver ILC2 numbers (Figure 5.6D). Intracellular TNF $\alpha$  and IFN $\gamma$  staining as well as an activation marker CD69 showed that IL-33 pre-treatment had no effects on ConA-induced T cell activation (Figure 5.6E). IL-33 and ConA treatments caused little changes in myeloid cell populations, although neutrophils and monocyte-derived macrophages appeared slightly higher in -IL33/+ConA group compared to +IL33/+ConA group (Figure 5.6F). Interestingly, IL-33 pre-treatment prevented increases in CD206<sup>+</sup> macrophages upon ConA treatment (Figure 5.6G). Quantification of fibrosis-related gene expression by RT-qPCR showed that *Colla1*, *Acta2* and *Timp1* were more highly expressed in -IL33/+ConA treated livers compared to +IL33/+ConA treated livers (Figure 5.6H). Picrosirius red staining also indicated higher amounts of collagen fibers in -IL33/+ConA livers than +IL33/+ConA livers (Figure 5.6I). These results suggest that lung ILC2s activated by i.n. IL-33 treatment migrate to the liver and attenuate ConA-induced acute hepatitis and cirrhosis, most likely by promoting tissue repair.

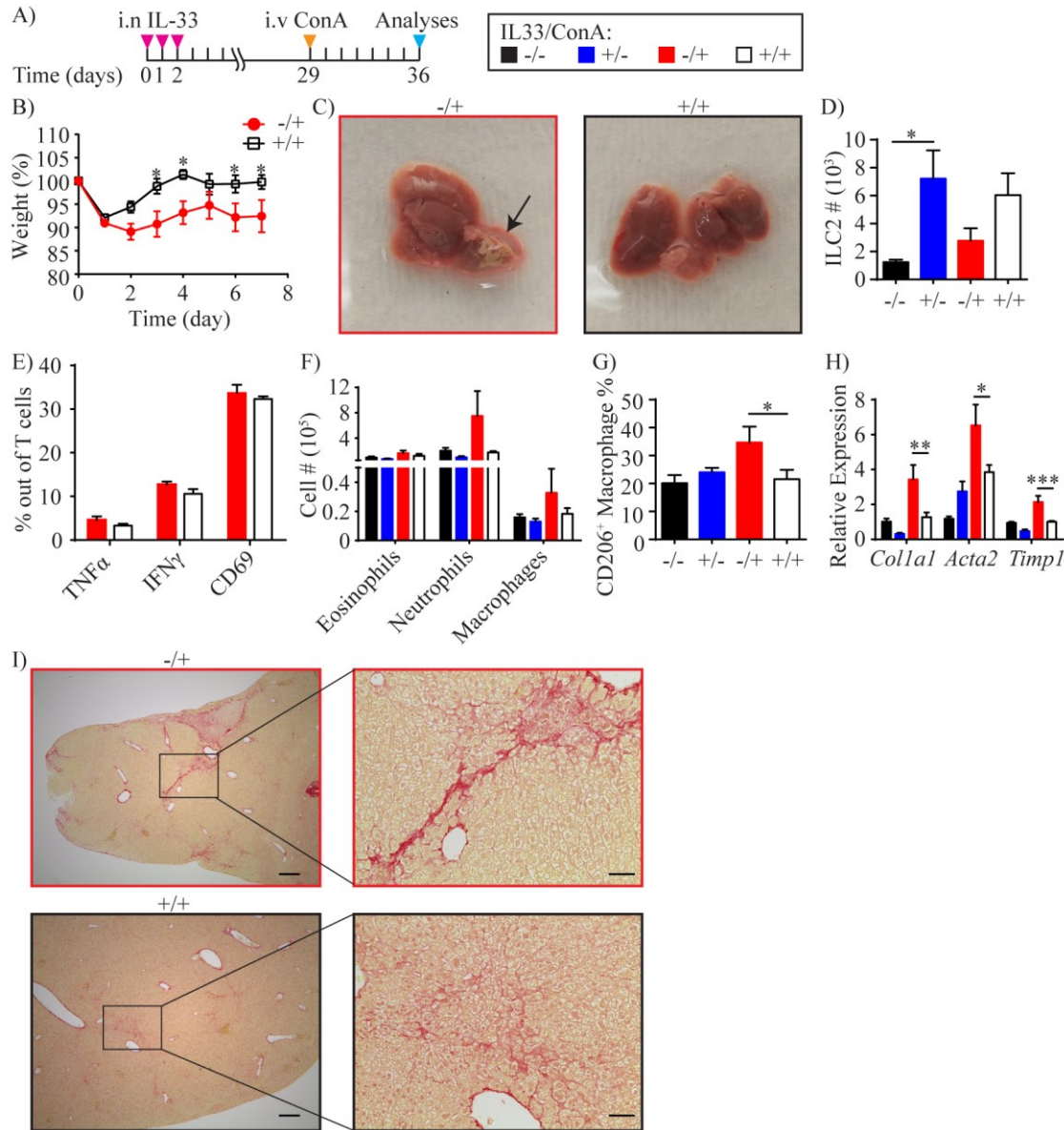


**Figure 5.6: I.n. IL-33 pre-treatment attenuates ConA-induced hepatitis**

(A) Treatment scheme for the data presented in B-I. Female WT mice received three daily i.n. administration of IL-33 followed by i.v. injection of ConA one month later. Mice were analyzed 1 week after ConA treatment. (B) Mice were weighed daily after ConA injections and the weight loss was calculated. Pictures of livers collected from -IL33/+ConA (left) and +IL33/+ConA treated (right) mice. The arrow indicates the discoloured region. ILC2s (D), percentages of T cells positive for indicated markers (E), myeloid cells (F), CD206<sup>+</sup> macrophages (G) and the expression of indicated genes (H) were quantified in the liver. “+/-” indicates the presence and absence of i.n. IL-33 and i.v. ConA treatments, respectively. (I) Picrosirius red staining of -IL33/+ConA (top) and +IL33/+ConA (bottom) treated livers at low (left, scale bar=200  $\mu$ m) and high (right, scale bar=50  $\mu$ m) magnifications. Data represented are mean  $\pm$  SEM. n=4-8; 2 independent experiments. Two-way ANOVA with Bonferroni correction was used to determine statistical significance, with a P value <0.05 being significant. \*P<0.05, \*\*P<0.01, \*\*\*P<0.001.

### 5.3 Discussion

The results presented here demonstrate that the migration of activated lung ILC2s has significant effects on immunity and inflammation in the liver. Repeated i.n. IL-33 administrations result in high numbers of lung ILC2s that migrate to the liver, leading to eosinophilic hepatitis and mild hepatic fibrosis. On the other hand, pre-treatment of mice with i.n. IL-33 administration attenuates ConA-induced acute hepatitis and severe fibrosis/cirrhosis. These two apparently opposing effects of lung-derived ILC2s are likely mediated by cytokines produced by lung-derived ILC2s in the liver. IL-5 produced by lung-derived ILC2s can drive eosinophilia while IL-13 can stimulate HSCs and induce upregulation of fibrotic genes (65) including *Colla1*, *Timp1* and *Acta2*, thus promoting liver fibrosis. ILC2s are critical for the development of eosinophilic hepatitis and fibrosis in the IL-33 treated mice as the ILC2-deficient CD127 cKO mice showed much reduced sign of eosinophilia and fibrosis even after repeated IL-33 treatments. IL-13 produced by lung-derived ILC2s also likely induces differentiation of macrophages into the M2 pathway and promotes type 2 skewing in the liver. It is therefore surprising that ConA treatment did not induce expansion of M2 macrophages in IL-33 pre-treated mice as +IL33/+ConA mice had significantly less M2 macrophages compared to -IL33/+ConA mice (Figure 5.6G). However, as the percentages of M2 macrophages at baseline before ConA treatment (-IL33/-ConA vs. +IL33/-ConA) are similar, lung-derived ILC2s most likely induce functional rather than quantitative changes in M2 macrophages. ConA-induced hepatitis is mediated, at least in part, by the prototypic Th1 cytokines IFN $\gamma$  and TNF $\alpha$  (370). As the IL-33 pre-treatment has no obvious effects on T cells expressing intracellular TNF $\alpha$  or IFN $\gamma$  (Figure 5.6E), it is unlikely that lung-derived ILC2s inhibit T cell activation by ConA. Instead, the type 2 immunity driven by lung-derived ILC2s likely promotes repair of damaged liver

tissues, as suggested by the rapid recovery from the initial weight loss in +IL33/+ConA mice. It is interesting to note that the results presented here are contradictory to previous publication showing that ILC2s promote ConA-induced hepatitis (356). It is possible that, in this model, the liver resident ILC2s cause tissue damage, while lung-derived liver ILC2s promote tissue repair, which could potentially be mediated by their differential cytokine production. Although I did not explore the role of IL-6 here, I have shown in Chapter 4 that lung-derived liver ILC2s produce IL-6 (Figure 4.4E-G), a hepatocyte growth factor (263,371). It is conceivable that IL-6 contributes to the repair of the damaged liver by promoting hepatocyte regeneration in IL-33 pre-treated mice.

It is not clear what evolutionary advantage there was for activated lung ILC2s to migrate specifically to the liver, but not to other organs. Considering the tissue residency of ILC2s, inducibility of their migration and their preference to settle in the liver, it is possible that this phenomenon was somehow selected for during evolution. In 1991, Margie Profet proposed the toxin hypothesis, which suggests that allergic responses are reactions towards materials that contain potentially toxic substances (372), and therefore, allergy has evolved as a mechanism to keep us away from harmful substances. Based on this theory, it is also probable that cells which are activated by allergens or irritants have a mechanism to “prepare” for potential danger. I have shown here that lung-derived ILC2s induce changes in the immune environment of the liver and protects the liver from ConA-induced damage. As the liver is one of the major organs that processes toxic substances, ILC2s may migrate to the liver upon stimulation in the lung to prepare to repair any damage caused by potentially poisonous substances.

Based on the results presented in this chapter, it is conceivable that PB ILC2s in asthma patients (236), which may derive from allergen-stimulated lungs, might also settle in the liver

and regulate hepatic inflammation and fibrosis. There have been case reports of patients simultaneously suffering from pulmonary fibrosis and liver cirrhosis (373) as well as asthmatic patients with eosinophilic hepatitis or cirrhosis (374,375). However, the results presented here have shown that lung-derived liver ILC2s can be pro- or anti- fibrotic depending on the immunological context, and confirming the protective or promoting effects of lung-derived liver ILC2s in hepatitis, fibrosis or cirrhosis would require detailed analyses of lymphocytes and myeloid cells in liver biopsy samples from asthma patients showing a sign of liver inflammation. If verified, the finding may lead to a new way of treating hepatitis patients.

## Chapter 6: Conclusion

### 6.1 Summary

Since their discovery in 2010, numerous studies have shown protective and pathological functions of ILC2s in various mouse and human organs. ILC2s seed tissues early after birth (83–85) and remain mostly tissue resident (86) for a long time during their lifetime. Therefore, ILC2s adapt to tissue specific cues and play critical roles in local immune responses (74), which is reflected by their phenotypic and functional diversity. In this thesis, I explored immunity provided by tissue-resident and migratory ILC2s upon i.n. IL-33 treatment, thereby challenging the idea of ILC2 tissue residency. In the first part of the thesis (Chapter 3), I investigated sex- and age-dependent regulation of lung-resident ILC2s, while in the second part (Chapters 4 and 5), I examined migratory potential of lung ILC2s as well as their roles in the liver after i.n. IL-33 stimulation.

In Chapter 3, I have shown enhanced responsiveness of female lung ILC2s compared to male ILC2s upon i.n. IL-33 stimulation, resulting in exacerbation of eosinophilic inflammation in post-pubertal female lungs (Figure 6.1). While the numbers of ILC2s in naïve female and male lungs were similar, the sex-dependent differences were likely imprinted at the naïve stage as ILC2s purified from naïve female lungs presented a more activated transcriptome profiles compared to those from male. Additionally, a greater frequency of female ILC2s were in cell cycle than male ILC2s as shown by higher percentages of Ki67<sup>+</sup> cells among naïve female compared to male ILC2s. Although I have also found increased expression of ILC2-activating cytokines, including IL-33, TSLP and IL-7, in naïve female lungs, endogenous IL-33 was not responsible for enhanced responsiveness of female lung ILC2s as sex difference in ILC2 expansion was still present in IL-33 deficient mice.



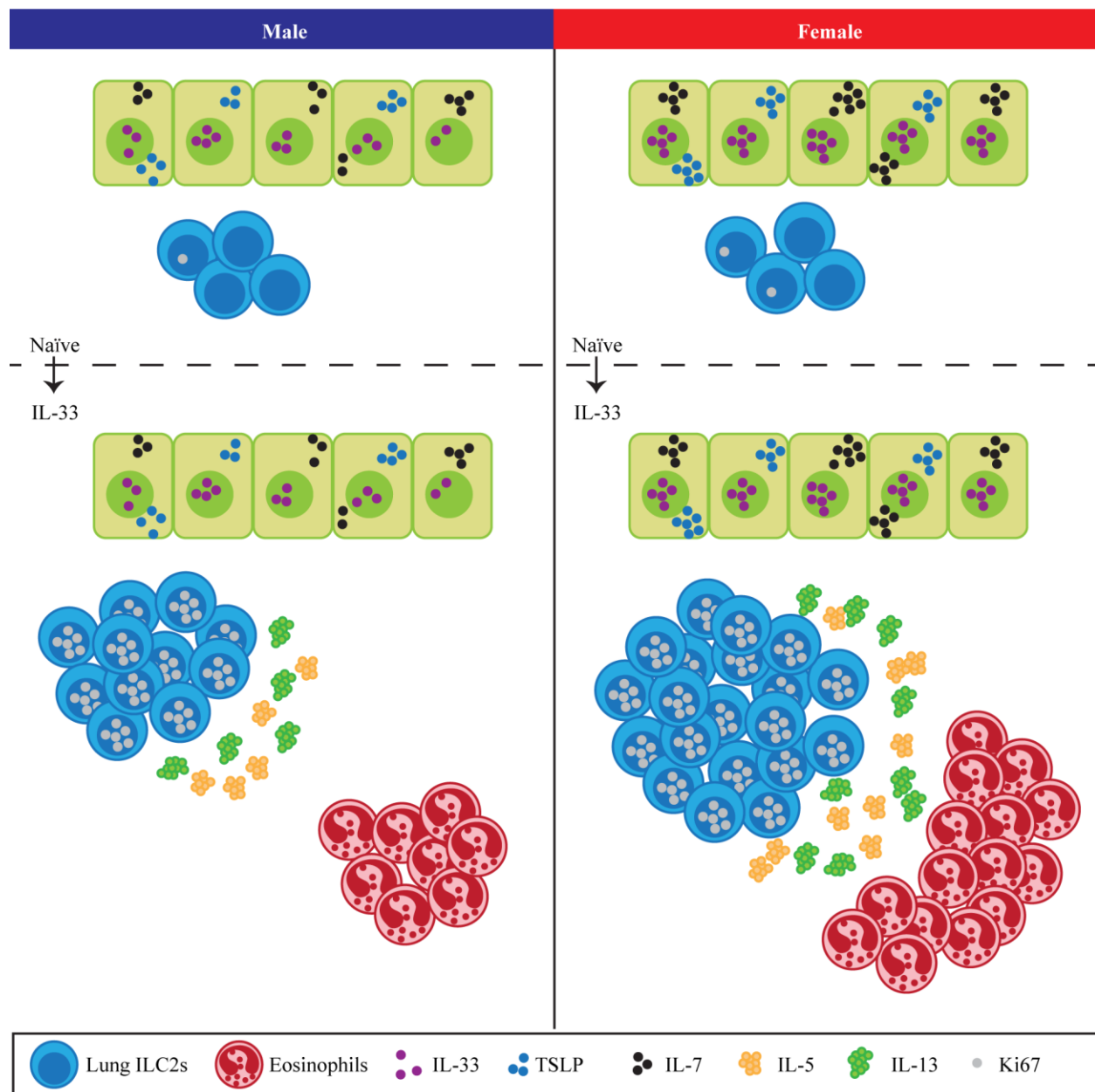


**Figure 6.1: Post-pubertal female lung ILC2s are more responsive than male lung ILC2s**

Post-pubertal naïve female lungs have greater percentages of Ki67<sup>+</sup> ILC2s as well as greater amounts of epithelium-derived cytokines compared to male lungs (top panel). Upon i.n. IL-33 treatment, female lung ILC2s proliferate more and produce greater amounts of IL-5 and IL-13 than male lung ILC2s, resulting in enhanced eosinophilia (bottom panel).

My work shown in Chapter 4 replicated a previous report showing tissue residency of ILC2s at steady state and upon activation (86). However, I found that i.n. administration of IL-33

caused expansion of ILC2s in the PB and liver in addition to the lung. Parabiosis experiments clearly indicated that these migratory ILC2s originated from the lung (Figure 6.2). While the majority of lung ILC2s upregulated CD103 upon i.n. IL-33 stimulation, migratory ILC2s lacked CD103 expression. Transcriptomic analyses demonstrated similarities between liver, PB and CD103<sup>-</sup> lung ILC2s, which more highly expressed genes related to cell cycle and DNA replication compared to CD103<sup>+</sup> lung ILC2s. ILC2s isolated from the liver after i.n. IL-33 treatment produced greater amounts of type 2 cytokines, Areg and IL-6 than lung ILC2s, although it is not clear whether it is an intrinsic property of the migratory ILC2s or due to the cues received from the liver environment. Nevertheless, this led me to investigate the functions of the lung-derived ILC2s in the liver in Chapter 5.

Lung-derived ILC2s induced alterations in the immune environment of the liver mainly by inducing eosinophilia and M2 macrophage polarization (Figure 6.2), which were diminished in ILC2 deficient CD127 cKO mice. Re-activation of ILC2s by a second set of i.n. IL-33 injections a month later further enhanced migration of lung ILC2s to the liver as well as eosinophilia and M2 polarization (Figure 6.3). Eosinophils formed a large cluster in the liver after repeated IL-33 treatments, indicative of eosinophilic hepatitis. In parallel, upregulation of fibrosis-related genes as well as collagen deposition was observed. In contrast, lung-derived ILC2s attenuated ConA-induced hepatitis, most probably by promoting tissue repair and recovery from liver injury (Figure 6.3).

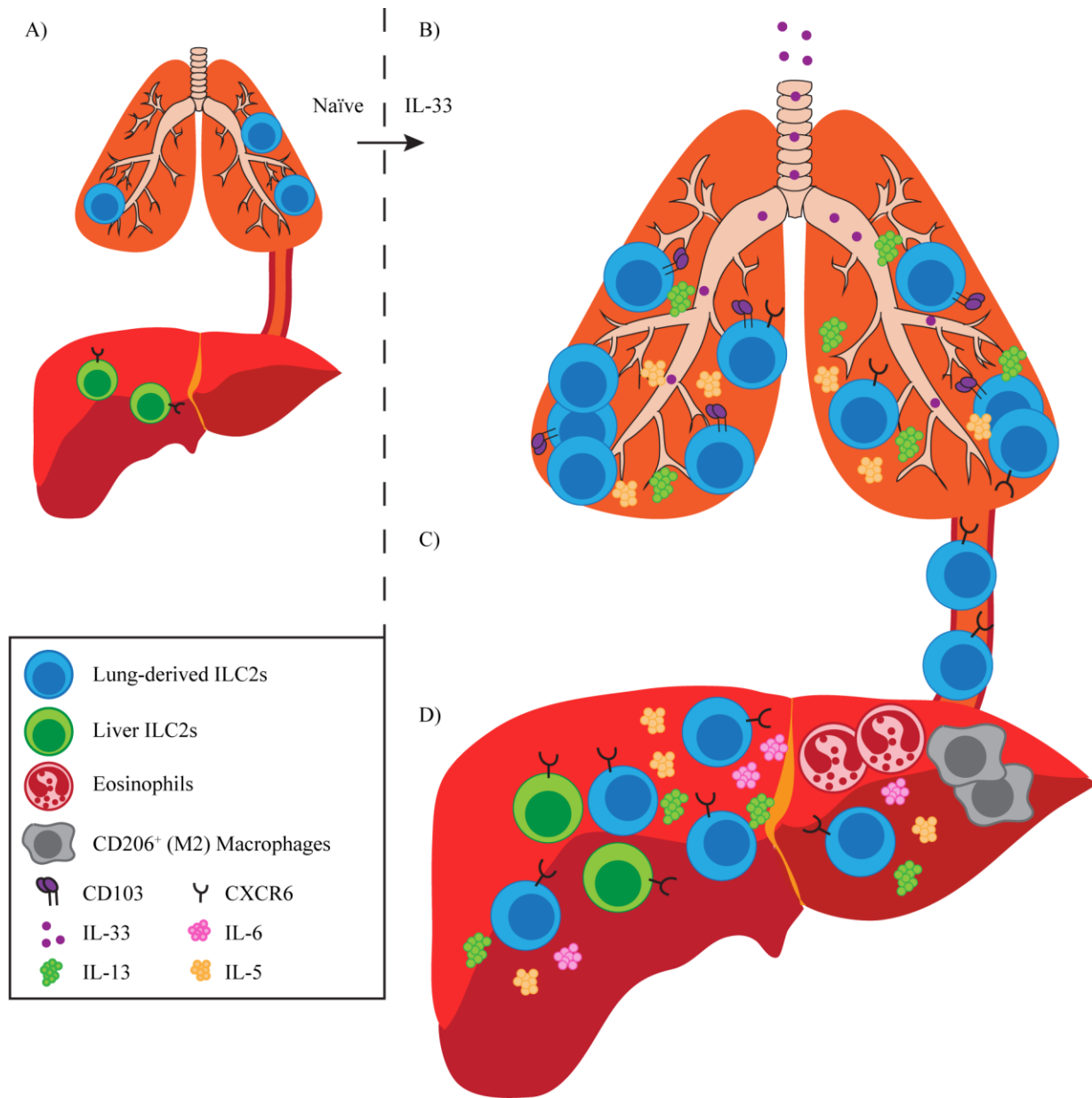


**Figure 6.2: Lung ILC2s migrate to the liver upon activation and alter the immune environment**  
 (A) There are few ILC2s in naïve lung and liver. (B, C) Upon i.n. IL-33 treatment, lung ILC2s upregulate CD103 and CXCR6. CD103<sup>+</sup> ILC2s remain in the lung (B), while CD103<sup>-</sup> ILC2s circulate through PB and migrate to the liver (C). (D) In the liver, lung-derived ILC2s produce IL-5, IL-13 and IL-6, leading to eosinophil recruitment and M2 macrophage polarization.

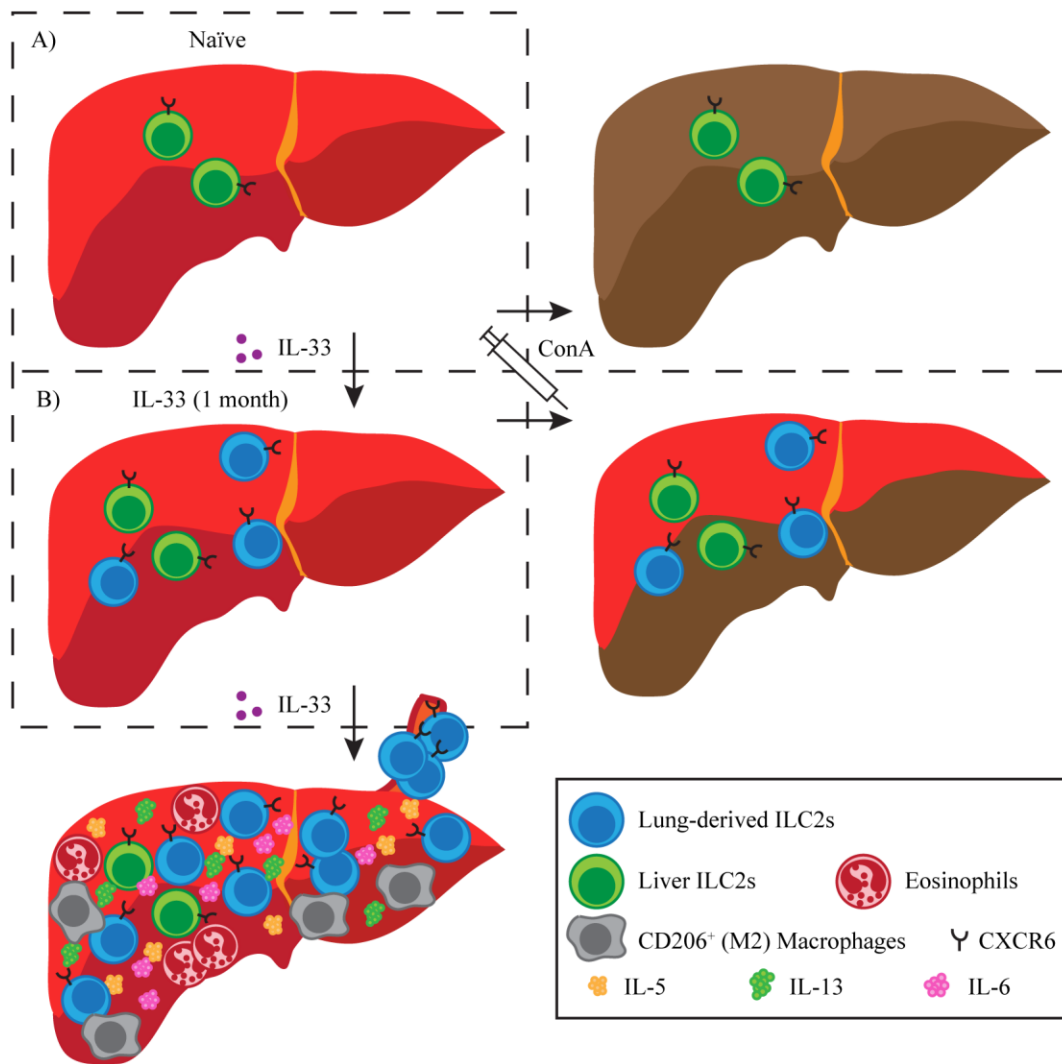


**Figure 6.3: Lung-derived ILC2s exert pro- and anti-fibrotic effects in the liver**

(A) There are few ILC2s in the naïve liver (left panel). I.v. injections of ConA into naïve mice result in severe hepatitis (right panel). (B) I.n. IL-33 administration induces lung ILC2 migration into the liver, and the numbers remain higher than those in naïve liver for more than a month (top left panel). A second set of i.n. IL-33 treatment causes migration of more ILC2s, leading to eosinophilic hepatitis and fibrosis-like inflammation (bottom panel), while IL-33 pre-treatment attenuates ConA-induced hepatitis (right panel).

In summary, the work presented in this thesis demonstrates (i) ILC2 intrinsic and environmental differences in naïve female and male lungs, (ii) the existence of a previously undescribed subset of CD103<sup>-</sup> migratory ILC2s which migrates to the liver upon activation in the lung, and (iii) pro- and anti-fibrotic roles of lung-derived ILC2s in the liver.

## 6.2 Significance

It has been known that asthma is more common among boys than girls, while this trend reverses after puberty (248), but the reason behind it has been unknown. My work shown in Chapter 3 demonstrates greater ILC2 responsiveness and enhanced eosinophilic inflammation in female lungs compared to male lungs upon i.n. IL-33 stimulation, which provides a potential mechanism behind epidemiological findings on sex bias in asthma prevalence. Although I did not investigate direct effects of sex steroid hormones on ILC2s, the differences in the ILC2 transcriptomes and the levels of ILC2 activating cytokines between female and male lungs suggest significant contributions of sex as an ILC2 regulatory factor. This raises awareness about potential adverse effects of hormone replacement therapy on type 2 airway inflammation, but also indicates that we must take precautions in selecting the sex of the mice used in ILC2 research as their intrinsic differences may lead to discrepancies in the results.

In the ILC field there has been a consensus that ILCs remain tissue resident, whereas there is mounting evidence of a migratory potential of ILC2s. The lung-liver axis of ILC2 migration and immune regulation, however, has never been reported, offering a novel insight into the complexity of ILC2-mediated immunity. My results suggest that pathogenic ILC2s in one human organ may have been activated elsewhere, prompting the need to investigate beyond specific tissues, which may lead to broadening of the potential targets for therapeutic intervention. Moreover, much of the human ILC2 research has so far relied on analyses of PB ILC2s, but their origins have been unknown. I have now shown that mouse ILC2s can enter circulation upon activation in the lung. As humans are constantly exposed to pathogens and allergens, this suggests that human PB ILC2s are probably a heterogeneous mixture of ILC2s activated in

various organs, and they may not be the best representation of the immunological events happening in one tissue.

The majority of mouse and human studies so far suggest pro-fibrotic roles of liver ILC2s (65,81,82,356), although ILC2s can exert mild protective effects in adenovirus-induced viral hepatitis model (237). Regardless, this is the first study clearly demonstrating both anti- and pro-fibrotic functions of ILC2s. Although it is uncertain whether it is a specific property of lung-derived ILC2s or liver resident ILC2s have similar capacity, these findings offer insight into context-dependent double-edged roles of ILC2s in liver inflammation.

### **6.3 Strengths and limitations**

Unlike other studies that reported the effects of sex steroid hormones on ILC2 development and responsiveness, I have focused on ILC2 intrinsic differences using transcriptomic analyses, which provided a global picture of the “more activated” state of naïve female lung ILC2s compared to male ILC2s. However, these analyses failed to pinpoint the exact mechanism behind the sex differences in ILC2s. Likewise, microarray analyses of the lung, liver and PB ILC2s also did not give insights into the mechanism behind ILC2 migration from the lung to the liver. One of the limitations of using microarray is that by using bulk RNA, microarray only detects average expression levels in a population of cells as a whole and does not give gene expression profiles at cellular or subset levels. More extensive analyses focusing on mechanistic aspect would require single cell RNA sequencing.

One of the difficulties I have faced in studying sex difference is that the difference in ILC2 numbers between IL-33 treated male and female lungs are relatively small to begin with. Consequently, it is not feasible to identify a pathway, gene or molecule that regulates ILC2 sex

bias, which is most likely mediated by many factors and the effect of a single factor in isolation may not appear significant. Therefore, by drawing conclusions based on statistical significance, biological relevance of a factor may be neglected.

In Chapter 4, I have used parabiosis mice to show that ILC2s that expand in the liver after i.n. IL-33 administration are of lung origin rather than liver resident ILC2s that are activated by IL-33 entering circulation. However, at this point, I cannot distinguish between liver resident ILC2s and lung-derived ILC2s in the liver, because there is no ILC2 specific marker, and thus, it is not feasible to label ILC2s in a tissue-specific manner. This poses issues in understanding specific roles of lung-derived ILC2s in comparison to liver resident ILC2s. Consequently, the conclusions I drew from my work presented in Chapters 4 and 5 are based on an assumption that the majority of liver ILC2s after i.n. IL-33 treatment is lung-derived and that the contribution of liver resident ILC2s is negligible.

Traditionally, ILC2 deficient mouse models were generated by transplantation of BM cells from ILC2 deficient *Rora*<sup>sg/sg</sup> mice (60,99), which do not survive into adulthood due to neurological defects (376,377). The newly generated ILC2 deficient CD127 cKO mice allowed me to study an ILC2 deficient system without having to perform BM transplantation. However, as I have shown in Figure 5.2 and Appendix C.1, some other immune cell populations are also reduced or increased in various tissues of CD127 cKO compared to WT mice, and it is unclear whether they have any effects. Moreover, some ILC2s either escape Cre-mediated deletion of *Il7ra* or do not depend on IL-7 signaling for their development, as implied by the presence of small numbers of ILC2s in *Il7ra*<sup>-/-</sup> mice (99,105), and consequently there are residual ILC2s in CD127 cKO mice. As can be seen in the mild expansion of eosinophils in CD127 cKO mouse liver upon i.n. IL-33 treatment (Figure 5.3C), these residual ILC2s are functionally competent

and contribute to mild inflammation. Furthermore, when repeated injections of IL-33 were given, ILC2 numbers in the liver in CD127 cKO mice reached 80 thousand cells, which is double the number of ILC2s in WT mouse liver after one set of IL-33 injections, posing limitations of the use of these mice as an ILC2 deficient mouse model.

While the IL-33 model is a simple system where the stimulation is relatively specific to ILC2s and is suitable for investigating mechanisms, it is highly artificial and not physiological. Moreover, repeated i.n. administrations of IL-33 used in Chapter 5 are not the best representation of chronic lung inflammation, where inflammation is persistent for a long period time. It is therefore necessary to study more physiological settings by using allergens, such as papain or HDM, to better recapitulate and understand the situations in humans.

Finally, it is currently not possible to find a link between human asthma and liver fibrosis to confirm my work in mice. While there have been reports showing patients simultaneously suffering from asthma and hepatitis or cirrhosis (374,375), if lung-derived ILC2s attenuate hepatitis as shown in ConA-induced hepatitis model, their effects will be undetected as it is not feasible to examine the liver of asthma patients without impaired liver functions. Thus, current and any further research on the functions of lung-derived ILC2s in the liver need to rely on the use of mouse models.

## **6.4 Future directions**

One of the questions left unanswered in Chapter 3 is the contribution of epithelium-derived cytokines to the difference in ILC2 responsiveness in male versus female mouse lungs. While I eliminated the possibility of IL-33 contribution, I did not explore the relevance of the sex differences in IL-7 and TSLP. Since TSLP signaling is unlikely required for ILC2 development



as suggested by normal numbers of lung ILC2s in TSLPR deficient mice (378), female and male ILC2 responsiveness upon IL-33 treatment can be studied using these mice. Investigation of the relevance of IL-7 signaling will not be feasible as IL-7 or IL-7R $\alpha$  deficient mice have significantly reduced numbers of ILC2s due to their developmental reliance on IL-7 signaling (22,99,105). Therefore, the use of an inducible IL-7 deletion mouse model or IL-7/IL-7R $\alpha$  neutralization will be necessary.

In Chapter 4, I have shown differential expression of CD103 and CXCR6 on lung, liver and PB ILC2s. However, their involvement in regulation of ILC2 migration was not explored and will require further investigation. I hypothesized that CD103 upregulation by lung ILC2s upon IL-33 treatment mediates retention of ILC2s in the lung, while CXCR6 is required for entrance of lung-derived ILC2s into the liver. This hypothesis can be tested by generating ILC2-selective CD103 and CXCR6 deficient mice (*Rora-Cre* x *Itgb7*<sup>fl/fl</sup> or *Rora-Cre* x *Cxcr6*<sup>fl/fl</sup>) and examining ILC2 migration patterns upon i.n. IL-33 treatment.

Although microarray analyses provided insight into the similarities between CD103<sup>-</sup> lung and liver ILC2s in that they express higher levels of cell cycle-related genes than CD103<sup>+</sup> lung ILC2s, phenotypic and functional analyses are necessary to understand their biological relevance. Flow cytometric analyses of surface molecule expression and cytokine profiling of the supernatants collected from ex vivo culture of each population will likely reveal their unique properties and suggest their biological functions.

My work in Chapter 5 demonstrated protective effects of lung-derived ILC2s in ConA-induced hepatitis. It is important to confirm that this is mediated by ILC2s by performing the same experiment in CD127 cKO mice. Additionally, the ILC2-mediated protection should also be tested in a more physiological model where mice are pre-treated with protease allergens or

HDM instead of IL-33. Once confirmed, the next critical question is how ILC2s exert their protective effects. I have shown in Chapter 4 that lung-derived ILC2s produce IL-6, which is a hepatocyte growth factor (263,371). Perhaps, *Rora-Cre* x *Il6<sup>fl/fl</sup>* mice can be generated to test the roles of ILC2-derived IL-6 in protection from ConA-induced hepatic injury. The direct mitogenic effects of ILC2-derived IL-6 on hepatocytes can also be assessed by incubating a hepatocyte cell line in culture supernatant collected from purified liver ILC2 culture in the presence or absence of IL-6 neutralizing antibody and measuring cell proliferation by *Ki67* expression in hepatocytes.

In the current study, ILC2s isolated from the liver after i.n. IL-33 treatment contain both liver resident ILC2s and lung-derived liver ILC2s, and it is not possible to distinguish between them. A potential approach for deciphering the differences between them is to analyze liver ILC2s before and after i.n. IL-33 treatment by single cell RNA sequencing to characterize liver resident and lung-derived liver ILC2s. If they are phenotypically and functionally distinct, this will allow us to specifically target one population without compromising the other, which may give us more specific therapeutic intervention for hepatic fibrosis.

## References

1. Turvey SE, Broide DH. Innate immunity (2010). *J Allergy Clin Immunol.* **125**:S24–32.
2. Vivier E, Artis D, Colonna M, Diefenbach A, Di Santo JP, et al. Innate Lymphoid Cells: 10 Years On (2018). *Cell.* **174**:1054–66.
3. Rider P, Voronov E, Dinarello CA, Apte RN, Cohen I. Alarmins: Feel the Stress (2017). *J Immunol.* **198**:1395–402.
4. Walsh D, McCarthy J, O'Driscoll C, Melgar S. Pattern recognition receptors-Molecular orchestrators of inflammation in inflammatory bowel disease (2013). *Cytokine Growth Factor Rev.* **24**:91–104.
5. Cooper MD, Alder MN. The evolution of adaptive immune systems (2006). *Cell.* **124**:815–22.
6. Germain RN. T-cell development and the CD4-CD8 lineage decision (2002). *Nat Rev Immunol.* **2**:309–22.
7. Klose CSN, Flach M, Möhle L, Rogell L, Hoyler T, et al. Differentiation of type 1 ILCs from a common progenitor to all helper-like innate lymphoid cell lineages (2014). *Cell.* **157**:340–56.
8. Gordon SM, Chaix J, Rupp LJ, Wu J, Madera S, et al. The Transcription Factors T-bet and Eomes Control Key Checkpoints of Natural Killer Cell Maturation (2012). *Immunity.* **36**:55–67.
9. Jiao Y, Huntington ND, Belz GT, Seillet C. Type 1 innate lymphoid cell biology: Lessons learnt from natural killer cells (2016). *Front Immunol.* **7**:426.
10. Zook EC, Kee BL. Development of innate lymphoid cells (2016). *Nat Immunol.* **17**:775–82.
11. Annunziato F, Romagnani C, Romagnani S. The 3 major types of innate and adaptive cell-mediated effector immunity (2015). *J Allergy Clin Immunol.* **135**:626–35.
12. Szabo SJ, Kim ST, Costa GL, Zhang X, Fathman CG, et al. A novel transcription factor, T-bet, directs Th1 lineage commitment (2000). *Cell.* **100**:655–69.
13. Szabo SJ, Sullivan BM, Sternmann C, Satoskar AR, Sleckman BP, et al. Distinct effects of T-bet in Th1 lineage commitment and IFN- $\gamma$  production in CD4 and CD8 T cells (2002). *Science.* **295**:338–42.
14. Pearce EL, Mullen AC, Martins GA, Krawczyk CM, Hutchins AS, et al. Control of Effector CD8<sup>+</sup> T Cell Function by the Transcription Factor Eomesodermin (2003). *Science.* **302**:1041–3.
15. Robinette ML, Colonna M. Immune modules shared by innate lymphoid cells and T cells (2016). *J Allergy Clin Immunol.* **138**:1243–51.
16. Mantovani A, Sica A, Sozzani S, Allavena P, Vecchi A, et al. The chemokine system in diverse forms of macrophage activation and polarization (2004). *Trends Immunol.* **25**:677–86.
17. Mills CD. M1 and M2 macrophages: Oracles of health and disease (2012). *Crit Rev Immunol.* **32**:463–88.
18. Newton AH, Cardani A, Braciale TJ. The host immune response in respiratory virus infection: balancing virus clearance and immunopathology (2016). *Semin Immunopathol.* **38**:471–82.
19. Jacobson Brown PM, Neuman MG. Immunopathogenesis of hepatitis C viral infection:

- Th1/Th2 responses and the role of cytokines (2001). *Clin Biochem.* **34**:167–71.
20. Damsker JM, Hansen AM, Caspi RR. Th1 and Th17 cells: Adversaries and collaborators (2010). *Ann N Y Acad Sci.* **1183**:211–21.
  21. Licona-Limón P, Kim LK, Palm NW, Flavell RA. TH2, allergy and group 2 innate lymphoid cells. (2013). *Nat Immunol.* **14**:536–42.
  22. Moro K, Yamada T, Tanabe M, Takeuchi T, Ikawa T, et al. Innate production of T(H)2 cytokines by adipose tissue-associated c-Kit(+)Sca-1(+) lymphoid cells (2010). *Nature.* **463**:540–4.
  23. Neill DR, Wong SH, Bellosi A, Flynn RJ, Daly M, et al. Nuocytes represent a new innate effector leukocyte that mediates type-2 immunity (2010). *Nature.* **464**:1367–70.
  24. Price AE, Liang H-E, Sullivan BM, Reinhardt RL, Eisley CJ, et al. Systemically dispersed innate IL-13-expressing cells in type 2 immunity (2010). *Proc Natl Acad Sci U S A.* **107**:11489–94.
  25. Mjösberg JM, Trifari S, Crellin NK, Peters CP, van Drunen CM, et al. Human IL-25- and IL-33-responsive type 2 innate lymphoid cells are defined by expression of CCR4 and CD161 (2011). *Nat Immunol.* **12**:1055–62.
  26. Halim TYF, Krauss RH, Sun AC, Takei F. Lung natural helper cells are a critical source of Th2 cell-type cytokines in protease allergen-induced airway inflammation (2012). *Immunity.* **36**:451–63.
  27. Wilhelm C, Hirota K, Stieglitz B, Van Snick J, Tolaini M, et al. An IL-9 fate reporter demonstrates the induction of an innate IL-9 response in lung inflammation (2011). *Nat Immunol.* **12**:1071–7.
  28. Monticelli LA, Sonnenberg GF, Abt MC, Alenghat T, Ziegler CGK, et al. Innate lymphoid cells promote lung-tissue homeostasis after infection with influenza virus (2011). *Nat Immunol.* **12**:1045–54.
  29. Scheinman EJ, Avni O. Transcriptional regulation of Gata3 in T helper cells by the integrated activities of transcription factors downstream of the interleukin-4 receptor and T cell receptor (2009). *J Biol Chem.* **284**:3037–48.
  30. Halim TYF, Steer CA, Mathä L, Gold MJ, Martinez-Gonzalez I, et al. Group 2 innate lymphoid cells are critical for the initiation of adaptive T helper 2 cell-mediated allergic lung inflammation (2014). *Immunity.* **40**:425–35.
  31. Zhang DH, Cohn L, Ray P, Bottomly K, Ray A. Transcription factor GATA-3 is differentially expressed in murine Th1 and Th2 cells and controls Th2-specific expression of the interleukin-5 gene (1997). *J Biol Chem.* **272**:21597–603.
  32. Zheng W, Flavell RA. The Transcription Factor GATA-3 Is Necessary and Sufficient for Th2 Cytokine Gene Expression in CD4 T Cells (1997). *Cell.* **89**:587–96.
  33. Zhu J, Min B, Hu-Li J, Watson CJ, Grinberg A, et al. Conditional deletion of Gata3 shows its essential function in TH1-TH2 responses (2004). *Nat Immunol.* **5**:1157–65.
  34. Kouro T, Takatsu K. IL-5- and eosinophil-mediated inflammation: From discovery to therapy (2009). *Int Immunol.* **21**:1303–9.
  35. Gour N, Wills-Karp M. IL-4 and IL-13 signaling in allergic airway disease (2015). *Cytokine.* **75**:68–78.
  36. Sharpe C, Thornton DJ, Grencis RK. A sticky end for gastrointestinal helminths; the role of the mucus barrier (2018). *Parasite Immunol.* **40**:e12517.
  37. Rubin BK. Secretion properties, clearance, and therapy in airway disease (2014). *Transl*

- Respir Med.* **2**:6.
38. de Vries J, Punnonen J, Cocks B, de Waal Malefyt R, Aversa G. Regulation of the human IgE response by IL4 and IL13 (1993). *Res Immunol.* **144**:597–601.
  39. Lebman DA, Coffman RL. Interleukin 4 causes isotype switching to IgE in T cell-stimulated clonal B cell cultures. (1988). *J Exp Med.* **168**:853–62.
  40. Hellman LT, Akula S, Thorpe M, Fu Z. Tracing the origins of IgE, mast cells, and allergies by studies of wild animals (2017). *Front Immunol.* **8**:1749.
  41. Townsend MJ, Fallon PG, Matthews DJ, Smith P, Jolin HE, et al. IL-9-deficient mice establish fundamental roles for IL-9 in pulmonary mastocytosis and goblet cell hyperplasia but not T cell development (2000). *Immunity.* **13**:573–83.
  42. Kearley J, Erjefalt JS, Andersson C, Benjamin E, Jones CP, et al. IL-9 governs allergen-induced mast cell numbers in the lung and chronic remodeling of the airways (2011). *Am J Respir Crit Care Med.* **183**:865–75.
  43. Stein M, Keshav S, Harris N, Gordon S. Interleukin 4 potently enhances murine macrophage mannose receptor activity: A marker of alternative immunologic macrophage activation (1992). *J Exp Med.* **176**:287–92.
  44. Doherty TM, Kastelein R, Menon S, Andrade S, Coffman RL. Modulation of murine macrophage function by IL-13. (1993). *J Immunol.* **151**:7151–60.
  45. Mills CD, Kincaid K, Alt JM, Heilman MJ, Hill AM. M-1/M-2 Macrophages and the Th1/Th2 Paradigm (2000). *J Immunol.* **164**:6166–73.
  46. Gieseck RL, Wilson MS, Wynn TA. Type 2 immunity in tissue repair and fibrosis (2018). *Nat Rev Immunol.* **18**:62–76.
  47. Withers DR, Hepworth MR. Group 3 innate lymphoid cells: Communications hubs of the intestinal immune system (2017). *Front Immunol.* **8**:1298.
  48. Dienz O, Rincon M. The effects of IL-6 on CD4 T cell responses (2009). *Clin Immunol.* **130**:27–33.
  49. Ivanov II, McKenzie BS, Zhou L, Tadokoro CE, Lepelley A, et al. The Orphan Nuclear Receptor ROR $\gamma$  Directs the Differentiation Program of Proinflammatory IL-17 + T Helper Cells (2006). *Cell.* **126**:1121–33.
  50. Leung S, Liu X, Fang L, Chen X, Guo T, et al. The cytokine milieu in the interplay of pathogenic Th1/Th17 cells and regulatory T cells in autoimmune disease (2010). *Cell Mol Immunol.* **7**:182–9.
  51. Stritesky GL, Yeh N, Kaplan MH. IL-23 Promotes Maintenance but Not Commitment to the Th17 Lineage (2008). *J Immunol.* **181**:5948–55.
  52. Beringer A, Miossec P. Systemic effects of IL-17 in inflammatory arthritis (2019). *Nat Rev Rheumatol.* **15**:491–501.
  53. Korn T, Bettelli E, Oukka M, Kuchroo VK. IL-17 and Th17 Cells (2009). *Annu Rev Immunol.* **27**:485–517.
  54. Borregaard N, Cowland JB. Granules of the human neutrophilic polymorphonuclear leukocyte (1997). *Blood.* **89**:3503–21.
  55. Pickert G, Neufert C, Leppkes M, Zheng Y, Wittkopf N, et al. STAT3 links IL-22 signaling in intestinal epithelial cells to mucosal wound healing. (2009). *J Exp Med.* **206**:1465–72.
  56. Tesmer LA, Lundy SK, Sarkar S, Fox DA. Th17 cells in human disease (2008). *Immunol Rev.* **223**:87–113.

57. Fort MM, Cheung J, Yen D, Li J, Zurawski SM, et al. IL-25 induces IL-4, IL-5, and IL-13 and Th2-associated pathologies in vivo (2001). *Immunity*. **15**:985–95.
58. Hurst SD, Muchamuel T, Gorman DM, Gilbert JM, Clifford T, et al. New IL-17 Family Members Promote Th1 or Th2 Responses in the Lung: In Vivo Function of the Novel Cytokine IL-25 (2002). *J Immunol*. **169**:443–53.
59. Fallon PG, Ballantyne SJ, Mangan NE, Barlow JL, Dasvarma A, et al. Identification of an interleukin (IL)-25-dependent cell population that provides IL-4, IL-5, and IL-13 at the onset of helminth expulsion (2006). *J Exp Med*. **203**:1105–16.
60. Halim TYF, MacLaren A, Romanish MT, Gold MJ, McNagny KM, et al. Retinoic-acid-receptor-related orphan nuclear receptor alpha is required for natural helper cell development and allergic inflammation (2012). *Immunity*. **37**:463–74.
61. Chang YJ, Kim HY, Albacker LA, Baumgarth N, McKenzie ANJ, et al. Innate lymphoid cells mediate influenza-induced airway hyper-reactivity independently of adaptive immunity (2011). *Nat Immunol*. **12**:631–8.
62. Kim BS, Siracusa MC, Saenz SA, Noti M, Monticelli LA, et al. TSLP elicits IL-33-independent innate lymphoid cell responses to promote skin inflammation. (2013). *Sci Transl Med*. **5**:170ra16.
63. Salimi M, Barlow JL, Saunders SP, Xue L, Gutowska-Owsiak D, et al. A role for IL-25 and IL-33-driven type-2 innate lymphoid cells in atopic dermatitis. (2013). *J Exp Med*. **210**:2939–50.
64. Roediger B, Kyle R, Yip KH, Sumaria N, Guy T V, et al. Cutaneous immunosurveillance and regulation of inflammation by group 2 innate lymphoid cells. (2013). *Nat Immunol*. **14**:564–73.
65. Mchedlidze T, Waldner M, Zopf S, Walker J, Rankin A, et al. Interleukin-33-dependent innate lymphoid cells mediate hepatic fibrosis (2013). *Immunity*. **39**:357–71.
66. Molofsky AB, Nussbaum JC, Liang HE, Dyken SJV, Cheng LE, et al. Innate lymphoid type 2 cells sustain visceral adipose tissue eosinophils and alternatively activated macrophages (2013). *J Exp Med*. **210**:535–49.
67. Brestoff JR, Kim BS, Saenz SA, Stine RR, Monticelli LA, et al. Group 2 innate lymphoid cells promote beiging of white adipose tissue and limit obesity (2015). *Nature*. **519**:242–6.
68. Lee MW, Odegaard JI, Mukundan L, Qiu Y, Molofsky AB, et al. Activated type 2 innate lymphoid cells regulate beige fat biogenesis (2015). *Cell*. **160**:74–87.
69. Dalmas E, Lehmann FM, Dror E, Wuest S, Thienel C, et al. Interleukin-33-Activated Islet-Resident Innate Lymphoid Cells Promote Insulin Secretion through Myeloid Cell Retinoic Acid Production (2017). *Immunity*. **47**:928–42.e7.
70. Bracamonte-Baran W, Chen G, Hou X, Talor MV, Choi HS, et al. Non-cytotoxic cardiac innate lymphoid cells are a resident and quiescent type 2-committed population (2019). *Front Immunol*. **10**:634.
71. Choi HS, Won T, Hou X, Chen G, Bracamonte-Baran W, et al. Innate Lymphoid Cells Play a Pathogenic Role in Pericarditis (2020). *Cell Rep*. **9**:2989–3003.e6.
72. Spits H, Artis D, Colonna M, Dieffenbach A, Di Santo JP, et al. Innate lymphoid cells-a proposal for uniform nomenclature (2013). *Nat Rev Immunol*. **13**:145–9.
73. Dutton EE, Camelo A, Sleeman M, Herbst R, Carlesso G, et al. Characterisation of innate lymphoid cell populations at different sites in mice with defective T cell immunity (2017). *Wellcome Open Res*. **2**:117.

74. Ricardo-Gonzalez RR, Van Dyken SJ, Schneider C, Lee J, Nussbaum JC, et al. Tissue signals imprint ILC2 identity with anticipatory function (2018). *Nat Immunol.* **19**:1093–9.
75. Schneider C, O’Leary CE, von Moltke J, Liang HE, Ang QY, et al. A Metabolite-Triggered Tuft Cell-ILC2 Circuit Drives Small Intestinal Remodeling (2018). *Cell.* **174**:271–84.e14.
76. Martinez-Gonzalez I, Mathä L, Steer CA, Ghaedi M, Poon GFT, et al. Allergen-Experienced Group 2 Innate Lymphoid Cells Acquire Memory-like Properties and Enhance Allergic Lung Inflammation (2016). *Immunity.* **45**:198–208.
77. Ghaedi M, Shen ZY, Orangi M, Martinez-Gonzalez I, Wei L, et al. Single-cell analysis of ROR $\alpha$  tracer mouse lung reveals ILC progenitors and effector ILC2 subsets (2020). *J Exp Med.* **217**:e20182293.
78. Hoyler T, Klose CSN, Souabni A, Turqueti-Neves A, Pfeifer D, et al. The transcription factor GATA-3 controls cell fate and maintenance of type 2 innate lymphoid cells. (2012). *Immunity.* **37**:634–48.
79. Kim BS, Wang K, Siracusa MC, Saenz SA, Brestoff JR, et al. Basophils Promote Innate Lymphoid Cell Responses in Inflamed Skin (2014). *J Immunol.* **193**:3717–25.
80. Simoni Y, Fehlings M, Kløverpris HN, McGovern N, Koo SL, et al. Human Innate Lymphoid Cell Subsets Possess Tissue-Type Based Heterogeneity in Phenotype and Frequency (2017). *Immunity.* **46**:148–61.
81. Forkel M, Berglin L, Kekäläinen E, Carlsson A, Svedin E, et al. Composition and functionality of the intrahepatic innate lymphoid cell-compartment in human nonfibrotic and fibrotic livers (2017). *Eur J Immunol.* **47**:1280–94.
82. Gonzalez-Polo V, Pucci-Molineris M, Cervera V, Gambaro S, Yantorno SE, et al. Group 2 innate lymphoid cells exhibit progressively higher levels of activation during worsening of liver fibrosis (2019). *Ann Hepatol.* **18**:366–72.
83. Steer CA, Martinez-Gonzalez I, Ghaedi M, Allinger P, Mathä L, et al. Group 2 innate lymphoid cell activation in the neonatal lung drives type 2 immunity and allergen sensitization (2017). *J Allergy Clin Immunol.* **140**:593–5.e3.
84. de Kleer IM, Kool M, de Bruijn MJW, Willart M, van Moorlegheem J, et al. Perinatal Activation of the Interleukin-33 Pathway Promotes Type 2 Immunity in the Developing Lung (2016). *Immunity.* **45**:1285–98.
85. Saluzzo S, Gorki AD, Rana BMJ, Martins R, Scanlon S, et al. First-Breath-Induced Type 2 Pathways Shape the Lung Immune Environment (2017). *Cell Rep.* **18**:1893–905.
86. Gasteiger G, Fan X, Dikiy S, Lee SY, Rudensky AY. Tissue residency of innate lymphoid cells in lymphoid and nonlymphoid organs (2015). *Science.* **350**:981–5.
87. Schneider C, Lee J, Koga S, Ricardo-Gonzalez RR, Nussbaum JC, et al. Tissue-Resident Group 2 Innate Lymphoid Cells Differentiate by Layered Ontogeny and In Situ Perinatal Priming (2019). *Immunity.* **50**:1425–38.e5.
88. Mjösberg J, Bernink J, Golebski K, Karrich JJ, Peters CP, et al. The Transcription Factor GATA3 Is Essential for the Function of Human Type 2 Innate Lymphoid Cells (2012). *Immunity.* **37**:649–59.
89. Constantinides MG, McDonald BD, Verhoef PA, Bendelac A. A committed precursor to innate lymphoid cells (2014). *Nature.* **508**:397–401.
90. Yang Q, Saenz SA, Zlotoff DA, Artis D, Bhandoola A. Cutting Edge: Natural Helper Cells Derive from Lymphoid Progenitors (2011). *J Immunol.* **187**:5505–9.

91. Ghaedi M, Steer CA, Martinez-Gonzalez I, Halim TYF, Abraham N, et al. Common-Lymphoid-Progenitor-Independent Pathways of Innate and T Lymphocyte Development (2016). *Cell Rep.* **15**:471–80.
92. Possot C, Schmutz S, Chea S, Boucontet L, Louise A, et al. Notch signaling is necessary for adult, but not fetal, development of ROR $\gamma$ <sup>+</sup> innate lymphoid cells (2011). *Nat Immunol.* **12**:949–58.
93. Yu X, Wang Y, Deng M, Li Y, Ruhn KA, et al. The basic leucine zipper transcription factor NFIL3 directs the development of a common innate lymphoid cell precursor (2014). *Elife.* **3**:e04406.
94. Yang Q, Li F, Harly C, Xing S, Ye L, et al. TCF-1 upregulation identifies early innate lymphoid progenitors in the bone marrow (2015). *Nat Immunol.* **16**:1044–50.
95. Yu Y, Tsang JCH, Wang C, Clare S, Wang J, et al. Single-cell RNA-seq identifies a PD-1hi ILC progenitor and defines its development pathway (2016). *Nature.* **539**:102–6.
96. Seillet C, Mielke LA, Amann-Zalcenstein DB, Su S, Gao J, et al. Deciphering the Innate Lymphoid Cell Transcriptional Program (2016). *Cell Rep.* **17**:436–47.
97. Xu W, Cherrier DE, Chea S, Vosshehrich C, Serafini N, et al. An Id2RFP-Reporter Mouse Redefines Innate Lymphoid Cell Precursor Potentials (2019). *Immunity.* **50**:1054–68.
98. Klein Wolterink RGJ, Serafini N, van Nimwegen M, Vosshehrich CAJ, De Bruijn MJW, et al. Essential, dose-dependent role for the transcription factor Gata3 in the development of IL-5<sup>+</sup> and IL-13<sup>+</sup> type 2 innate lymphoid cells (2013). *Proc Natl Acad Sci U S A.* **110**:10240–5.
99. Wong SH, Walker JA, Jolin HE, Drynan LF, Hams E, et al. Transcription factor ROR $\alpha$  is critical for nuocyte development (2012). *Nat Immunol.* **13**:229–36.
100. Yagi R, Zhong C, Northrup DL, Yu F, Bouladoux N, et al. The transcription factor GATA3 is critical for the development of all IL-7R $\alpha$ -expressing innate lymphoid cells (2014). *Immunity.* **40**:378–88.
101. Harly C, Cam M, Kaye J, Bhandoola A. Development and differentiation of early innate lymphoid progenitors (2018). *J Exp Med.* **215**:249–62.
102. Califano D, Cho JJ, Uddin MN, Lorentsen KJ, Yang Q, et al. Transcription Factor Bcl11b Controls Identity and Function of Mature Type 2 Innate Lymphoid Cells (2015). *Immunity.* **43**:354–68.
103. Walker JA, Oliphant CJ, Englezakis A, Yu Y, Clare S, et al. Bcl11b is essential for group 2 innate lymphoid cell development (2015). *J Exp Med.* **212**:875–82.
104. Yu Y, Wang C, Clare S, Wang J, Lee SC, et al. The transcription factor Bcl11b is specifically expressed in group 2 innate lymphoid cells and is essential for their development (2015). *J Exp Med.* **212**:865–74.
105. Robinette ML, Bando JK, Song W, Ulland TK, Gilfillan S, et al. IL-15 sustains IL-7R-independent ILC2 and ILC3 development (2017). *Nat Commun.* **8**:14601.
106. Lei AH, Xiao Q, Liu GY, Shi K, Yang Q, et al. ICAM-1 controls development and function of ILC2 (2018). *J Exp Med.* **215**:2157–74.
107. Dinarello CA. Overview of the IL-1 family in innate inflammation and acquired immunity (2018). *Immunol Rev.* **281**:8–27.
108. Carriere V, Roussel L, Ortega N, Lacorre DA, Americh L, et al. IL-33, the IL-1-like cytokine ligand for ST2 receptor, is a chromatin-associated nuclear factor in vivo (2007). *Proc Natl Acad Sci U S A.* **104**:282–7.



109. Moussion C, Ortega N, Girard JP. The IL-1-like cytokine IL-33 is constitutively expressed in the nucleus of endothelial cells and epithelial cells in vivo: A novel “Alarmin”? (2008). *PLoS One*. **3**:e3331.
110. Küchler AM, Pollheimer J, Balogh J, Sponheim J, Manley L, et al. Nuclear interleukin-33 is generally expressed in resting endothelium but rapidly lost upon angiogenic or proinflammatory activation (2008). *Am J Pathol*. **173**:1229–42.
111. Pichery M, Mirey E, Mercier P, Lefrancais E, Dujardin A, et al. Endogenous IL-33 is highly expressed in mouse epithelial barrier tissues, lymphoid organs, brain, embryos, and inflamed tissues: in situ analysis using a novel Il-33-LacZ gene trap reporter strain. (2012). *J Immunol*. **188**:3488–95.
112. Dahlgren MW, Jones SW, Cautivo KM, Dubinin A, Ortiz-Carpena JF, et al. Adventitial Stromal Cells Define Group 2 Innate Lymphoid Cell Tissue Niches (2019). *Immunity*. **50**:707–22.e6.
113. Zhao W, Hu Z. The enigmatic processing and secretion of interleukin-33 (2010). *Cell Mol Immunol*. **7**:260–2.
114. Baekkevold ES, Roussigné M, Yamanaka T, Johansen FE, Jahnsen FL, et al. Molecular characterization of NF-HEV, a nuclear factor preferentially expressed in human high endothelial venules (2003). *Am J Pathol*. **163**:69–79.
115. Lefrançais E, Roga S, Gautier V, Gonzalez-de-Peredo A, Monsarrat B, et al. IL-33 is processed into mature bioactive forms by neutrophil elastase and cathepsin G (2012). *Proc Natl Acad Sci U S A*. **109**:1673–8.
116. Travers J, Rochman M, Miracle CE, Habel JE, Brusilovsky M, et al. Chromatin regulates IL-33 release and extracellular cytokine activity (2018). *Nat Commun*. **9**:3244.
117. Cayrol C, Girard JP. The IL-1-like cytokine IL-33 is inactivated after maturation by caspase-1 (2009). *Proc Natl Acad Sci U S A*. **106**:9021–6.
118. Lefrançais E, Duval A, Mirey E, Roga S, Espinosa E, et al. Central domain of IL-33 is cleaved by mast cell proteases for potent activation of group-2 innate lymphoid cells (2014). *Proc Natl Acad Sci U S A*. **111**:15502–7.
119. Palmer G, Lipsky BP, Smithgall MD, Meininger D, Siu S, et al. The IL-1 receptor accessory protein (AcP) is required for IL-33 signaling and soluble AcP enhances the ability of soluble ST2 to inhibit IL-33 (2008). *Cytokine*. **42**:358–64.
120. Schmitz J, Owyang A, Oldham E, Song Y, Murphy E, et al. IL-33, an interleukin-1-like cytokine that signals via the IL-1 receptor-related protein ST2 and induces T helper type 2-associated cytokines (2005). *Immunity*. **23**:479–90.
121. Furusawa J, Moro K, Motomura Y, Okamoto K, Zhu J, et al. Critical Role of p38 and GATA3 in Natural Helper Cell Function (2013). *J Immunol*. **191**:1818–26.
122. Monin L, Gaffen SL. Interleukin 17 family cytokines: Signaling mechanisms, biological activities, and therapeutic implications (2018). *Cold Spring Harb Perspect Biol*. **10**:a028522.
123. von Moltke J, Ji M, Liang HE, Locksley RM. Tuft-cell-derived IL-25 regulates an intestinal ILC2-epithelial response circuit (2016). *Nature*. **529**:221–5.
124. Kang CM, Jang AS, Ahn MH, Shin JA, Kim JH, et al. Interleukin-25 and interleukin-13 production by alveolar macrophages in response to particles (2005). *Am J Respir Cell Mol Biol*. **33**:290–6.
125. Ikeda K, Nakajima H, Suzuki K, Kagami SI, Hirose K, et al. Mast cells produce

- interleukin-25 upon FcεRI-mediated activation (2003). *Blood*. **101**:3594–6.
126. Wang YH, Angkasekwinai P, Lu N, Voo KS, Arima K, et al. IL-25 augments type 2 immune responses by enhancing the expansion and functions of TSLP-DC-activated Th2 memory cells (2007). *J Exp Med*. **204**:1837–47.
  127. Barlow JL, Bellosi A, Hardman CS, Drynan LF, Wong SH, et al. Innate IL-13-producing nuocytes arise during allergic lung inflammation and contribute to airways hyperreactivity (2012). *J Allergy Clin Immunol*. **129**:191–8.e1–4.
  128. Barlow JL, Peel S, Fox J, Panova V, Hardman CS, et al. IL-33 is more potent than IL-25 in provoking IL-13-producing nuocytes (type 2 innate lymphoid cells) and airway contraction (2013). *J Allergy Clin Immunol*. **132**:933–41.
  129. Huang Y, Guo L, Qiu J, Chen X, Hu-Li J, et al. IL-25-responsive, lineage-negative KLRG1 hi cells are multipotential “inflammatory” type 2 innate lymphoid cells (2015). *Nat Immunol*. **16**:161–9.
  130. Huang Y, Mao K, Chen X, Sun MA, Kawabe T, et al. S1P-dependent interorgan trafficking of group 2 innate lymphoid cells supports host defense (2018). *Science*. **359**:114–9.
  131. Roan F, Obata-Ninomiya K, Ziegler SF. Epithelial cell-derived cytokines: More than just signaling the alarm (2019). *J Clin Invest*. **129**:1441–51.
  132. Rochman Y, Kashyap M, Robinson GW, Sakamoto K, Gomez-Rodriguez J, et al. Thymic stromal lymphopoietin-mediated STAT5 phosphorylation via kinases JAK1 and JAK2 reveals a key difference from IL-7-induced signaling (2010). *Proc Natl Acad Sci U S A*. **107**:19455–60.
  133. Guo L, Wei G, Zhu J, Liao W, Leonard WJ, et al. IL-1 family members and STAT activators induce cytokine production by Th2, Th17, and Th1 cells (2009). *Proc Natl Acad Sci U S A*. **106**:13463–8.
  134. Mohapatra A, Van Dyken SJ, Schneider C, Nussbaum JC, Liang HE, et al. Group 2 innate lymphoid cells utilize the IRF4-IL-9 module to coordinate epithelial cell maintenance of lung homeostasis (2016). *Mucosal Immunol*. **9**:275–86.
  135. Camelo A, Rosignoli G, Ohne Y, Stewart RA, Overed-Sayer C, et al. IL-33, IL-25, and TSLP induce a distinct phenotypic and activation profile in human type 2 innate lymphoid cells (2017). *Blood Adv*. **1**:577–89.
  136. Soumelis V, Reche PA, Kanzler H, Yuan W, Edward G, et al. Human epithelial cells trigger dendritic cell-mediated allergic inflammation by producing TSLP (2002). *Nat Immunol*. **3**:673–80.
  137. Taylor BC, Zaph C, Troy AE, Du Y, Guild KJ, et al. TSLP regulates intestinal immunity and inflammation in mouse models of helminth infection and colitis (2009). *J Exp Med*. **206**:655–67.
  138. Rimoldi M, Chieppa M, Salucci V, Avogadri F, Sonzogni A, et al. Intestinal immune homeostasis is regulated by the crosstalk between epithelial cells and dendritic cells (2005). *Nat Immunol*. **6**:507–14.
  139. Spolski R, Li P, Leonard WJ. Biology and regulation of IL-2: from molecular mechanisms to human therapy (2018). *Nat Rev Immunol*. **18**:648–59.
  140. Moro K, Kabata H, Tanabe M, Koga S, Takeno N, et al. Interferon and IL-27 antagonize the function of group 2 innate lymphoid cells and type 2 innate immune responses (2016). *Nat Immunol*. **17**:76–86.

141. Chen N, Wang X. Role of IL-9 and STATs in hematological malignancies (Review) (2014). *Oncol Lett.* **7**:602–10.
142. Turner JE, Morrison PJ, Wilhelm C, Wilson M, Ahlfors H, et al. IL-9-mediated survival of type 2 innate lymphoid cells promotes damage control in helminth-induced lung inflammation (2013). *J Exp Med.* **210**:2951–65.
143. Martin CE, Spasova DS, Frimpong-Boateng K, Kim HO, Lee M, et al. Interleukin-7 Availability Is Maintained by a Hematopoietic Cytokine Sink Comprising Innate Lymphoid Cells and T Cells (2017). *Immunity.* **47**:171–82.e4.
144. Hara T, Shitara S, Imai K, Miyachi H, Kitano S, et al. Identification of IL-7–Producing Cells in Primary and Secondary Lymphoid Organs Using IL-7–GFP Knock-In Mice (2012). *J Immunol.* **189**:1577–84.
145. Mazzucchelli RI, Warming S, Lawrence SM, Ishii M, Abshari M, et al. Visualization and identification of IL-7 producing cells in reporter mice (2009). *PLoS One.* **4**:e7637.
146. Ceredig R, Rolink AG. The key role of IL-7 in lymphopoiesis (2012). *Semin Immunol.* **24**:159–64.
147. Jin J-O, Yu Q. Systemic administration of TLR3 agonist induces IL-7 expression and IL-7-dependent CXCR3 ligand production in the lung (2013). *J Leukoc Biol.* **93**:413–25.
148. Adachi T, Kobayashi T, Sugihara E, Yamada T, Ikuta K, et al. Hair follicle-derived IL-7 and IL-15 mediate skin-resident memory T cell homeostasis and lymphoma (2015). *Nat Med.* **21**:1272–9.
149. Zhang W, Du JY, Yu Q, Jin JO. Interleukin-7 produced by intestinal epithelial cells in response to *Citrobacter rodentium* infection plays a major role in innate immunity against this pathogen (2015). *Infect Immun.* **83**:3213–23.
150. Sawa Y, Arima Y, Ogura H, Kitabayashi C, Jiang JJ, et al. Hepatic Interleukin-7 Expression Regulates T Cell Responses (2009). *Immunity.* **30**:447–57.
151. Junttila IS. Tuning the cytokine responses: An update on interleukin (IL)-4 and IL-13 receptor complexes (2018). *Front Immunol.* **9**:888.
152. Motomura Y, Morita H, Moro K, Nakae S, Artis D, et al. Basophil-derived interleukin-4 controls the function of natural helper cells, a member of ILC2s, in lung inflammation (2014). *Immunity.* **40**:758–71.
153. Bal SM, Bernink JH, Nagasawa M, Groot J, Shikhagaie MM, et al. IL-1 $\beta$ , IL-4 and IL-12 control the fate of group 2 innate lymphoid cells in human airway inflammation in the lungs (2016). *Nat Immunol.* **17**:636–45.
154. Dinarello CA, Novick D, Kim S, Kaplanski G. Interleukin-18 and IL-18 binding protein (2013). *Front Immunol.* **4**:289.
155. Aggarwal BB. Signalling pathways of the TNF superfamily: A double-edged sword (2003). *Nat Rev Immunol.* **3**:745–56.
156. Richard AC, Ferdinand JR, Meylan F, Hayes ET, Gabay O, et al. The TNF-family cytokine TL1A: from lymphocyte costimulator to disease co-conspirator (2015). *J Leukoc Biol.* **98**:333–45.
157. Yu X, Pappu R, Ramirez-Carrozzi V, Ota N, Caplazi P, et al. TNF superfamily member TL1A elicits type 2 innate lymphoid cells at mucosal barriers (2014). *Mucosal Immunol.* **7**:730–40.
158. Meylan F, Hawley ET, Barron L, Barlow JL, Penumetcha P, et al. The TNF-family cytokine TL1A promotes allergic immunopathology through group 2 innate lymphoid

- cells (2014). *Mucosal Immunol.* **7**:958–68.
159. Clouthier DL, Watts TH. Cell-specific and context-dependent effects of GITR in cancer, autoimmunity, and infection (2014). *Cytokine Growth Factor Rev.* **25**:91–106.
  160. Nagashima H, Okuyama Y, Fujita T, Takeda T, Motomura Y, et al. GITR cosignal in ILC2s controls allergic lung inflammation (2018). *J Allergy Clin Immunol.* **141**:1939–43.e8.
  161. Galle-Treger L, Sankaranarayanan I, Hurrell BP, Howard E, Lo R, et al. Costimulation of type-2 innate lymphoid cells by GITR promotes effector function and ameliorates type 2 diabetes (2019). *Nat Commun.* **10**:713.
  162. Kamachi F, Isshiki T, Harada N, Akiba H, Miyake S. ICOS promotes group 2 innate lymphoid cell activation in lungs (2015). *Biochem Biophys Res Commun.* **463**:739–45.
  163. Debeuf N, Lambrecht BN. Eicosanoid control over antigen presenting cells in asthma (2018). *Front Immunol.* **9**:2006.
  164. Peters-Golden M, Gleason MM, Togias A. Cysteinyl leukotrienes: Multi-functional mediators in allergic rhinitis (2006). *Clin Exp Allergy.* **36**:689–703.
  165. Doherty TA, Khorram N, Lund S, Mehta AK, Croft M, et al. Lung type 2 innate lymphoid cells express cysteinyl leukotriene receptor 1, which regulates TH2 cytokine production (2013). *J Allergy Clin Immunol.* **132**:205–13.
  166. McGinty JW, Ting HA, Billipp TE, Nadsjombati MS, Khan DM, et al. Tuft-Cell-Derived Leukotrienes Drive Rapid Anti-helminth Immunity in the Small Intestine but Are Dispensable for Anti-protist Immunity (2020). *Immunity.* **52**:528–41.
  167. von Moltke J, O’Leary CE, Barrett NA, Kanaoka Y, Austen KF, et al. Leukotrienes provide an NFAT-dependent signal that synergizes with IL-33 to activate ILC2s (2017). *J Exp Med.* **214**:27–37.
  168. Lund SJ, Portillo A, Cavagnero K, Baum RE, Naji LH, et al. Leukotriene C4 Potentiates IL-33–Induced Group 2 Innate Lymphoid Cell Activation and Lung Inflammation (2017). *J Immunol.* **199**:1096–104.
  169. Salimi M, Stöger L, Liu W, Go S, Pavord I, et al. Cysteinyl leukotriene E4 activates human group 2 innate lymphoid cells and enhances the effect of prostaglandin D2 and epithelial cytokines (2017). *J Allergy Clin Immunol.* **140**:1090–100.e11.
  170. Lewis RA, Soter NA, Diamond PT, Austen KF, Oates JA, et al. Prostaglandin D2 generation after activation of rat and human mast cells with anti-IgE. (1982). *J Immunol.* **129**:1627–31.
  171. Oguma T, Asano K, Ishizaka A. Role of prostaglandin D2 and its receptors in the pathophysiology of asthma (2008). *Allergol Int.* **57**:307–12.
  172. Tait Wojno ED, Monticelli LA, Tran SV, Alenghat T, Osborne LC, et al. The prostaglandin D2 receptor CRTH2 regulates accumulation of group 2 innate lymphoid cells in the inflamed lung (2015). *Mucosal Immunol.* **8**:1313–23.
  173. Xue L, Salimi M, Panse I, Mjösberg JM, McKenzie ANJ, et al. Prostaglandin D2 activates group 2 innate lymphoid cells through chemoattractant receptor-homologous molecule expressed on TH2 cells. (2014). *J Allergy Clin Immunol.* **133**:1184–94.e7.
  174. Barnig C, Cernadas M, Dutilleul S, Liu X, Perrella MA, et al. Lipoxin A4 regulates natural killer cell and type 2 innate lymphoid cell activation in asthma (2013). *Sci Transl Med.* **5**:174ra26.
  175. Chang JE, Doherty TA, Baum R, Broide D. Prostaglandin D2 regulates human type 2

- innate lymphoid cell chemotaxis (2014). *J Allergy Clin Immunol.* **133**:899–901.e3.
176. Sternberg EM. Neural regulation of innate immunity: A coordinated nonspecific host response to pathogens (2006). *Nat Rev Immunol.* **6**:318–28.
  177. Klose CSN, Mahlaköiv T, Moeller JB, Rankin LC, Flamar AL, et al. The neuropeptide neuromedin U stimulates innate lymphoid cells and type 2 inflammation (2017). *Nature.* **549**:282–6.
  178. Wallrapp A, Riesenfeld SJ, Burkett PR, Abdulnour REE, Nyman J, et al. The neuropeptide NMU amplifies ILC2-driven allergic lung inflammation (2017). *Nature.* **549**:351–6.
  179. Cardoso V, Chesné J, Ribeiro H, Garcia-Cassani B, Carvalho T, et al. Neuronal regulation of type 2 innate lymphoid cells via neuromedin U (2017). *Nature.* **549**:277–81.
  180. Martinez VG, O’Driscoll L. Neuromedin U: A multifunctional neuropeptide with pleiotropic roles (2015). *Clin Chem.* **61**:471–82.
  181. Kobayashi Y, Tata PR. Pulmonary Neuroendocrine Cells: Sensors and Sentinels of the Lung (2018). *Dev Cell.* **45**:425–6.
  182. Russell FA, King R, Smillie SJ, Kodji X, Brain SD. Calcitonin gene-related peptide: physiology and pathophysiology (2014). *Physiol Rev.* **94**:1099–142.
  183. Sui P, Wiesner DL, Xu J, Zhang Y, Lee J, et al. Pulmonary neuroendocrine cells amplify allergic asthma responses (2018). *Science.* **360**:eaan8546.
  184. Nussbaum JC, Van Dyken SJ, von Moltke J, Cheng LE, Mohapatra A, et al. Type 2 innate lymphoid cells control eosinophil homeostasis (2013). *Nature.* **502**:245–8.
  185. Talbot S, Abdulnour REE, Burkett PR, Lee S, Cronin SJF, et al. Silencing Nociceptor Neurons Reduces Allergic Airway Inflammation (2015). *Neuron.* **87**:341–54.
  186. Delgado M, Ganea D. Vasoactive intestinal peptide: A neuropeptide with pleiotropic immune functions (2013). *Amino Acids.* **45**:25–39.
  187. Gour N, Smole U, Yong HM, Lewkowich IP, Yao N, et al. C3a is required for ILC2 function in allergic airway inflammation (2018). *Mucosal Immunol.* **11**:1653–62.
  188. Maazi H, Patel N, Sankaranarayanan I, Suzuki Y, Rigas D, et al. ICOS:ICOS-Ligand Interaction Is Required for Type 2 Innate Lymphoid Cell Function, Homeostasis, and Induction of Airway Hyperreactivity. (2015). *Immunity.* **42**:538–51.
  189. Salimi M, Xue L, Jolin H, Hardman C, Cousins DJ, et al. Group 2 Innate Lymphoid Cells Express Functional NKp30 Receptor Inducing Type 2 Cytokine Production (2016). *J Immunol.* **196**:45–54.
  190. Trabanelli S, Chevalier MF, Martinez-Usatorre A, Gomez-Cadena A, Salomé B, et al. Tumour-derived PGD2 and NKp30-B7H6 engagement drives an immunosuppressive ILC2-MDSC axis (2017). *Nat Commun.* **8**:593.
  191. Trinchieri G. Type I interferon: Friend or foe? (2010). *J Exp Med.* **207**:2053–63.
  192. Duerr CU, McCarthy CDA, Mindt BC, Rubio M, Meli AP, et al. Type I interferon restricts type 2 immunopathology through the regulation of group 2 innate lymphoid cells (2016). *Nat Immunol.* **17**:65–75.
  193. Maazi H, Banie H, Aleman Muench GR, Patel N, Wang B, et al. Activated plasmacytoid dendritic cells regulate type 2 innate lymphoid cell-mediated airway hyperreactivity (2018). *J Allergy Clin Immunol.* **141**:893–905.e6.
  194. Kudo F, Ikutani M, Seki Y, Otsubo T, Kawamura YI, et al. Interferon- $\gamma$  constrains cytokine production of group 2 innate lymphoid cells (2016). *Immunology.* **147**:21–9.

195. Molofsky AB, Van Gool F, Liang H-E, Van Dyken SJ, Nussbaum JC, et al. Interleukin-33 and Interferon- $\gamma$  Counter-Regulate Group 2 Innate Lymphoid Cell Activation during Immune Perturbation. (2015). *Immunity*. **43**:161–74.
196. Bi J, Cui L, Yu G, Yang X, Chen Y, et al. NK Cells Alleviate Lung Inflammation by Negatively Regulating Group 2 Innate Lymphoid Cells (2017). *J Immunol*. **198**:3336–44.
197. Vignali DAA, Kuchroo VK. IL-12 family cytokines: immunological playmakers (2012). *Nat Immunol*. **13**:722–8.
198. Mchedlidze T, Kindermann M, Neves AT, Voehringer D, Neurath MF, et al. IL-27 suppresses type 2 immune responses in vivo via direct effects on group 2 innate lymphoid cells (2016). *Mucosal Immunol*. **9**:1384–94.
199. Zdanov A. Structural Features of the Interleukin-10 Family of Cytokines (2004). *Curr Pharm Des*. **10**:3873–84.
200. Verma R, Balakrishnan L, Sharma K, Khan AA, Advani J, et al. A network map of Interleukin-10 signaling pathway (2016). *J Cell Commun Signal*. **10**:61–7.
201. Morita H, Arae K, Unno H, Miyauchi K, Toyama S, et al. An Interleukin-33-Mast Cell-Interleukin-2 Axis Suppresses Papain-Induced Allergic Inflammation By Promoting Regulatory T Cell Numbers (2015). *Immunity*. **43**:175–86.
202. Ogasawara N, Poposki JA, Klingler AI, Tan BK, Weibman AR, et al. IL-10, TGF- $\beta$  and glucocorticoid prevent the production of type 2 cytokines in human group 2 innate lymphoid cells (2018). *J Allergy Clin Immunol*. **141**:1147–51.
203. Rigas D, Lewis G, Aron JL, Wang B, Banie H, et al. Type 2 innate lymphoid cell suppression by regulatory T cells attenuates airway hyperreactivity and requires inducible T-cell costimulator–inducible T-cell costimulator ligand interaction (2017). *J Allergy Clin Immunol*. **139**:1468–77.e2.
204. Zhou Y, Wang W, Zhao C, Wang Y, Wu H, et al. Prostaglandin E2 inhibits group 2 innate lymphoid cell activation and allergic airway inflammation through E-prostanoid 4-cyclic adenosine monophosphate signaling (2018). *Front Immunol*. **9**:501.
205. Maric J, Ravindran A, Mazzurana L, Björklund ÅK, Van Acker A, et al. Prostaglandin E2 suppresses human group 2 innate lymphoid cell function (2018). *J Allergy Clin Immunol*. **141**:1761–73.e6.
206. Sreeramkumar V, Fresno M, Cuesta N. Prostaglandin E2 and T cells: Friends or foes (2012). *Immunol Cell Biol*. **90**:579–86.
207. Zhou W, Toki S, Zhang J, Goleniewksa K, Newcomb DC, et al. Prostaglandin I2 signaling and inhibition of group 2 innate lymphoid cell responses (2016). *Am J Respir Crit Care Med*. **193**:31–42.
208. Simons B, Ferrini ME, Carvalho S, Bassett DJP, Jaffar Z, et al. PGI<sub>2</sub> Controls Pulmonary NK Cells That Prevent Airway Sensitization to House Dust Mite Allergen (2017). *J Immunol*. **198**:461–71.
209. Scanzano A, Cosentino M. Adrenergic regulation of innate immunity: A review (2015). *Front Pharmacol*. **6**:171.
210. Moriyama S, Brestoff JR, Flamar AL, Moeller JB, Klose CSN, et al.  $\beta$ 2-adrenergic receptor-mediated negative regulation of group 2 innate lymphoid cell responses (2018). *Science*. **359**:1056–61.
211. Ding X, Luo Y, Zhang X, Zheng H, Yang X, et al. IL-33-driven ILC2/eosinophil axis in fat is induced by sympathetic tone and suppressed by obesity (2016). *J Endocrinol*.

- 231:35–48.**
212. Galle-Treger L, Suzuki Y, Patel N, Sankaranarayanan I, Aron JL, et al. Nicotinic acetylcholine receptor agonist attenuates ILC2-dependent airway hyperreactivity (2016). *Nat Commun.* **7**:13202.
  213. Picciotto MR, Higley MJ, Mineur YS. Acetylcholine as a Neuromodulator: Cholinergic Signaling Shapes Nervous System Function and Behavior (2012). *Neuron.* **76**:116–29.
  214. Laffont S, Blanquart E, Savignac M, Cénac C, Laverny G, et al. Androgen signaling negatively controls group 2 innate lymphoid cells (2017). *J Exp Med.* **214**:1581–92.
  215. Cephus JY, Stier MT, Fuseini H, Yung JA, Toki S, et al. Testosterone Attenuates Group 2 Innate Lymphoid Cell-Mediated Airway Inflammation (2017). *Cell Rep.* **21**:2487–99.
  216. Kadel S, Ainsua-Enrich E, Hatipoglu I, Turner S, Singh S, et al. A Major Population of Functional KLRG1 – ILC2s in Female Lungs Contributes to a Sex Bias in ILC2 Numbers (2018). *ImmunoHorizons.* **2**:74–86.
  217. Pegram HJ, Andrews DM, Smyth MJ, Darcy PK, Kershaw MH. Activating and inhibitory receptors of natural killer cells (2011). *Immunol Cell Biol.* **89**:216–24.
  218. Blaser C, Kaufmann M, Pircher H. Virus-activated CD8 T cells and lymphokine-activated NK cells express the mast cell function-associated antigen, an inhibitory C-type lectin. (1998). *J Immunol.* **161**:6451–4.
  219. Hanke T, Corral L, Vance RE, Raulet DH. 2F1 antigen, the mouse homolog of the rat “mast cell function-associated antigen”, is a lectin-like type II transmembrane receptor expressed by natural killer cells (1998). *Eur J Immunol.* **28**:4409–17.
  220. Qin W, Hu L, Zhang X, Jiang S, Li J, et al. The Diverse Function of PD-1/PD-L Pathway Beyond Cancer (2019). *Front Immunol.* **10**:2298.
  221. Taylor S, Huang Y, Mallett G, Stathopoulou C, Felizardo TC, et al. PD-1 regulates KLRG1+ group 2 innate lymphoid cells (2017). *J Exp Med.* **214**:1663–78.
  222. Wills-Karp M. Interleukin-13 in asthma pathogenesis (2004). *Immunol Rev.* **202**:175–90.
  223. Zhu Z, Homer RJ, Wang Z, Chen Q, Geba GP, et al. Pulmonary expression of interleukin-13 causes inflammation, mucus hypersecretion, subepithelial fibrosis, physiologic abnormalities, and eotaxin production (1999). *J Clin Invest.* **103**:779–88.
  224. Gordon S. Alternative activation of macrophages (2003). *Nat Rev Immunol.* **3**:23–35.
  225. Lund S, Walford HH, Doherty TA. Type 2 Innate Lymphoid Cells in Allergic Disease (2013). *Curr Immunol Rev.* **9**:214–21.
  226. Knight PA, Brown JK, Pemberton AD. Innate immune response mechanisms in the intestinal epithelium: Potential roles for mast cells and goblet cells in the expulsion of adult *Trichinella spiralis* (2008). *Parasitology.* **135**:655–70.
  227. Herbert DR, Yang JQ, Hogan SP, Groschwitz K, Khodoun M, et al. Intestinal epithelial cell secretion of RELM- $\beta$  protects against gastrointestinal worm infection (2009). *J Exp Med.* **206**:2947–57.
  228. Schwartz C, Khan AR, Floudas A, Saunders SP, Hams E, et al. ILC2s regulate adaptive Th2 cell functions via PD-L1 checkpoint control (2017). *J Exp Med.* **214**:2507–21.
  229. Camelo A, Barlow JL, Drynan LF, Neill DR, Ballantyne SJ, et al. Blocking IL-25 signalling protects against gut inflammation in a type-2 model of colitis by suppressing nuocyte and NKT derived IL-13 (2012). *J Gastroenterol.* **47**:1198–211.
  230. Kim HY, Chang Y-J, Subramanian S, Lee H-H, Albacker L a, et al. Innate lymphoid cells responding to IL-33 mediate airway hyperreactivity independently of adaptive immunity

- (2012). *J Allergy Clin Immunol.* **129**:216–27.e1–6.
231. Bartemes KR, Iijima K, Kobayashi T, Kephart GM, McKenzie AN, et al. IL-33-responsive lineage- CD25<sup>+</sup> CD44(hi) lymphoid cells mediate innate type 2 immunity and allergic inflammation in the lungs. (2012). *J Immunol.* **188**:1503–13.
  232. Doherty TA, Khorram N, Chang JE, Kim HK, Rosenthal P, et al. STAT6 regulates natural helper cell proliferation during lung inflammation initiated by *Alternaria* (2012). *Am J Physiol Lung Cell Mol Physiol.* **303**:L577–88.
  233. Klein Wolterink RGJ, Kleinjan A, van Nimwegen M, Bergen I, de Bruijn M, et al. Pulmonary innate lymphoid cells are major producers of IL-5 and IL-13 in murine models of allergic asthma. (2012). *Eur J Immunol.* **42**:1106–16.
  234. Sugita K, Steer CA, Martinez-Gonzalez I, Altunbulakli C, Morita H, et al. Type 2 innate lymphoid cells disrupt bronchial epithelial barrier integrity by targeting tight junctions through IL-13 in asthmatic patients (2018). *J Allergy Clin Immunol.* **141**:300–10.e11.
  235. Christianson CA, Goplen NP, Zafar I, Irvin C, Good JT, et al. Persistence of asthma requires multiple feedback circuits involving type 2 innate lymphoid cells and IL-33 (2015). *J Allergy Clin Immunol.* **136**:59–68.e14.
  236. Bartemes KR, Kephart GM, Fox SJ, Kita H. Enhanced innate type 2 immune response in peripheral blood from patients with asthma (2014). *J Allergy Clin Immunol.* **134**:671–8.e4.
  237. Liang Y, Jie Z, Hou L, Aguilar-Valenzuela R, Vu D, et al. IL-33 Induces Neutrophils and Modulates Liver Injury in Viral Hepatitis (2013). *J Immunol.* **190**:5666–75.
  238. Schipper HS, Prakken B, Kalkhoven E, Boes M. Adipose tissue-resident immune cells: Key players in immunometabolism (2012). *Trends Endocrinol Metab.* **23**:407–15.
  239. Sekar R, Wang L, Chow BKC. Central control of feeding behavior by the secretin, pacap, and glucagon family of peptides (2017). *Front Endocrinol.* **8**:18.
  240. Spencer SP, Wilhelm C, Yang Q, Hall JA, Bouladoux N, et al. Adaptation of innate lymphoid cells to a micronutrient deficiency promotes type 2 barrier immunity. (2014). *Science.* **343**:432–7.
  241. Calderón MA, Cox L, Casale TB, Moingeon P, Demoly P. Multiple-allergen and single-allergen immunotherapy strategies in polysensitized patients: Looking at the published evidence (2012). *J Allergy Clin Immunol.* **129**:929–34.
  242. Dharmage SC, Perret JL, Custovic A. Epidemiology of asthma in children and adults (2019). *Front Pediatr.* **7**:246.
  243. Eder W, Ege MJ, Von Mutius E. The asthma epidemic (2006). *N Engl J Med.* **355**:2226–35.
  244. Torgerson DG, Ampleford EJ, Chiu GY, Gauderman WJ, Gignoux CR, et al. Meta-analysis of genome-wide association studies of asthma in ethnically diverse North American populations (2011). *Nat Genet.* **43**:887–92.
  245. Hirota T, Takahashi A, Kubo M, Tsunoda T, Tomita K, et al. Genome-wide association study identifies three new susceptibility loci for adult asthma in the Japanese population (2011). *Nat Genet.* **43**:893–6.
  246. Bønnelykke K, Sleiman P, Nielsen K, Kreiner-Møller E, Mercader JM, et al. A genome-wide association study identifies CDHR3 as a susceptibility locus for early childhood asthma with severe exacerbations (2014). *Nat Genet.* **46**:51–5.
  247. Moffatt MF, Gut IG, Demenais F, Strachan DP, Bouzigon E, et al. A large-scale, consortium-based genomewide association study of asthma (2010). *N Engl J Med.*



- 363:1211–21.
248. Chen Y, Stewart P, Johansen H, McRae L, Taylor G. Sex difference in hospitalization due to asthma in relation to age (2003). *J Clin Epidemiol*. **56**:180–7.
  249. Barnes PJ. Intrinsic asthma: Not so different from allergic asthma but driven by superantigens? (2009). *Clin Exp Allergy*. **39**:1145–51.
  250. Kuruvilla ME, Lee FEH, Lee GB. Understanding Asthma Phenotypes, Endotypes, and Mechanisms of Disease (2019). *Clin Rev Allergy Immunol*. **56**:219–33.
  251. Fahy JV. Type 2 inflammation in asthma-present in most, absent in many (2015). *Nat Rev Immunol*. **15**:57–65.
  252. Hauber HP, Hamid Q. The role of interleukin-9 in asthma (2005). *Allergol Int*. **54**:71–8.
  253. Voehringer D, Reese TA, Huang X, Shinkai K, Locksley RM. Type 2 immunity is controlled by IL-4/IL-13 expression in hematopoietic non-eosinophil cells of the innate immune system (2006). *J Exp Med*. **203**:1435–46.
  254. Dunican EM, Fahy JV. The role of type 2 inflammation in the pathogenesis of asthma exacerbations (2015). *Ann Am Thorac Soc*. **12**:S144–9.
  255. Poss KD. Advances in understanding tissue regenerative capacity and mechanisms in animals (2010). *Nat Rev Genet*. **11**:710–22.
  256. Zhao A, Qin H, Fu X. What determines the regenerative capacity in animals? (2016). *Bioscience*. **66**:735–46.
  257. Cordero-Espinoza L, Huch M. The balancing act of the liver: tissue regeneration versus fibrosis (2018). *J Clin Invest*. **128**:85–96.
  258. Zhang CY, Yuan WG, He P, Lei JH, Wang CX. Liver fibrosis and hepatic stellate cells: Etiology, pathological hallmarks and therapeutic targets (2016). *World J Gastroenterol*. **22**:10512–22.
  259. Ramakrishna G, Rastogi A, Trehanpati N, Sen B, Khosla R, et al. From Cirrhosis to Hepatocellular Carcinoma: New Molecular Insights on Inflammation and Cellular Senescence (2013). *Liver Cancer*. **2**:367–83.
  260. Asrani SK, Devarbhavi H, Eaton J, Kamath PS. Burden of liver diseases in the world (2019). *J Hepatol*. **70**:151–71.
  261. Macdonald RA. “Lifespan” of Liver Cells: Autoradiographic Study Using Tritiated Thymidine in Normal, Cirrhotic, and Partially Hepatectomized Rats (1961). *Arch Intern Med*. **107**:335–43.
  262. Mihm S. Danger-associated molecular patterns (DAMPs): Molecular triggers for sterile inflammation in the liver (2018). *Int J Mol Sci*. **19**:3104.
  263. Cressman DE, Greenbaum LE, DeAngelis RA, Ciliberto G, Furth EE, et al. Liver failure and defective hepatocyte regeneration in interleukin-6- deficient mice (1996). *Science*. **274**:1379–83.
  264. Yamada Y, Kirillova I, Peschon JJ, Fausto N. Initiation of liver growth by tumor necrosis factor: Deficient liver regeneration in mice lacking type I tumor necrosis factor receptor (1997). *Proc Natl Acad Sci U S A*. **94**:1441–6.
  265. Selzner N, Selzner M, Odermatt B, Tian Y, Van Rooijen N, et al. ICAM-1 triggers liver regeneration through leukocyte recruitment and Kupffer cell-dependent release of TNF- $\alpha$ /IL-6 in mice (2003). *Gastroenterology*. **124**:692–700.
  266. Matsuoka M, Tsukamoto H. Stimulation of hepatic lipocyte collagen production by Kupffer cell-derived transforming growth factor  $\beta$ : Implication for a pathogenetic role in

- alcoholic liver fibrogenesis (1990). *Hepatology*. **11**:599–605.
267. Rockey DC, Weymouth N, Shi Z. Smooth muscle  $\alpha$  actin (Acta2) and myofibroblast function during hepatic wound healing. (2013). *PLoS One*. **8**:e77166.
  268. Melhem A, Muhanna N, Bishara A, Alvarez CE, Ilan Y, et al. Anti-fibrotic activity of NK cells in experimental liver injury through killing of activated HSC (2006). *J Hepatol*. **45**:60–71.
  269. Radaeva S, Sun R, Jaruga B, Nguyen VT, Tian Z, et al. Natural killer cells ameliorate liver fibrosis by killing activated stellate cells in NKG2D-dependent and tumor necrosis factor-related apoptosis-inducing ligand-dependent manners (2006). *Gastroenterology*. **130**:435–52.
  270. Glässner A, Eisenhardt M, Krämer B, Körner C, Coenen M, et al. NK cells from HCV-infected patients effectively induce apoptosis of activated primary human hepatic stellate cells in a TRAIL-, FasL- and NKG2D-dependent manner (2012). *Lab Invest*. **92**:967–77.
  271. Hammerich L, Bangen JM, Govaere O, Zimmermann HW, Gassler N, et al. Chemokine receptor CCR6-dependent accumulation of  $\gamma\delta$  T cells in injured liver restricts hepatic inflammation and fibrosis (2014). *Hepatology*. **59**:630–42.
  272. Troeger JS, Mederacke I, Gwak GY, Dapito DH, Mu X, et al. Deactivation of hepatic stellate cells during liver fibrosis resolution in mice (2012). *Gastroenterology*. **143**:1073–83.e22.
  273. Kisseleva T, Cong M, Paik YH, Scholten D, Jiang C, et al. Myofibroblasts revert to an inactive phenotype during regression of liver fibrosis (2012). *Proc Natl Acad Sci U S A*. **109**:9448–53.
  274. Karlmark KR, Weiskirchen R, Zimmermann HW, Gassler N, Ginhoux F, et al. Hepatic recruitment of the inflammatory Gr1<sup>+</sup> monocyte subset upon liver injury promotes hepatic fibrosis (2009). *Hepatology*. **50**:261–74.
  275. Bray F, Ferlay J, Soerjomataram I, Siegel RL, Torre LA, et al. Global cancer statistics 2018: GLOBOCAN estimates of incidence and mortality worldwide for 36 cancers in 185 countries (2018). *CA Cancer J Clin*. **68**:394–424.
  276. Swann JB, Smyth MJ. Immune surveillance of tumors (2007). *J Clin Invest*. **117**:1137–46.
  277. Wellenstein MD, de Visser KE. Cancer-Cell-Intrinsic Mechanisms Shaping the Tumor Immune Landscape (2018). *Immunity*. **48**:399–416.
  278. Van Dalen FJ, Van Stevendaal MHME, Fennemann FL, Verdoes M, Ilina O. Molecular repolarisation of tumour-associated macrophages (2019). *Molecules*. **24**:9.
  279. Bie Q, Zhang P, Su Z, Zheng D, Ying X, et al. Polarization of ILC2s in peripheral blood might contribute to immunosuppressive microenvironment in patients with gastric cancer (2014). *J Immunol Res*. **2014**:923135.
  280. Salimi M, Wang R, Yao X, Li X, Wang X, et al. Activated innate lymphoid cell populations accumulate in human tumour tissues (2018). *BMC Cancer*. **18**:341.
  281. Wu Y, Yan Y, Su Z, Bie Q, Chen X, et al. Enhanced circulating ILC2s and MDSCs may contribute to ensure maintenance of Th2 predominant in patients with lung cancer (2017). *Mol Med Rep*. **15**:4374–81.
  282. Carrega P, Loiacono F, Di Carlo E, Scaramuccia A, Mora M, et al. NCR + ILC3 concentrate in human lung cancer and associate with intratumoral lymphoid structures (2015). *Nat Commun*. **6**:8280.
  283. Long A, Dominguez D, Qin L, Chen S, Fan J, et al. Type 2 Innate Lymphoid Cells

- Impede IL-33–Mediated Tumor Suppression (2018). *J Immunol.* **201**:3456–64.
284. Saranchova I, Han J, Zaman R, Arora H, Huang H, et al. Type 2 Innate Lymphocytes Actuate Immunity Against Tumours and Limit Cancer Metastasis (2018). *Sci Rep.* **8**:2924.
  285. Moral JA, Leung J, Rojas LA, Ruan J, Zhao J, et al. ILC2s amplify PD-1 blockade by activating tissue-specific cancer immunity (2020). *Nature.* **579**:130–5.
  286. Chou SJ, Babot Z, Leingärtner A, Studer M, Nakagawa Y, et al. Geniculocortical input drives genetic distinctions between primary and higher-order visual areas (2013). *Science.* **340**:1239–42.
  287. McCaughy TM, Etzensperger R, Alag A, Tai X, Kurtulus S, et al. Conditional deletion of cytokine receptor chains reveals that IL-7 and IL-15 specify CD8 cytotoxic lineage fate in the thymus (2012). *J Exp Med.* **209**:2263–76.
  288. Rossi FMV, Corbel SY, Merzaban JS, Carlow DA, Gossens K, et al. Recruitment of adult thymic progenitors is regulated by P-selectin and its ligand PSGL-1 (2005). *Nat Immunol.* **6**:626–34.
  289. Romera-Hernández M, Mathä L, Steer CA, Ghaedi M, Takei F. Identification of Group 2 Innate Lymphoid Cells in Mouse Lung, Liver, Small Intestine, Bone Marrow, and Mediastinal and Mesenteric Lymph Nodes (2019). *Curr Protoc Immunol.* **125**:e73.
  290. Tuominen V, Ruotoistenmäki S, Viitanen A, Jumppanen M, Isola J. ImmunoRatio: A publicly available web application for quantitative image analysis of estrogen receptor (ER), progesterone receptor (PR), and Ki-67 (2010). *Breast Cancer Res.* **12**:R56.
  291. Subramanian A, Tamayo P, Mootha VK, Mukherjee S, Ebert BL, et al. Gene set enrichment analysis: A knowledge-based approach for interpreting genome-wide expression profiles (2005). *Proc Natl Acad Sci U S A.* **102**:15545–50.
  292. Godec J, Tan Y, Liberzon A, Tamayo P, Bhattacharya S, et al. Compendium of Immune Signatures Identifies Conserved and Species-Specific Biology in Response to Inflammation (2016). *Immunity.* **44**:194–206.
  293. Maere S, Heymans K, Kuiper M. BiNGO: A Cytoscape plugin to assess overrepresentation of Gene Ontology categories in Biological Networks (2005). *Bioinformatics.* **21**:3448–9.
  294. Merico D, Isserlin R, Stueker O, Emili A, Bader GD. Enrichment map: A network-based method for gene-set enrichment visualization and interpretation (2010). *PLoS One.* **5**:e13984.
  295. Fabregat A, Sidiropoulos K, Viteri G, Forner O, Marin-Garcia P, et al. Reactome pathway analysis: A high-performance in-memory approach (2017). *BMC Bioinformatics.* **18**:142.
  296. Sidiropoulos K, Viteri G, Sevilla C, Jupe S, Webber M, et al. Reactome enhanced pathway visualization (2017). *Bioinformatics.* **33**:3461–7.
  297. Livak KJ, Schmittgen TD. Analysis of relative gene expression data using real-time quantitative PCR and the 2- $\Delta\Delta$ CT method (2001). *Methods.* **25**:402–8.
  298. Almqvist C, Worm M, Leynaert B. Impact of gender on asthma in childhood and adolescence: a GA2LEN review (2008). *Allergy.* **63**:47–57.
  299. Sears MR, Burrows B, Flannery EM, Herbison GP, Holdaway MD. Atopy in childhood. I. Gender and allergen related risks for development of hay fever and asthma (1993). *Clin Exp Allergy.* **23**:941–8.
  300. SIDRIA (Italian Studies on Respiratory Disorders in Childhood and the Environment). Asthma and respiratory symptoms in 6-7 yr old Italian children: Gender, latitude,

- urbanization and socioeconomic factors (1997). *Eur Respir J*. **10**:1780–6.
301. Luyt DK, Burton PR, Simpson H. Epidemiological study of wheeze, doctor diagnosed asthma, and cough in preschool children in Leicestershire (1993). *Br Med J*. **306**:1386–90.
  302. Melén E, Kere J, Pershagen G, Svartengren M, Wickman M. Influence of male sex and parental allergic disease on childhood wheezing: Role of interactions (2004). *Clin Exp Allergy*. **34**:839–44.
  303. Mandhane PJ, Greene JM, Cowan JO, Taylor DR, Sears MR. Sex differences in factors associated with childhood- and adolescent-onset wheeze (2005). *Am J Respir Crit Care Med*. **172**:45–54.
  304. Anderson HR, Pottier AC, Strachan DP. Asthma from birth to age 23: Incidence and relation to prior and concurrent atopic disease (1992). *Thorax*. **47**:537–42.
  305. Venn A, Lewis S, Cooper M, Hill J, Britton J. Questionnaire study of effect of sex and age on the prevalence of wheeze and asthma in adolescence (1998). *Br Med J*. **316**:1945–6.
  306. Chen Y, Dales R, Tang M, Krewski D. Sex-related interactive effect of smoking and household pets on asthma incidence (2002). *Eur Respir J*. **20**:1162–6.
  307. Nicolai T, Pereszlenyiova-Bliznakova L, Illi S, Reinhardt D, Von Mutius E. Longitudinal follow-up of the changing gender ratio in asthma from childhood to adulthood: Role of delayed manifestation in girls (2003). *Pediatr Allergy Immunol*. **14**:280–3.
  308. Leynaert B, Sunyer J, Garcia-Esteban R, Svanes C, Jarvis D, et al. Gender differences in prevalence, diagnosis and incidence of allergic and non-allergic asthma: a population-based cohort (2012). *Thorax*. **67**:625–31.
  309. Melgert BN, Postma DS, Kuipers I, Geerlings M, Luinge MA, et al. Female mice are more susceptible to the development of allergic airway inflammation than male mice (2005). *Clin Exp Allergy*. **35**:1496–503.
  310. Blacqui re MJ, Hylkema MN, Postma DS, Geerlings M, Timens W, et al. Airway inflammation and remodeling in two mouse models of asthma: Comparison of males and females (2010). *Int Arch Allergy Immunol*. **153**:173–81.
  311. Takeda M, Tanabe M, Ito W, Ueki S, Konno Y, et al. Gender difference in allergic airway remodelling and immunoglobulin production in mouse model of asthma (2013). *Respirology*. **18**:797–806.
  312. Warren KJ, Sweeter JM, Pavlik JA, Nelson AJ, Devasure JM, et al. Sex differences in activation of lung-related type 2 innate lymphoid cells in experimental asthma (2017). *Ann Allergy, Asthma Immunol*. **118**:233–4.
  313. Bartemes K, Chen C-C, Iijima K, Drake L, Kita H. IL-33-Responsive Group 2 Innate Lymphoid Cells Are Regulated by Female Sex Hormones in the Uterus (2018). *J Immunol*. **200**:229–36.
  314. Ahnstedt H, Roy-O'Reilly M, Spychala MS, Mobley AS, Bravo-Alegria J, et al. Sex differences in adipose tissue CD8<sup>+</sup> T cells and regulatory T cells in middle-aged mice (2018). *Front Immunol*. **9**:659.
  315. Afshan G, Afzal N, Qureshi S. CD4<sup>+</sup>CD25<sup>hi</sup> regulatory T cells in healthy males and females mediate gender difference in the prevalence of autoimmune diseases (2012). *Clin Lab*. **58**:567–71.
  316. Fan X, Rudensky AY. Hallmarks of Tissue-Resident Lymphocytes (2016). *Cell*. **164**:1198–211.
  317. Stier MT, Zhang J, Goleniewska K, Cephus JY, Rusznak M, et al. IL-33 promotes the

- egress of group 2 innate lymphoid cells from the bone marrow (2018). *J Exp Med.* **215**:263–81.
318. Karta MR, Rosenthal PS, Beppu A, Vuong CY, Miller M, et al.  $\beta$ 2integrins rather than  $\beta$ 1integrins mediate *Alternaria*-induced group 2 innate lymphoid cell trafficking to the lung (2018). *J Allergy Clin Immunol.* **141**:329–38.e12.
  319. Ricardo-Gonzalez RR, Schneider C, Liao C, Lee J, Liang H-E, et al. Tissue-specific pathways extrude activated ILC2s to disseminate type 2 immunity (2020). *J Exp Med.* **217**:e20191172.
  320. Hunter MC, Teixeira A, Halin C. T cell trafficking through lymphatic vessels (2016). *Front Immunol.* **7**:613.
  321. Kurebayashi S, Ueda E, Sakaue M, Patel DD, Medvedev A, et al. Retinoid-related orphan receptor gamma (RORgamma) is essential for lymphoid organogenesis and controls apoptosis during thymopoiesis (2000). *Proc Natl Acad Sci.* **97**:10132–7.
  322. Wehr A, Baeck C, Heymann F, Niemietz PM, Hammerich L, et al. Chemokine Receptor CXCR6-Dependent Hepatic NK T Cell Accumulation Promotes Inflammation and Liver Fibrosis (2013). *J Immunol.* **190**:5226–36.
  323. Cepek KL, Shaw SK, Parker CM, Russell GJ, Morrow JS, et al. Adhesion between epithelial cells and T lymphocytes mediated by E-cadherin and the  $\alpha\beta$ 7 integrin (1994). *Nature.* **372**:190–3.
  324. “CDC6 association with the ORC:origin complex”. Reactome, version 72, <https://reactome.org>. Stable ID: R-MMU-68689 (Apr 15, 2020).
  325. “RNA polymerase I promoter opening”. Reactome, version 72, <https://reactome.org>. Stable ID: R-MMU-73728 (Apr 15, 2020).
  326. “Mitotic metaphase/anaphase transition”. Reactome, version 72, <https://reactome.org>. Stable ID: R-MMU-68881 (Apr 15, 2020).
  327. “Unwinding of DNA”. Reactome, version 72, <https://reactome.org>. Stable ID: R-MMU-176974 (Apr 15, 2020).
  328. “Packaging of telomere ends”. Reactome, version 72, <https://reactome.org>. Stable ID: R-MMU-171306 (Apr 15, 2020).
  329. “TP53 regulates transcription of genes involved in G2 cell cycle arrest”. Reactome, version 72, <https://reactome.org>. Stable ID: R-MMU-6804114 (Apr 15, 2020).
  330. “Assembly of ORC complex at the origin of replication”. Reactome, version 72, <https://reactome.org>. Stable ID: R-MMU-68616 (Apr 15, 2020).
  331. “Phosphorylation of Emi1”. Reactome, version 72, <https://reactome.org>. Stable ID: R-MMU-176417 (Apr 15, 2020).
  332. “Activation of NIMA kinases NEK9, NEK6, NEK7”. Reactome, version 72, <https://reactome.org>. Stable ID: R-MMU-2980767 (Apr 15, 2020).
  333. “G2/M DNA replication checkpoint”. Reactome, version 72, <https://reactome.org>. Stable ID: R-MMU-69478 (Apr 15, 2020).
  334. Cayrol C, Girard JP. Interleukin-33 (IL-33): A nuclear cytokine from the IL-1 family (2018). *Immunol Rev.* **281**:154–68.
  335. Zaidman NA, O’Grady KE, Patil N, Milavetz F, Maniak PJ, et al. Airway epithelial anion secretion and barrier function following exposure to fungal aeroallergens: Role of oxidative stress (2017). *Am J Physiol Cell Physiol.* **313**:C68–79.
  336. Uchida M, Anderson EL, Squillace DL, Patil N, Maniak PJ, et al. Oxidative stress serves

- as a key checkpoint for IL-33 release by airway epithelium (2017). *Allergy Eur J Allergy Clin Immunol.* **72**:1521–31.
337. Cohen ES, Scott IC, Majithiya JB, Rapley L, Kemp BP, et al. Oxidation of the alarmin IL-33 regulates ST2-dependent inflammation (2015). *Nat Commun.* **6**:8327.
  338. Förster R, Schubel A, Breitfeld D, Kremmer E, Renner-Müller I, et al. CCR7 coordinates the primary immune response by establishing functional microenvironments in secondary lymphoid organs (1999). *Cell.* **99**:23–33.
  339. Woodfin A, Voisin MB, Beyrau M, Colom B, Caille D, et al. The junctional adhesion molecule JAM-C regulates polarized transendothelial migration of neutrophils in vivo (2011). *Nat Immunol.* **12**:761–9.
  340. Nourshargh S, Renshaw SA, Imhof BA. Reverse Migration of Neutrophils: Where, When, How, and Why? (2016). *Trends Immunol.* **37**:273–86.
  341. Matloubian M, David A, Engel S, Ryan JE, Cyster JG. A transmembrane CXC chemokine is a ligand for HIV-coreceptor Bonzo (2000). *Nat Immunol.* **1**:298–304.
  342. Wilbanks A, Zondlo SC, Murphy K, Mak S, Soler D, et al. Expression Cloning of the STRL33/BONZO/TYMSTR Ligand Reveals Elements of CC, CXC, and CX3C Chemokines (2001). *J Immunol.* **166**:5145–54.
  343. Schön MP, Arya A, Murphy EA, Adams CM, Strauch UG, et al. Mucosal T lymphocyte numbers are selectively reduced in integrin alpha E (CD103)-deficient mice. (1999). *J Immunol.* **162**:6641–9.
  344. Campbell ID, Humphries MJ. Integrin structure, activation, and interactions (2011). *Cold Spring Harb Perspect Biol.* **3**:a004994.
  345. Meng F, Wang K, Aoyama T, Grivennikov SI, Paik Y, et al. Interleukin-17 signaling in inflammatory, Kupffer cells, and hepatic stellate cells exacerbates liver fibrosis in mice (2012). *Gastroenterology.* **143**:765–76.
  346. Lo BC, Gold MJ, Hughes MR, Antignano F, Valdez Y, et al. The orphan nuclear receptor ROR $\alpha$  and group 3 innate lymphoid cells drive fibrosis in a mouse model of Crohn's disease (2016). *Sci Immunol.* **1**:eaaf8864.
  347. Chiaramonte MG, Donaldson DD, Cheever AW, Wynn TA. An IL-13 inhibitor blocks the development of hepatic fibrosis during a T-helper type 2-dominated inflammatory response (1999). *J Clin Invest.* **104**:777–85.
  348. Sugimoto R, Enjoji M, Nakamuta M, Ohta S, Kohjima M, et al. Effect of IL-4 and IL-13 on collagen production in cultured LI90 human hepatic stellate cells (2005). *Liver Int.* **25**:420–8.
  349. Liu Y, Meyer C, Müller A, Herweck F, Li Q, et al. IL-13 Induces Connective Tissue Growth Factor in Rat Hepatic Stellate Cells via TGF- $\beta$ -Independent Smad Signaling (2011). *J Immunol.* **187**:2814–23.
  350. Gharaee-Kermani M, McGarry B, Lukacs N, Huffnagle G, Egan RW, et al. The role of IL-5 in bleomycin-induced pulmonary fibrosis (1998). *J Leukoc Biol.* **64**:657–66.
  351. Cho JY, Miller M, Baek KJ, Han JW, Nayar J, et al. Inhibition of airway remodeling in IL-5-deficient mice (2004). *J Clin Invest.* **113**:551–60.
  352. Reiman RM, Thompson RW, Feng CG, Hari D, Knight R, et al. Interleukin-5 (IL-5) augments the progression of liver fibrosis by regulating IL-13 activity (2006). *Infect Immun.* **74**:1471–9.
  353. Huaux F, Liu T, McGarry B, Ullenbruch M, Xing Z, et al. Eosinophils and T

- Lymphocytes Possess Distinct Roles in Bleomycin-Induced Lung Injury and Fibrosis (2003). *J Immunol.* **171**:5470–81.
354. Wynn TA. Fibrotic disease and the TH1/TH2 paradigm (2004). *Nat Rev Immunol.* **4**:583–94.
  355. Madala SK, Pesce JT, Ramalingam TR, Wilson MS, Minnicozzi S, et al. Matrix Metalloproteinase 12-Deficiency Augments Extracellular Matrix Degrading Metalloproteinases and Attenuates IL-13–Dependent Fibrosis (2010). *J Immunol.* **184**:3955–63.
  356. Neumann K, Karimi K, Meiners J, Voetlaue R, Steinmann S, et al. A Proinflammatory Role of Type 2 Innate Lymphoid Cells in Murine Immune-Mediated Hepatitis (2017). *J Immunol.* **198**:128–37.
  357. Cavada BS, Pinto-Junior VR, Osterne VJS, Nascimento KS. ConA-like lectins: High similarity proteins as models to study structure/biological activities relationships (2019). *Int J Mol Sci.* **20**:30.
  358. Clark WR. An antigen-specific component of lectin-mediated cytotoxicity (1975). *Cell Immunol.* **17**:505–16.
  359. Pilarski LM, Bretscher PA, Baum LL. Helper T cells are required for the polyclonal stimulation of cytotoxic T cells by concanavalin A (1977). *J Exp Med.* **145**:1237–49.
  360. Tiegs G, Hentschel J, Wendel A. A T cell-dependent experimental liver injury in mice inducible by concanavalin A (1992). *J Clin Invest.* **90**:196–203.
  361. Mizuhara H, O’neill E, Seki N, Ogawa T, Kusunoki C, et al. T cell activation-associated hepatic injury: Mediation by tumor necrosis factors and protection by interleukin 6 (1994). *J Exp Med.* **179**:1529–37.
  362. Ballegeer M, Libert C. Different Cell Types Involved in Mediating Concanavalin A Induced Liver Injury: A Comprehensive Overview (2016). *Gastroenterol Hepatol Res.* **1**:001.
  363. Kusters S, Gantner F, Kunstle G, Tiegs G. Interferon gamma plays a critical role in T cell-dependent liver injury in mice initiated by concanavalin A (1996). *Gastroenterology.* **111**:462–71.
  364. Nakamura K, Okada M, Yoneda M, Takamoto S, Nakade Y, et al. Macrophage inflammatory protein-2 induced by TNF- $\alpha$  plays a pivotal role in concanavalin A-induced liver injury in mice (2001). *J Hepatol.* **35**:217–24.
  365. Tagawa Y, Sekikawa K, Iwakura Y. Suppression of concanavalin A-induced hepatitis in IFN-gamma(-/-) mice, but not in TNF-alpha(-/-) mice: role for IFN-gamma in activating apoptosis of hepatocytes. (1997). *J Immunol.* **159**:1418–28.
  366. Ksontini R, Colagiovanni DB, Josephs MD, Edwards CK, Tannahill CL, et al. Disparate roles for TNF-alpha and Fas ligand in concanavalin A-induced hepatitis. (1998). *J Immunol.* **160**:4082–9.
  367. Gantner F, Leist M, Lohse AW, Germann PG, Tiegs G. Concanavalin A-induced T-cell-Mediated hepatic injury in mice: The role of tumor necrosis factor (1995). *Hepatology.* **21**:190–8.
  368. Junqueira LCU, Bignolas G, Brentani RR. Picrosirius staining plus polarization microscopy, a specific method for collagen detection in tissue sections (1979). *Histochem J.* **11**:447–55.
  369. Junqueira LCU, Cossermelli W, Brentani R. Differential Staining of Collagens Type I, II

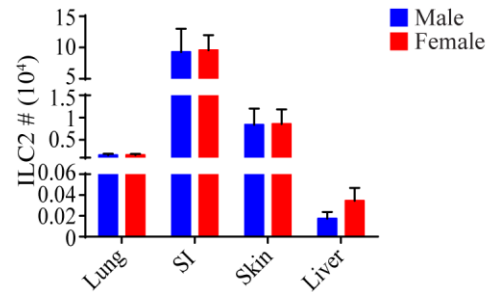
- and III by Sirius Red and Polarization Microscopy (1978). *Arch Histol Jpn.* **41**:267–74.
370. Heymann F, Hamesch K, Weiskirchen R, Tacke F. The concanavalin A model of acute hepatitis in mice (2015). *Lab Anim.* **49**:12–20.
  371. Streetz KL, Luedde T, Manns MP, Trautwein C. Interleukin 6 and liver regeneration (2000). *Gut.* **47**:309–12.
  372. Profet M. The function of allergy: Immunological defense against toxins (1991). *Q Rev Biol.* **66**:23–62.
  373. Carulli L, Dei Cas A, Nascimbeni F. Synchronous cryptogenic liver cirrhosis and idiopathic pulmonary fibrosis: A clue to telomere involvement (2012). *Hepatology.* **56**:2001–3.
  374. Omata F, Shibata M, Nakano M, Jacobs JL, Yasuharu T, et al. Chronic hepatitis with eosinophilic infiltration associated with asthma (2009). *Intern Med.* **48**:1945–9.
  375. Terasaki S, Nakanuma Y, Hosono M, Ogino H, Unoura M, et al. Three cases of primary biliary cirrhosis associated with bronchial asthma (1995). *J Gastroenterol.* **30**:667–71.
  376. Sidman RL, Lane PW, Dickie MM. Staggerer, a new mutation in the mouse affecting the cerebellum (1962). *Science.* **137**:610–2.
  377. Herrup K, Mullen RJ. Staggerer chimeras: Intrinsic nature of purkinje cell defects and implications for normal cerebellar development (1979). *Brain Res.* **178**:443–57.
  378. Van Dyken SJ, Mohapatra A, Nussbaum JC, Molofsky AB, Thornton EE, et al. Chitin activates parallel immune modules that direct distinct inflammatory responses via innate lymphoid type 2 and  $\gamma\delta$  T cells (2014). *Immunity.* **40**:414–24.



## Appendices

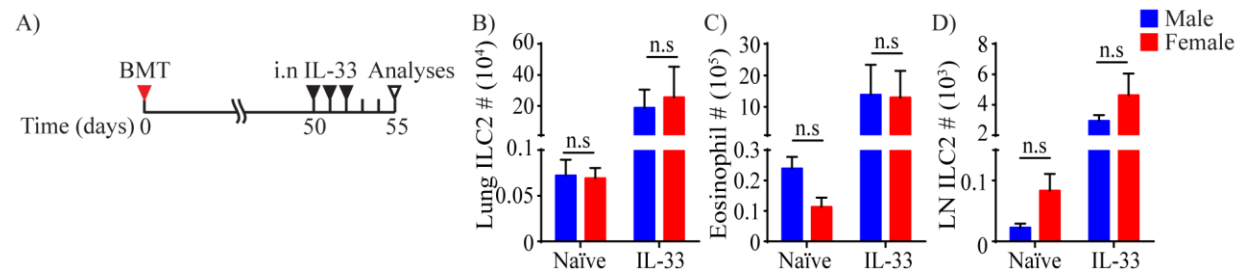
### Appendix A

#### A.1 Sex has no effects on ILC2 development



Numbers of ILC2s in various tissues of post-pubertal naïve male and female mice. Data represented are mean  $\pm$  SEM. n=4-9;  $\geq 2$  independent experiments. Unpaired two-tailed t-test was used to determine statistical significance, with a P value <0.05 being significant.

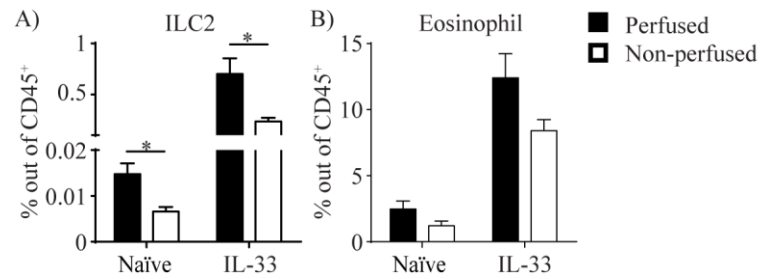
#### A.2 Female and male ILC2s respond similarly in female host



Ten million BM cells isolated from female and male B6 mice were transplanted into lethally irradiated female Pep3b recipients. Fifty days later when donor cells reconstituted the recipient mice, mice were given three consecutive days of i.n. IL-33 treatment and lungs and medLN were analyzed three days after the last treatment (A). ILC2s were quantified in the lung (B) and medLN (D) and eosinophils were quantified in the lung (C). Data represented are mean  $\pm$  SEM. n=4; 1 experiment. Two-way ANOVA with Bonferroni correction was used to assess statistical significance, with a P value <0.05 being significant. n.s., not significantly different [P>0.05]. BMT=BM transplantation.

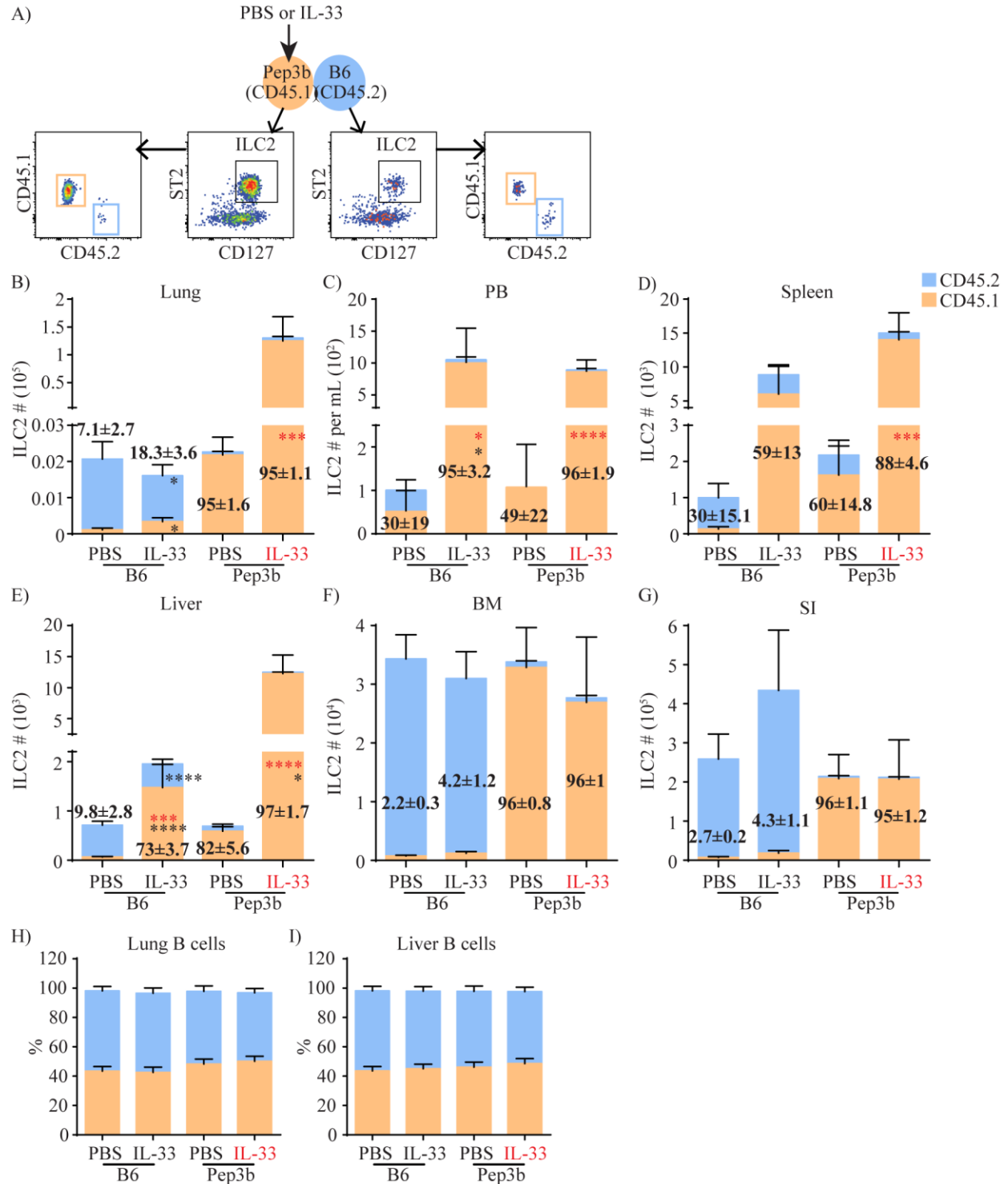
## Appendix B

### B.1 Perfusion has little effect on the frequencies of liver ILC2s and eosinophils



The frequencies of ILC2s (A) and eosinophils (B) were quantified in perfused (black bars) and non-perfused (white bars) livers collected from naïve or IL-33 treated female or male mice (analyses on day 5 in Figure 4.1C). n=4-5; 1 (IL-33 treated) or 2 (naïve) experiments. Unpaired two-tailed t-test was used to determine statistical significance, with a P value <0.05 being significant. \*P<0.05.

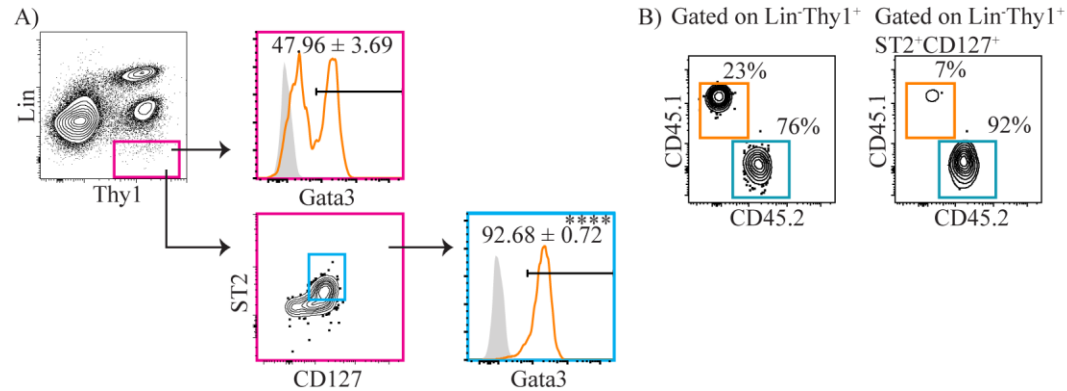
## B.2 Analyses of parabiosis mice after i.n. IL-33 administration into Pep3b mice



(A) Female B6 and Pep3b mice were conjoined by parabiosis surgery. Pep3b mice were given three daily i.n. PBS or IL-33 and both B6 and Pep3b mice were analyzed on day 7. (B-G) CD45.1<sup>+</sup> (orange) and CD45.2<sup>+</sup> (blue) ILC2s were quantified in the lung (B), PB (C), spleen (D), liver (E), BM (F) and SI (G). (H and I) Percentages of CD45.1<sup>+</sup>

(orange) and CD45.2<sup>+</sup> (blue) B cells in the lung (H) and liver (I) were calculated. The x-axes show the strains of mice analyzed (B6 or Pep3b) and treatment groups (PBS or IL-33). IL-33 highlighted in red indicates the mouse that received IL-33 injections. Numbers within graphs indicate the percentages of CD45.1<sup>+</sup> ILC2s. Black and red asterisks indicate statistical significance of percentages and cell numbers, respectively, of CD45.2<sup>+</sup> (within blue bars) and CD45.1<sup>+</sup> (within orange bars) ILC2s compared to PBS treated pairs. Data represented are mean  $\pm$  SEM. n=4-6 (except SI, where n=3);  $\geq 3$  independent experiments. Two-way ANOVA with Bonferroni correction was used to determine statistical significance, with a P value <0.05 being significant. \*P<0.05, \*\*\*P<0.001, \*\*\*\*P<0.0001.

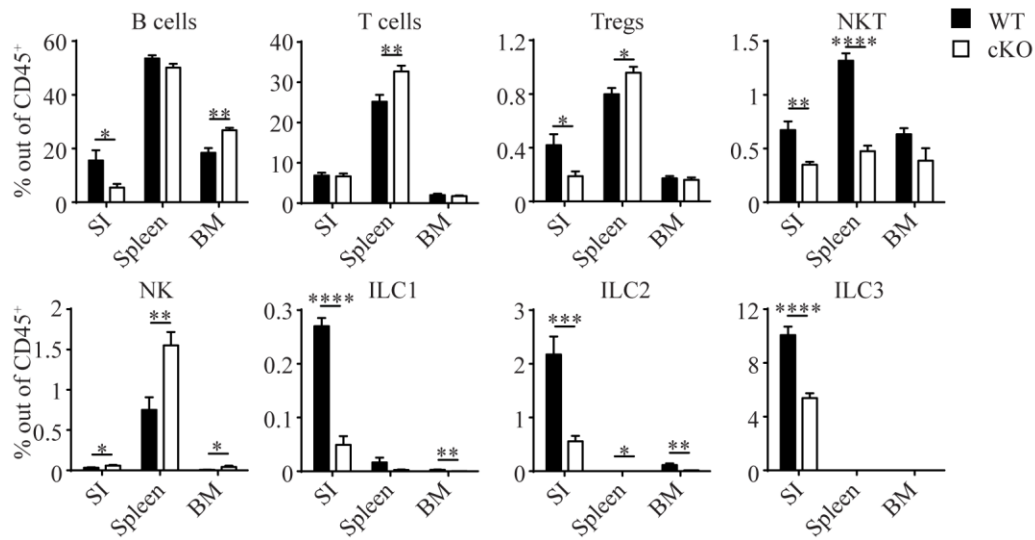
### B.3 Lin<sup>-</sup>Thy1<sup>+</sup> cells contain non-ILC2s



(A) GATA 3 expression was analyzed in Lin<sup>-</sup>Thy1<sup>+</sup> cells and Lin<sup>-</sup>Thy1<sup>+</sup>ST2<sup>+</sup>CD127<sup>+</sup> cells in naïve female or male B6 mouse lung (solid orange lines). Shaded=FMO. Numbers indicate mean  $\pm$  SEM percentages of GATA3<sup>+</sup> cells. n=8; 1 experiment. Paired two-tailed t-test was used to determine statistical significance, with a P value <0.05 being significant. \*\*\*\*P<0.0001. (B) Lin<sup>-</sup>Thy1<sup>+</sup> cells (left panel) and Lin<sup>-</sup>Thy1<sup>+</sup>ST2<sup>+</sup>CD127<sup>+</sup> cells (right panel) in the lungs of naïve female B6 parabiont were analyzed for CD45.2<sup>+</sup> (blue) and CD45.1<sup>+</sup> (orange) expression. Numbers indicate the mean percentages of the cells in each gate. n=6;  $\geq 2$  independent experiments.

## Appendix C

### C.1 Characterization of CD127 cKO mouse SI, spleen and BM



Frequencies of various lymphocytes within CD45<sup>+</sup> cells were quantified in the SI, spleen and BM of naïve female or male WT (black bars) and CD127 cKO (white bars) mice. Gating strategies used for identification of each population are shown in Figure 2.1. Tregs=regulatory T cells. Data represented are mean  $\pm$  SEM. n=5-6; 2 independent experiments. Unpaired two-tailed t test was used to determine statistical significance, with a P value <0.05 being significant. \*P<0.05, \*\*P<0.01, \*\*\*P<0.001, \*\*\*\*P<0.0001.